

**PHOTOGRAMMETRIC EVALUATION OPTIONS
FOR ANCIENT STRUCTURES IN
HYPOKREMNOS, PAGOS, PARADISO AND NYSA**

**A Thesis Submitted to
the Graduate School of Engineering and Sciences of
İzmir Institute of Technology
in Partial Fulfillment of the Requirements for the Degree of**

**MASTER OF SCIENCE
in Architectural Restoration**

**by
Funda UYGUN**

**June 2013
İZMİR**

We approve the thesis of **Funda UYGUN**

Examining Committee Members:

Assist. Prof. Dr. Mine HAMAMCIOĞLU TURAN

Department of Architectural Restoration, İzmir Institute of Technology

Prof. Dr. Başak İPEKOĞLU

Department of Architectural Restoration, İzmir Institute of Technology

Prof. Dr. Hasan BÖKE

Department of Architectural Restoration, İzmir Institute of Technology

Assist. Prof. Dr. Ömür SAYGIN

Department of City and Regional Planning, İzmir Institute of Technology

Dr. Ogan OCALI

District of Technology Development, İzmir Institute of Technology

11 June 2013

Assist. Prof. Dr. Mine HAMAMCIOĞLU TURAN

Supervisor, Department of Architectural Restoration
İzmir Institute of Technology

Prof. Dr. Başak İPEKOĞLU

Head of the Department of
Architectural Restoration

Prof. Dr. R. Tuğrul SENGER

Dean of the Graduate School of
Engineering and Sciences

ACKNOWLEDGMENTS

First of all, I would like to express my special gratitude to my supervisor, Assist. Prof. Dr. Mine Hamamciođlu Turan for her scientific support, guidance and incredible patience throughout my thesis. This thesis could not be completed without her moral and technical support.

I thank Prof. Dr. Bařak İpekođlu, head of the Department of Architectural Restoration, for her support and tolerance, and also for constructive comments about the thesis.

I would like to express my thanks to the jury members; Prof. Dr. Bařak İpekođlu, Prof. Dr. Hasan Bke, Assist. Prof. Dr. mr Saygın, Dr. Ogan Ocalı and Assoc. Prof. Dr. Selim Sarp Tunoku for kindly attending my thesis defense exam and important contributions they provided.

Special thanks go to Prof. Dr. Gnter Pomaska for his scientific support and guidance during my Erasmus study. I am also very grateful to Dr. Ogan Ocalı for his helps and technical support for 3D modeling process via Tgi3D. I also thank Spec. Dr. Elif Uđurlu Sađın for her technical support during laboratory analysis.

My special thanks go to my dear friend Ziřan Karayazılı for her friendship and support. She never left me alone at the site surveys in spite of all bad conditions. And special thanks to my special friend Mehmet Gencer for his encouragement during this study.

Finally, I am indebted to my father Hasan Uygun, my mother Glhan Uygun their endless love, support and patience throughout my life. This thesis is dedicated to them.

ABSTRACT

PHOTOGRAMMETRIC EVALUATION OPTIONS FOR ANCIENT STRUCTURES IN HYPOKREMNOS, PAGOS, PARADISO AND NYSA

This study has focused on 3D reconstruction of ancient monuments based on photogrammetric documentation. The aim of the thesis is to search the limits of automatic and manual photogrammetric evaluation and modeling processes for interpreting of morphologic characteristics of ancient monuments with different geometries, positions, site conditions, and documentation necessities. Emphasis is made on documentation of historical structural characteristics for their conservation aim.

In the methodology of the study, three parameters effecting the quality of the photogrammetric documentation are considered. First parameter is the type of the photogrammetric evaluation software. Manual photogrammetric software; Tgi3D SU and two automated photogrammetric software; Photosynth and Autodesk 123D are used in the study. Variation in the form, size and displacement of the monuments has been defined as the second parameter. In turn, four ancient monuments which have different characteristic features are studied; Hypokremnos Viaduct, Pagos Cistern, Paradiso Aqueduct and Nysa Library. Type of the 3D model and scale of documentation is defined as the last parameter of this thesis. A three dimensional way of documenting structural characteristics of ancient monuments is searched. 1/50 and 1/130 is selected for automatic documentation techniques as documentation scale, while 1/20 scale is selected for manual documentation technique.

This study proves that documentation of structural characteristics of ancient structures may be realized in a successful way with manual photogrammetric technique. The 3D model is much more satisfactory compared to those based on automatic photogrammetric techniques in terms of accuracy control, level of geometric detail and documentation of surfaces.

Consequently, while automatic evaluation is insufficient for providing data leading to structural evaluation, manual photogrammetric evaluation enriches the content of documentation of a historical structure. Structural system detail and 3D model to be used in intervention decisions of structural system can be produced with the help of the manual photogrammetric technique without the necessity of any further documentation.

ÖZET

HYPOKREMNOS, PAGOS, PARADISO VE NYSA' DAKİ ANTİK YAPILAR İÇİN FOTOGRA METRİK DEĞERLENDİRME SEÇENEKLERİ

Bu çalışma antik yapıların fotogrametrik belgelemeye dayalı olarak üç boyutlu modellenmesini arařtırmaktadır. Tezin amacı, farklı geometri, konum ve çevre şartlarına sahip antik yapıların morfolojik özelliklerini ve belgeleme gereksinimlerini ortaya çıkarmak için otomatik ve manuel fotogrametrik değerlendirme ve modellemenin sınırlarını arařtırmaktır. Tarihi strüktür sistemlerinin karakteristiklerinin koruma amaçlı belgelenmesi vurgulanmıştır.

Çalışmanın yönteminde, fotogrametrik belgelenmenin kalitesini etkileyen üç parametre dikkate alınmıştır. İlk parametre fotogrametrik belgeleme yönteminin çeşididir. Çalışmada tamamen manuel bir fotogrametrik yazılım olan Tgi3D SU ve otomatik fotogrametrik yazılımlar olan Photosynth ve Autodesk 123D kullanılmıştır. Yapıların form, boyut ve konumlarındaki çeşitlilik ikinci parametre olarak belirlenmiştir. Bu doğrultuda farklı karakteristik özelliklere sahip dört antik yapı çalışılmıştır: Hypokremnos Köprüsü, Pagos Sarnıcı, Paradiso Su Kemerleri ve Nysa Kütüphanesi. Son parametre olarak, üç boyutlu modelin çeşidi ve belgeleme ölçeği belirlenmiştir. Antik yapıların yapım özelliklerinin üç boyutlu belgelenmesinin kapsamı arařtırılmıştır. Otomatik belgeleme teknikleri için belgeleme ölçeği 1/50 ve 1/130, manuel belgeleme tekniği için ise 1/20 olarak seçilmiştir.

Bu çalışma; antik yapıların manuel fotogrametrik teknikle yapım özelliklerinin başarıyla belgelenebileceğini kanıtlamıştır. Sonuçta elde edilen 3b model hata kontrolü, geometrik detay düzeyi ve yüzeylerin belgelenmesi açısından otomatik fotogrametrik tekniklerle elde edilen modellerden çok daha yeterlidir.

Sonuç olarak, otomatik değerlendirme yapım özelliklerinin değerlendirilmesine yardımcı olacak yeterli bilgiyi sağlayamazken, manuel değerlendirme tarihi bir strüktürün belgelenmesinin içeriğini zenginleştirmektedir. Strüktür sistemiyle ilgili müdahale kararlarında kullanılacak sistem detayı ve üç boyutlu model, başka bir ek belgelemeye gerek olmadan, manuel fotogrametrik model yardımıyla üretilmektedir.

TABLE OF CONTENTS

LIST OF FIGURES	ix
LIST OF TABLES	xiii
LIST OF ABBREVIATIONS.....	xiv
CHAPTER 1. INTRODUCTION	1
1.1. Phases of Heritage Documentation	3
1.1.1. Data Gathering and Processing	4
1.1.2. Imaged Based 3D Modeling.....	6
1.2. Literature Review	7
1.2.1. Studies on Surveying with Passive Sensors	7
1.2.2. Studies on 3D Modeling.....	10
1.3. Definition of Research Problem, Aim and Content.....	12
1.4. Methodology and Tools.....	13
1.5. Content	14
CHAPTER 2. DOCUMENTATION PROCESS	16
2.1. Antique Monument Documentation	16
2.2. Data Gathering and Processing	17
2.2.1. Taking Photographs for Automatic Photogrammetric Documentation	17
2.2.2. Taking Photographs for Manual Photogrammetric Documentation	20
2.3. Data Processing	25
2.3.1. Automatic Photogrammetric Evaluation.....	25
2.3.1.1. Point Cloud Generation	26
2.3.1.2. Modeling.....	29
2.3.2. Manual Photogrammetric Evaluation	32
2.3.2.1. Point Cloud Generation	32
2.3.2.2. Modeling.....	37

CHAPTER 3. CHARACTERISTICS OF THE CASE STUDIES	43
3.1. Hypokremnos Viaduct.....	43
3.1.1. Historical Background	44
3.1.2. Site Characteristics.....	48
3.1.3. Construction Technique	51
3.2. Pagos Cistern.....	57
3.2.1. Historical Background	59
3.2.2. Site Characteristics.....	60
3.2.3. Construction Technique	62
3.3. Paradiso Aqueduct.....	64
3.3.1. Historical Background	65
3.3.2. Site Characteristics.....	66
3.3.3. Construction Technique	69
3.4. Nysa Library.....	70
3.4.1. Historical Background	72
3.4.2. Site Characteristics.....	73
3.4.3. Construction Technique	76
 CHAPTER 4. HISTORICAL RESEARCH, COMPARATIVE STUDY AND RESTITUTION OF HYPOKREMNOS VIADUCT.....	 80
4.1. History of the Site	80
4.2. History of Ancient Viaduct in Anatolia	81
4.3. Comparison of Ancient Anatolian Viaducts with the Case Study	85
4.3.1. Façade Composition.....	87
4.3.2. Architectural Elements.....	88
4.3.3. Structural Elements	90
4.3.4. Construction Technique and Material Usage.....	95
4.3.5. Historical Evaluation.....	97
4.4. Restitution of Hypokremnos Viaduct.....	98
4.4.1. Restitution of Site Characteristics.....	99
4.4.2. Restitution of Morphologic Characteristics	101
4.4.3. Restitution of Structural Characteristics	101
4.3.3.1. Structural System Detail	102

4.3.3.2. Construction Phases of the Viaduct.....	106
CHAPTER 5. DISCUSSION.....	109
5.1. Advantages and Disadvantages of Automatic Photogrammetric Evaluation Software	110
5.2. Advantages and Disadvantages of Manual Photogrammetric Evaluation Software	115
CHAPTER 6. CONCLUSION	122
REFERENCES	126
APPENDICES	
APPENDIX A. MATERIAL CHARACTERISTICS OF THE MORTAR SAMPLE FROM HYPOKREMNOS VIADUCT.....	134
APPENDIX B. ORTHOGRAPHIC VIEWS OF THE 3D MODEL OF HYPOKREMNOS VIADUCT.....	141
APPENDIX C. AXONOMETRIC VIEWS OF THE 3D MODEL OF HYPOKREMNOS VIADUCT.....	145
APPENDIX D. DRAWINGS OF STRUCTURAL SYSTEM DETAIL OF HYPOKREMNOS VIADUCT IN 1/20 SCALE.....	147

LIST OF FIGURES

<u>Figure</u>	<u>Page</u>
Figure 1.1. Comparison of Photosynth and conventional photogrammetry in Treasury..	8
Figure 1.2. Integration of multi-resolution data for 3D modeling of the Pompeii Forum	9
Figure 1.3. The three-dimensional model of <i>Basilica da Ascension</i> in Spain.....	10
Figure 1.4. Surface construction by directly using the images through interactive plotting and analyzing point clouds	11
Figure 1.5. Texturing in Blender	12
Figure 2.1. Nikon D70 digital SLR camera	17
Figure 2.2. Steel tape (20 meter) and ladder	18
Figure 2.3. General and overlapping photos for Autodesk 123D and Photosynth	18
Figure 2.4. Detailed photos for Photosynth	19
Figure 2.5. Image blocks of Pagos Cistern	20
Figure 2.6. Image blocks of Paradiso Aqueduct	20
Figure 2.7. Target (Scale: 1/1)	21
Figure 2.8. Shooting positions	21
Figure 2.9. Organization of the image block of the plan	22
Figure 2.10. Organization of the image block of the facades	23
Figure 2.11. Organization of the image blocks of the arches	23
Figure 2.12. Organization of photo positions	24
Figure 2.13. Systemization of targets	24
Figure 2.14. Selection of two targets for scaling model	25
Figure 2.15. Exporting point cloud and camera parameters via SynthExport	26
Figure 2.16. Exporting different coordinate system	27
Figure 2.17. Manual stitching in Autodesk 123D.....	28
Figure 2.18. Point cloud and mesh construction, Paradiso Aqueduct	29
Figure 2.19. Align tool and point based gluing command.....	30
Figure 2.20. Combined pieces, Hypokremnos Viaduct	31
Figure 2.21. Combined mesh model of Pagos Cistern in SketchUp.....	31
Figure 2.22. Problematic photos	32
Figure 2.23. Point errors	35

Figure 2.24. Automatic addition of control points.....	36
Figure 2.25. Export settings	36
Figure 2.26. Line command and Tgi3D toolbar	37
Figure 2.27. Move command and Tgi3D Toolbar	37
Figure 2.28. Upsample mesh and Tgi3D image-based surface modeler toolbar	38
Figure 2.29. Multi segment surface command and Tgi3D image-based surface modeler	38
Figure 2.30. Determining number of iterations	38
Figure 2.31. Making component.....	39
Figure 2.32. Problems	40
Figure 2.33. Tgi3D toolbar	41
Figure 2.34. Tgi3D Su Move command and Tgi3D toolbar.....	41
Figure 2.35. Paste in place command	42
Figure 3.1. Hypokremnos Viaduct.....	43
Figure 3.2. Ancient settlements	44
Figure 3.3. Ancient settlements in Urla Region.....	45
Figure 3.4. Location of Hypokremnos.....	46
Figure 3.5. Ionia in Roman Period.....	47
Figure 3.6. The historical caravan route in Ottoman Period.....	48
Figure 3.7. Water sources in Çeşme, Karaburun and Urla regions	49
Figure 3.8. Tatar Brook and Hypokremnos (İçmeler)	50
Figure 3.9. Location of the Hypokremnos Viaducts.....	51
Figure 3.10. Model of structural elements	52
Figure 3.11. Dressing system of the facades	54
Figure 3.12. Double layered facing stones of the viaduct	54
Figure 3.13. Model of the facing stones	55
Figure 3.14. Semicircular arch and keystone in the smallest arch.....	56
Figure 3.15. Model of rubble sstone pavements	56
Figure 3.16. Parapet walls.....	57
Figure 3.17. Pagos Cistern.....	58
Figure 3.18. Location of Pagos Cistern and aqueducts.....	58
Figure 3.19. Location of Pagos Cistern	61
Figure 3.20. Plan of Pagos Cistern	62
Figure 3.21. Model of partial part of Pagos Cistern	63

Figure 3.22. Piers, arches, gaps above the piers and plasters	64
Figure 3.23. Unclear and incomplete structural details	64
Figure 3.24. Paradiso Aqueduct.....	65
Figure 3.25. Positions of Paradiso Aqueducts	66
Figure 3.26. Waterways in İzmir (a. Karapınar Waterway)	67
Figure 3.27. Travelers' Route underneath the waterway.....	68
Figure 3.28. Old photo of Ste-Anne (Paradiso) Aqueduct	68
Figure 3.29. Model of Paradiso Aqueduct.....	69
Figure 3.30. Dimensions of piers and arches, type of arches	70
Figure 3.31. Unclear details	70
Figure 3.32. Scaffoldings (Source: Adam 2005)	71
Figure 3.33. Nysa Library	72
Figure 3.34. Location of Nysa	74
Figure 3.35. Ground floor plan of Nysa Library.....	75
Figure 3.36. Model of Nysa Library	76
Figure 3.37. Model of rubble stone facing.....	77
Figure 3.38. Model of <i>Chequer work</i>	77
Figure 3.39. Model of <i>Opus Africanum</i>	78
Figure 3.40. Semicircular arches of niches	78
Figure 4.1. Ionia in Roman Period.....	81
Figure 4.2. A Roman Viaduct; Aizonai, Penkalas Brook.....	82
Figure 4.3. A rectangular formed Roman Viaduct; Taş Viaduct, Seyhan, Adana.....	83
Figure 4.4. A Byzantine Viaduct; Çobançeşme Viaduct	83
Figure 4.5. Different coloured and sized cut stone blocks in a Seljukid Viaduct; Bayramiç Viaduct.....	85
Figure 4.6. Ottoman Viaduct; Sinanlı Viaduct	85
Figure 4.7. Characteristics of ancient viaducts in Anatolia	86
Figure 4.8. Façade form of case study viaduct	87
Figure 4.9. Babaeski Viaduct with its kiosks.....	89
Figure 4.10. Floor covering of Hypokremnos Viaduct.....	89
Figure 4.11. Structural elements of a Viaduct	90
Figure 4.12. Timber piled foundation system.....	91
Figure 4.13. The principle of a Roman cofferdam	92
Figure 4.14. Spandrel walls	93

Figure 4.15. Semicircular arches	93
Figure 4.16. Centering	94
Figure 4.17. Keystone of the arch of Hypokremnos Viaduct	95
Figure 4.18. Facing materials and patterns of facades.....	97
Figure 4.19. Ancient road passing through Hypokremnos	99
Figure 4.20. Hypokremnos Region in Roman Period.....	100
Figure 4.21. Restitution of southern facade	101
Figure 4.22. Data gathering positions	103
Figure 4.23. Bringing together data gathered from different parts of the object	105
Figure 4.24. Structural system detail	105
Figure 4.25. Construction phases of Hypokremnos Viaduct	108
Figure 5.1. Model and photo positions by Autodesk 123D in Nysa Library.....	110
Figure 5.2. Unclear details by Autodesk 123D, in Nysa Library	111
Figure 5.3. Incomplete surfaces by Autodesk 123D, in Pagos Cistern	112
Figure 5.4. Comparison of models gained by Autodesk 123D and Photosynth+Meshlab in Nysa Library	112
Figure 5.5. Model of Pagos Cistern by Autodesk 123D.....	113
Figure 5.6. Model of Paradiso Aqueduct by Autodesk 123D.....	114
Figure 5.7. Model of Hypokremnos Viaduct by Autodesk 123D.....	114
Figure 5.8. Reality based model of Nysa Library by Autodesk 123D.....	115
Figure 5.9. Maximum and global point error.....	116
Figure 5.10. Model of Hypokremnos Viaduct by Tgi3D	117
Figure 5.11. Detailed 3D model of Hypokremnos Viaduct by Tgi3D	118
Figure 5.12. Orthographic view of the model without incomplete surfaces and holes	118
Figure 5.13. Problem of inclusion of sky.....	120
Figure 5.14. Drooping problem	121
Figure 6.1. Tilted photos and color differences	123
Figure 6.2. Analyzed spots on the reality based 3D model for system detail.....	124
Figure 6.3. Structural system detail	125
Figure 6.4. Structural system detail as view on the mixed 3D model	125

LIST OF TABLES

<u>Table</u>	<u>Page</u>
Table 1.1. Methodology.....	14
Table 3.1. Construction technique and material usage of structural and architectural elements	53
Table 4.1. Dating of Hypokremnos Viaduct.....	98
Table 4.2. Characteristics of Hypokremnos Viaduct.....	104
Table 5.1. Duration of calibration and modeling.....	119
Table 5.2. Calibration time	119
Table 6.1. Evaluation of documentation techniques.....	123

LIST OF ABBREVIATIONS

<u>Abbreviations</u>	<u>Definition</u>	<u>Release date</u>
Tgi3D	Tgi3D SU PhotoScan Calibration Tool	October 12, 2012
SketchUp 8	Trimble SketchUp 8	May 21, 2013
SketchUp	Google SketchUp	August, 2000
Photosynth	Microsoft®'s Photosynth™	March 18, 2010
Autodesk 123D	Autodesk 123D Catch	March 20, 2012
Meshlab	Meshlab v1.3.2	August 3, 2012
AutoCad	AutoCad 2012	2012
Artlantis	Artlantis Studio 2	2008
m	meter	
cm	centimeter	

CHAPTER 1

INTRODUCTION

Measuring with traditionally, tachometry, photogrammetry, and laser scanning are the methods of gathering data with measured survey purposes of architectural heritage (Böhler and Heinz 1999, Arias, et al. 2005, Remondino 2011). In this thesis, photogrammetric methods are emphasized.

The term photogrammetry was firstly introduced in 1867 as title of an article from Meydenbauer which was published in the *Wochenblatt des Architektenvereins zu Berlin* (Berlin Architectural Society - Weekly Journal). Since 1980s, photogrammetry has provided the primary source data for Geographic Information System. There has been a continuing development of close-range photogrammetric techniques to many other fields; architecture, engineering, archeology, etc. (Meydenbauer 1912, Blachut and Burkhardt 1988, Grimm 2007). According to specific needs in architectural documentation, the different kinds of image based systems were developed; digital image rectification, stereoscopic image measurement and multi-image measurement (Fellbaum 1992, Grussenmeyer, et al. 2002).

Consequently, measured survey data is structured either in 2D or 3D forms to produce architectural presentations. Today photogrammetric data is naturally composed of 3D point cloud and 3D surfaces. In turn, it is possible to produce very accurate reality based models from photogrammetric surveys. Reality-based models employ hardware and software to metrically survey the reality as it is, documenting in 3D the actual visible situation of a site by means of images, range-data, CAD drawing and maps, classical surveying (GPS, total station, etc.) or an integration of the aforementioned techniques (Manferdini and Remondino 2010). If the reality based model stems from photogrammetric survey data, then it is often referred with the name image based model.

Image based modeling has been widely used method for geometric surfaces of architectural objects for twenty years (Streilein 1994, Grussenmeyer, et al. 2002, Remondino and El-Hakim 2006). Since the last a few years, softwares for multi-image

measurement techniques creating realistic image-based 3D models with textures from photographs by matching photos manually or automatically have been developed.

The examination of the suitability of the point clouds gained by multi-image modeling techniques for survey of architectural heritage is a contemporary research topic questioned by scholars from various disciplines. This point clouds can be obtained by tachometric, photogrammetric or laser scanning techniques (Böhler and Heinz 1999, Arias, et al. 2005). Establishment of a multi-scale survey (Grussenmeyer et. al, 2002), on the other hand, makes possible the fundamental classification of heritage information since scale for architecture is a means to filter information displayed.

On the other hand, virtual reality models are also possible for architectural heritage applications. Virtual reality is a concept that has its roots in 1860s. It refers to an illusion in an artificial world and enables a participant to sense that he/she is occupying an environment other than that which he physically occupies (Wikipedia 2010). Virtual reality technology was started to be used with the development of CAD software of graphic hardware in cultural heritage presentations. It was based on computer graphics software (3D Studio, Maya, SketchUp, etc.) or procedural modeling and they allow the generation of 3D data without any metric survey as input or knowledge of heritage sites (Manferdini and Remondino 2010). It had a potential in museums to make people understand ancient life, lost heritages, etc. It was firstly used in an interactive walk-through of a 3D reconstruction of Dudley Castle, England in 1994. Thus, virtual reality enables heritage sites to be recreated extremely accurately, so that the recreations can be published in various media. In turn, lost heritage or vulnerable heritage may be made visible to a great number of people. 3D virtual reality may be widely used for preparation of projects for development and presentation of historical environment (Wikipedia 2010). It may be claimed that virtual reality based models can be effective tools for single building restoration projects.

In this study, photogrammetric survey of a number of architectural heritage is made and surveyed data is structured with the tools of image based modeling technology. Thus, a number of reality based models are produced. In addition, restitution model of one of the selected heritage is developed combining the tools of virtual reality technology with reality based modeling technology. In turn, a mixed 3D model is produced.

In this study, reality based 3D model is referred as reality based 3D model, 3D model, model or photogrammetric 3D model. However, the mixed model is always pointed out clearly.

1.1. Phases of Heritage Documentation

Geometric data acquisition represents the first step of an architectural restoration project for conservation aimed documentations (Salonia, et al. 2007, Salonia, et al. 2009).

Reality-based 3D surveying and modeling of architectural heritage is meant as the digital recording and 3D reconstruction of the existing fabric using active sensors, passive sensors, classical surveying tools (e.g. total station) and an integration of the mentioned techniques (Böhler and Heinz 1999, Arias, et al. 2005, Remondino 2011).

The choice of a technique or their integration depends on the required accuracy, object dimensions, location constraints, surface characteristics, working team experience, project budget, etc. 3D surveying and modeling have some problems and challenges (Remondino, and El-Hakim 2006, Remondino 2011):

- Selecting the appropriate methodology (sensor, hardware, software) and data processing procedure.
- Designing the proper production workflow.
- Speeding up the data processing time with as much automation as possible.
- Being able to fluently display and interact.

Although many technologies and sensors are available to achieve a good and realistic 3D model containing the required level of detail nowadays, the best approach is still the combination of different techniques. In fact, as a single technique is not able to give satisfactory results in all situations, concerning high geometric accuracy, portability, automation, photo-realism, low-costs, flexibility and efficiency; image and range data are generally combined to fully exploit intrinsic potentialities of each approach (El-Hakim, et al. 2004, Guidi, et al. 2008). Within the limits of this study, techniques of reality-based 3D surveying with passive sensors and 3D modeling are discussed below, respectively. Image-based modeling techniques are preferred in case

of lost monuments or monuments with regular geometric shapes; small objects with free form shapes and low budget terrestrial projects (Remondino and El-Hakim 2006, Remondino 2011).

1.1.1. Data Gathering and Processing

Optical recording sensors are divided into two as passive and active sensors (Böhler and Heinz 1999, Guidi, et al. 2008, Remondino 2011).

- Passive sensors (e.g. digital cameras), deliver image data which are then processed for some mathematical formulations to infer 3D information from 2D image measurements (Remondino and El-Hakim 2006).
- Active sensors (e.g. laser scanner) can provide data directly for 3D information (Blais 2004).

Photogrammetry is considered as the best technique for the processing of image data gathered with digital cameras. It is able to deliver at any scale of application accurate, metric, and detailed 3D information. Normally at least 2 images are required and 3D data can be derived using the rules of projective geometry (Grussenmeyer, et al. 2002, Remondino 2011).

Images can be acquired using satellite, aerial and terrestrial sensors. Then, these images are processed following the typical photogrammetric pipeline (Gruen, et al. 2004, Remondino 2011):

- Sensor calibration
- Image orientation
- Surface measurement
- Feature extraction
- Orthophoto generation

The performance of the conventional photogrammetry is already known in terms of its metric accuracy and acquisition quickness, but time is required in the restitution step because of the manual homologous point recognition from different panoramas (Annibale 2011). The conventional photogrammetric software such as Socced Set, Rolleimetric, Pictran, Tgi3D Su Photo Scan, and Z-Glif utilize accurate matching methods.

In recent years, computer vision community has developed several techniques for architectural heritage reconstruction at a very high level of automation (Photosynth, Bundler, Arc 3D, Photo Modeler and Autodesk 123D). The image orientation phase in terrestrial applications is done without targets in these recent web based and open source software, and they are promising reliable results (Barazzetti, et al. 2010, Remondino 2011). Nowadays, open source software such as Photosynth and Bundler has been discussed from the view point of the accuracy of their point clouds and the ease they provide in data gathering and evaluation; e.g. reduction of the time required for the restitution and automation of the process (Rosnell and Honkavaara 2012). The provided point clouds are useful benchmarks to start with the model reconstruction even if lacking in detail and scale. Especially, Photosynth is a user friendly web service to automatically orient scattered photo making use of few on line steps. Its web interface allows the user to navigate in a virtual scene where its oriented photos are combined with the produced point cloud. Lastly, camera calibration and tie points are exported with an additional software: Synthexport (Annibale 2011). SynthExport allows one to extract the point cloud as well as the camera parameter data of a synth on Photosynth. Point clouds are downloaded automatically and converted to formats that are compatible with most 3D graphics applications. Camera information such as position, focal length and lens distortion of each image is stored as a CSV file. Once a set of images has been oriented, the surface measurements step can be performed with manual and automated matching procedures, depending on the application, aim and scene investigation. Afterwards, the point cloud is transferred into a polygonal mesh texturing engine for visualization (Barazzetti, et al. 2010).

The quality of a point cloud can be characterized by two major quality indicators: the completeness of the point cloud and the accuracy of the individual points. The performance of the matching method directly affects the point density and the accuracy. In addition, the amount of blocked parts of an image by obstructions affects the completeness of the point cloud (Rosnell and Honkavaara 2012).

In turn, establishment of an appropriate integration of conventional photogrammetric software and open source ones for data gathering and evaluation in the documentation of an architectural heritage is an ongoing research problem (El Hakim 2004, Annibale 2011, Rosnell and Honkavaara 2012).

In order to achieve good performance of the point cloud generation techniques, performance assessment criteria have been established. These criteria are below:

- Independent check points should be used for calculating the accuracy of the point cloud (Grussenmeyer, et al. 2002, Honkavaara 2008, Rosnell and Honkavaara 2012).
- The point clouds surveyed with different techniques should be visualized in a unique 3D digital environment and compared (Annibale 2011).
- The same set of images acquired for the studied object should be used as input for the evaluation process with different techniques (Annibale 2011).
- The image block should be designed well (Rosnell and Honkavaara 2012).
- Basic photograph taking rules such as correct exposure time, avoiding back light, avoiding shaking, etc. should be followed (Swallow, et al. 2004).
- Each photograph should overlap with its neighbors (Grussenmeyer, et al. 2002, Swallow, et al. 2004).
- The quality of the image block should be controlled after collection, and unqualified images should be eliminated (Rosnell and Honkavaara 2012).
- Survey control measurements should be provided by theodolite (Swallow, et al. 2004).

1.1.2. Image Based 3D Modeling

3D reality based modeling is the generation of structured 3D data from surveyed unstructured data (Remondino 2011). Images contain all the useful information to derive geometry and texture for a 3D modeling application, but the reconstruction of detailed, accurate and photorealistic 3D models from images is still a difficult task, particularly for large and complex sites, especially if uncalibrated or widely separated images are used (Guidi, et al. 2008, Barazzetti, et al. 2010). 3D modeling consists of geometric and appearance modeling. Geometric modeling deals with the data registration processing (editing, cleaning, meshing), while appearance modeling deals with texturing, blending and rendering. (Lensch, et al. 2003, Remondino 2011).

Once a point cloud (unstructured data) is available, a polygonal model (mesh, structured data) can be generated. A mathematical formulation is required to transfer 2D image measurement into 3D coordinates (Horn and Brooks 1989, Guidi, et al. 2008).

The produced polygonal model demands time consuming repairing to close holes, fix incorrect faces or non-recurring parts (Remondino 2011).

An appearance model is photorealistic and there is no difference between a view rendered from the model and a photograph taken from the view point. It is achieved with texture mapping; in other words, projecting one or more rectified images on the 3D geometry (Lensch, et al. 2003, Remondino 2011). Problems might rise from various factors: time consumption in image quality of building geometry registration, presence of occlusions, specular surfaces, and variations in lighting and camera settings (Remondino 2011).

1.2. Literature Review

For the aim of this thesis, the previous studies on surveying of cultural heritage with quick digital photogrammetric techniques, conventional photogrammetric techniques and combined techniques; and techniques of modeling surveyed data have been evaluated.

1.2.1. Studies on Surveying with Passive Sensors

The type of photogrammetric evaluation software is the primary parameter that affects the quality of the architectural heritage survey. There are a number of studies (Böhler and Heinz 1999, El Hakim 2004, Remondino and El Hakim 2006, Guidi, et al. 2008, Barazzetti, et al. 2010, Annibale 2011, Rosnell and Honkavaara 2012, etc.) comparing the point clouds restituted with quick, simple, low-cost, web based, and open source photogrammetric software such as Photosynth™ and Bundler+CMVS2+PMVS2; and those restituted with conventional photogrammetric software. The first requires less restitution time, because it works without any orientation information, but the point cloud acquired with the second is more accurate. The first has a great potential if the orientation process is improved in time (Barazzetti, et al. 2010). The integration of the two software groups in order to benefit from the advantages of both is an ongoing research problem (El Hakim 2004).

The study of Annibale (2011) discusses how conventional and quick photogrammetric techniques can be used for optimizing the 3D modeling process of a complex architecture. The conventional Fangi 2007, 2008, 2009, 2010 software and the web based softwares of Photosynth and Bundler+CMVS2+PMVS2 were the tools used (Figure 1.1). The case of the Treasury, Nabatean Architecture in Petra was studied. Using the same photograph dataset, point clouds were generated with the two software groups.

The point cloud restituted by the web based software was a useful benchmark to start with the model reconstruction, but it lacked detail and scale. This preliminary model was used as a reference, and its details and scale were provided with the usage of point cloud acquired with conventional techniques.

In addition to the photogrammetric evaluation software preference, the characteristic of the building element is a parameter taken into consideration, while deciding on the strategy of the survey. Guidi, et al. (2008) points out that the building elements with different geometric qualities should be surveyed with different strategies (Figure 1.2). For example, flat surfaces require a few points for modeling; but irregular and deficient building elements, and ornamentations require dense point clouds.

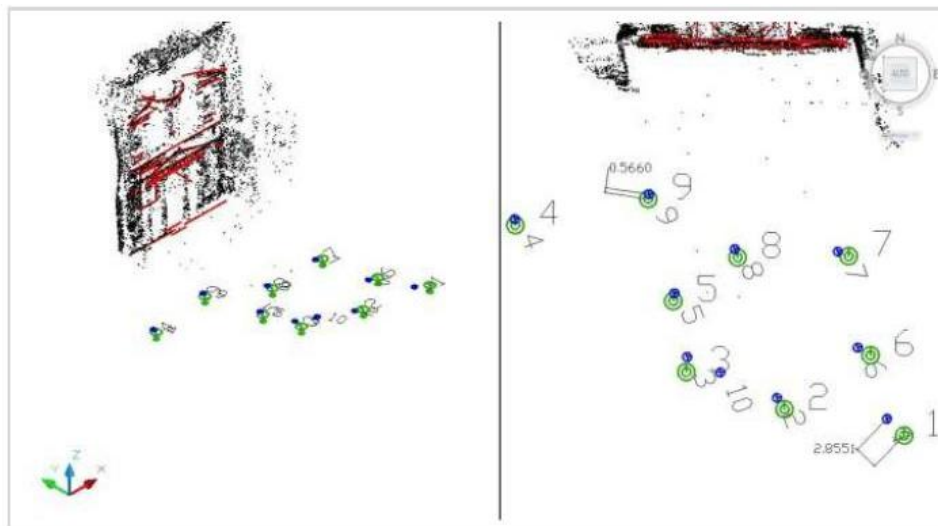


Figure 1.1. Comparison of Photosynth and conventional photogrammetry in Treasury (Source: Annibale 2011)

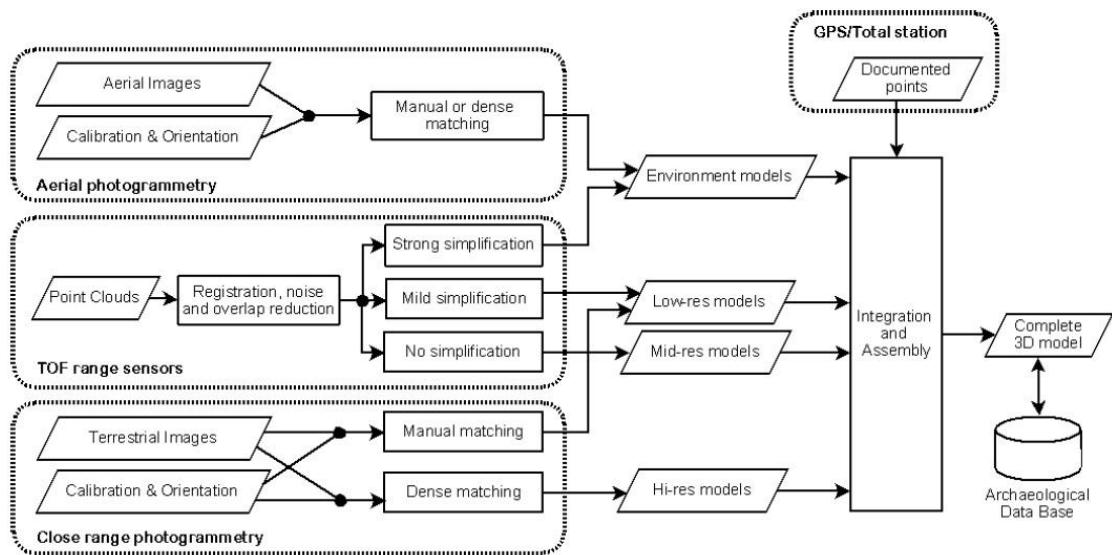


Figure 1.2. Integration of multi-resolution data for 3D modeling of the Pompeii Forum (Source: Guidi, et al. 2008)

The third parameter affecting the strategy of the survey is the type of the 3D model aimed for. If structural characteristics, deficiencies and failures are desired to be represented (Arias, et al. 2005), a conventional photogrammetric software (Photomodeler Pro 4.0.) should be preferred. In turn, the structured data such as the positioning, size and form of the walls and their openings can be taken as a reliable input in the identification of structural characteristics (Figure 1.3).

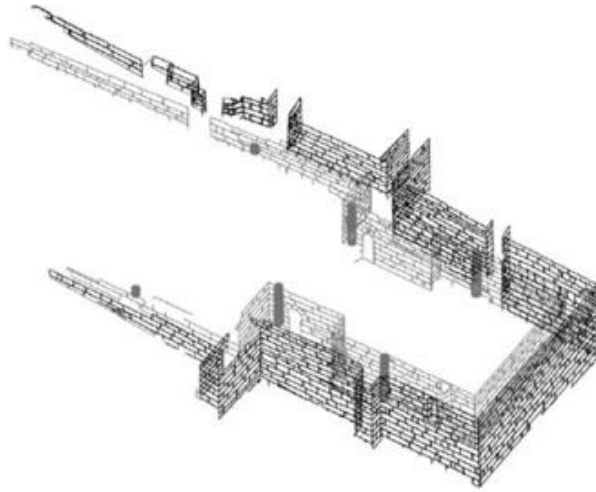


Figure 1.3. The three-dimensional model of *Basilica da Ascension* in Spain
(Source: Arias, et al. 2005)

1.2.2. Studies on 3D Modeling

In this part, previous studies about modeling of cultural heritage, including conversion from point cloud to mesh and processing of mesh and creation of texture on the mesh surface, are evaluated.

Surface reconstruction and texturing of unstructured data extracted from manual and automatic photogrammetric techniques were carried out by professional or web-based free softwares.

In the study of Barazzetti, et al. (2011), a complete manual and a complete automatic photogrammetric evaluation were carried out. The Temple in Myson was modeled by analyzing the point clouds and using oriented images. The creation of 3D model with manual measurements was carried out by using the oriented images. In this case, an operator (human) selected the same point in at least two images and the 3D position of the selected element was estimated by using the intersection of homologous rays (Figure 1.4).

The automatic creation of a 3D model could be performed by using the point cloud extracted from the images with PhotoModeler Scanner or PMVS. Point cloud was processed with a meshing algorithm in Geomagic Studio. This software allowed direct mesh reconstruction through a network of triangles connecting the measured image points (Figure 1.4).



Figure 1.4. Surface construction by directly using the images through interactive plotting and analyzing point clouds (Source: Barazzetti, et al. 2011)

Meshlab, an open source software, was preferred in modeling in most of the automatic applications. In the study of Callieri, et al (2011), facades of the case of Piazza Della Signoria were constructed with triangulation using filter in Meshlab to indicate the possibility of modeling with this open source tool instead of costly and difficult to use software. Mapping of photogrammetric information onto 3D data was also carried out with an external tool in Meshlab.

Cignoni, et al. (2008) presented a complete free software pipeline for the 3D digital acquisition of cultural heritage. There are two main tools; Arc 3D for data acquisition and Meshlab for data processing. Meshlab provided a specific tool for importing data produced by Arc 3D service.

In the study of Annibale (2011) comparing automatic and manual photogrammetric techniques, Meshlab was used for visualizing and processing of point cloud extracted automatically. Mesh model was textured using the UV modifier of 3D Studio Max Software because of its performance in terms of interactive modeling. This research dealt with an efficient and low cost methodology to obtain a metric and photorealistic survey of a complex architecture.

In the study of Pomaska (2009), the model reconstructed with Meshlab was textured with Blender, an open source tool for 3D content creation. Blender supports UV mapping with tools for unwrapping faces and stitching them onto the image atlas (Figure 1.5).

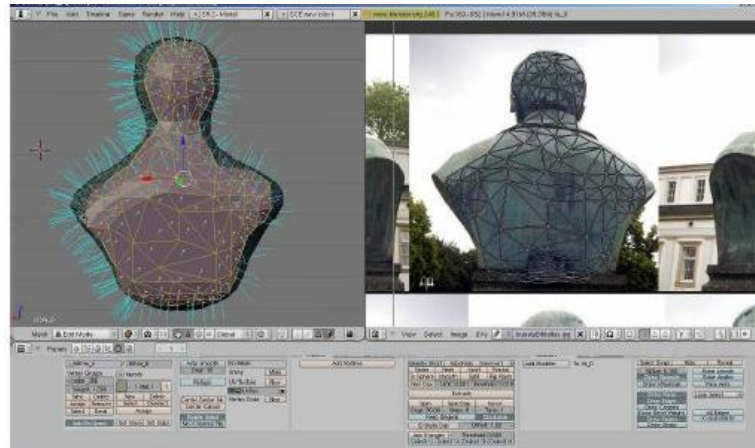


Figure 1.5. Texturing in Blender
(Source: Pomaska 2009)

1.3. Definition of the Research Problem and Aim

It is claimed that automatic, quick, simple, low-cost, web-based, and open source photogrammetric software can be sufficient for the reality-based 3D surveying and modeling of historical structures, if only visual analysis of the heritage characteristics is aimed. Manual photogrammetric software should be preferred for precise documentation of historical structural systems and related building elements. The geometric characteristics of the building such as linear or massive; location of the building such as in depressed ground or on plain ground; presence of obstacles around the building such as shrubs, brook or sea; and the desired documentation scale such as 1/100 or 1/20 are the parameters that determine the surveying methodology. In order to test these parameters, four case studies were selected. So, the aim of the study is to search the limits of automatic and manual photogrammetric evaluation and modeling processes for interpreting of ancient morphologic characteristics of objects with different geometries, positions, site conditions, and documentation necessities. Emphasis is made on documentation of historical structural characteristics for their conservation aimed documentation.

1.4. Methodology and Tool

In this study, both complete manual photogrammetric software (Tgi3D) and two automated photogrammetric software (Photosynth and Autodesk 123D) was used. Professional camera (Nikon D70 digital SLR camera with 28-80 mm lens) was preferred. Photosynth was used only for point cloud generation and then surface reconstruction of point clouds was carried out in Meshlab, free mesh processing software. However, Autodesk 123D is fully automatic software which carried out evaluation and modeling phases together.

These software were tested on four different case studies which have different geometries, placements and site conditions; Hypokremnos Viaduct, Paradiso Aqueduct, Pagos Cistern and Nysa Library. The Hypokremnos Viaduct, Urla, Izmir is a 16.37 m long linear objects with 3.49 m width and 1.93 m maximum height. It is an independent structure. The viaduct was documented by both manual and automatic photogrammetric software. For manual documentation, the study scale was 1/20, while 1/50 was preferred for automatic software. The Paradiso Aqueduct, Buca, Izmir, is also a high linear object (approximately 120x3x120 m), whereas it is surrounded by shrubs and trees and a brook. The Pagos Cistern, Kadifekale, Izmir (approximately 35.79 x 20 x 5.20 m) is a cubical object at a depressed position. The Nysa Library, Aydın (approximately 25x14x6 m) is a mass composed of two independent prisms and surrounded by some shrubs and debris. These three case structures were just studied with automatic software to gain models in 1/50 scale (Table 1.1).

Table 1.1. Methodology

	Software	Geometry	Position	Site Restrictions	Scale
Hypokremnos Viaduct	Photosynth+Meshlab	Linear+Low	Parallel to coastline	Splashing sea waves	1/50
	Autodesk 123D				1/50
	Tgi3D				1/20
Pagos Cistern	Photosynth+Meshlab	Prismatic	Depressed on ground	Elevated landscape in its surrounding	1/50
	Autodesk 123D				
Paradiso Aqueduct	Photosynth+Meshlab	Linear+High	On a brook	Surrounded by shrubs and trees	1/130
	Autodesk 123D				
Nysa Library	Photosynth+Meshlab	Prismatic	On plain ground	Some shrubs and debris in its vicinity	1/50
	Autodesk 123D				

1.5. Content

In the first chapter, general information on phases of heritage documentation is mentioned. The previous studies which were carried on data gathering, processing, and modeling in documentation are analyzed in detail. The study problem, its aim, methodology, and tools of the study are explained, respectively.

In the second chapter, how data was gathered and processed with a manual photogrammetric technique (Tgi3D); and automatic photogrammetric documentation techniques (Photosynth and Autodesk 123D) are stated in detail.

In the third chapter, characteristics of case studies which were documented with photogrammetric techniques are explained. Historical backgrounds; site, morphologic and structural characteristics of each case study are stated. Additionally, structural characteristics of Hypokremnos Viaduct are assessed with reference to manual photogrammetric documentation.

In the fourth chapter, historical research on ancient viaducts in Anatolia and comparison of Hypokremnos Viaduct with these viaducts was carried out. Lastly, restitution of Hypokremnos viaduct is discussed with its morphologic and structural aspects. Structural system detail and construction phases of Hypokremnos viaduct are identified and modeled.

In conclusion, the content of structural documentation suitable for an antique monument is clarified. Advantages and disadvantages of automatic and manual photogrammetric evaluation are discussed.

CHAPTER 2

DOCUMENTATION PROCESS

This study considers the documentation of four ancient structures in Western Turkey; the Hypokremnos Viaduct in Urla, İzmir; Pagos Cistern, Kadifekale, İzmir; Paradiso Aqueduct, Buca, İzmir; and Nysa Library, Nysa, Aydın. The Hypokremnos Viaduct, has been documented with both manual and automatic techniques, while the others were only documented with automatic techniques. The study also considers the interpreting of structural characteristics of these heritages.

2.1. Antique Monument Documentation

If an antique monument is documented for conservation purposes, the following factors should be taken into consideration:

- An antique monument is an irregular formed object as a result of its long life span. This age is revealed in various evidences whose source is either alterations or failures and deteriorations. In turn, the related representation should be a realistic expression of the irregularity of the monument.
- Since scale is a means of filtering information, the determination of representation scale should be the first step in the documentation process so that the appropriate framework for classifying heritage information can be developed. For example, 1/200 may be appropriate for formulating site decisions, 1/50 may be appropriate for formulating consolidation decisions and 1/20 may be appropriate for application details.
- Historical research of each monument should be planned so that the original building and composition can be interpreted.

2.2. Data Gathering and Processing

Taking photographs is the first step of data gathering. The differences in the strategies of taking photographs for manual and automatic processing are pointed out below.

2.2.1. Taking Photographs for Automatic Photogrammetric Documentation

The equipment which was used while taking photographs for automatic documentation are listed below:

- Nikon D70 digital SLR camera, equipped with 28-80 mm lense (Figure 2.1)
- Ladder (Figure 2.2)
- Steel tape (20 meter) (Figure 2.2)



Figure 2.1. Nikon D70 digital SLR camera



Figure 2.2. Steel tape (20 meter) and ladder

Image blocks were organized according to the software which was used for modeling and characteristics of case studies.

Two different software for automatic photogrammetric documentation were preferred; Autodesk 123D and Photosynth with Meshlab. Photos were taken with different organizations according to this software.

The principles followed while taking photographs are below:

1) Designing Image Blocks

For Autodesk 123D, general and overlapping photos are taken by surrounding the case study buildings (Figure 2.3). Number of photos should be around 50 and should not exceed 70. However, to gain a detailed point cloud in Photosynth, both detailed and general photos are necessary. Angle between the detailed photos is limited at least 15 per full rotation and maximum 25 degrees angle (Figure 2.4).

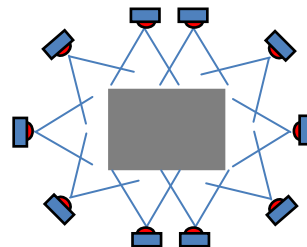


Figure 2.3. General and overlapping photos for Autodesk 123D and Photosynth

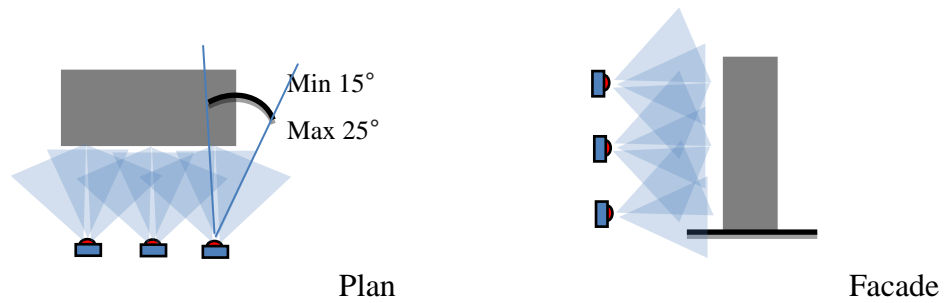


Figure 2.4. Detailed photos for Photosynth

Each case study has different geometry and position. Nysa library has a cubical mass and has no occlusions around. Paradiso Aqueduct is a linear structure and has accessibility problems. Pagos Cistern has a depressed position. Hypokremnos Viaduct has linear structure, and has no occlusions around, excluding sea. The image block designs mentioned above were adopted to the necessities of each case study.

Nysa library's detailed photographs are taken from three different levels, while Pagos Cistern, Paradiso Aqueduct, and Hypokremnos Viaduct were taken from two different levels. The reason of using three levels in the library is the short shooting distance contrary to other case studies.

2) Calculation of Shooting distance

The shooting distance was calculated according to the below formula (Swallow, et al. 2004). The drawing scale was determined as 1/50 for the automatic photogrammetric documentation.

For 1/50 scale:

Negative scale range 1/150 to 1/250

Negative Scale = Focal length / Distance

Focal lengths were arranged according to the possible shooting distances. In Nysa Library, Hypokremnos Viaduct and Pagos Cistern, focal length was preferred as 28 mm (Figure 2.5).

$$1/200 = 28 \text{ mm}/d$$

$d \approx 5,5 \text{ m}$ (max shooting distance for
Nysa Library and Hypokremnos Viaduct)

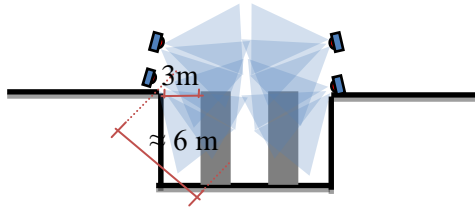


Figure 2.5. Image blocks of Pagos Cistern

However, Paradiso Aqueduct has accessibility problem, the shooting distance is about 25 m. To be able to take both general photos and also detail photos, focal length was arranged as 55 mm. By using these values, scale was calculated as 1/130 for Paradiso Aqueduct (Figure 2.6).

For 1/130 scale:

Negative scale 1/520

$$1/520 = f/d$$

$$520 \times 55 \text{ mm} = d$$

$$d \text{ max} = 28.6 \text{ m (max shooting distance for Paradiso Aqueduct)}$$

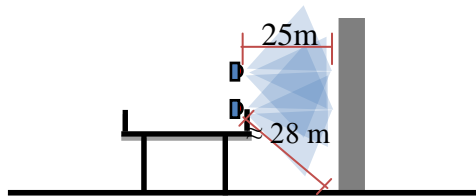


Figure 2.6. Image blocks of Paradiso Aqueduct

2.2.2. Taking Photographs for Manual Photogrammetric Documentation

The equipment which was listed in automatic documentation was used for the manual documentation. Nikon D70 digital SLR camera was just preferred to take photos. Additionally, targets were used by stitching to surfaces of the case study for the calibration phase (Figure 2.7).

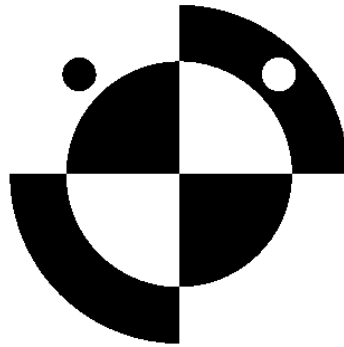


Figure 2.7. Target (Scale: 1/1)

The principles followed while taking photographs are as in the below:

1) Calculation of shooting distance:

The shooting distance was calculated according to the formula which was mentioned in automatic photogrammetric documentation. Shooting distances were calculated as 2.25 meter for 1/20 scale and 5.5 meter for 1/50 scale (Figure 2.8).

For 1/50 scale:

Negative scale of 1/50 = 1/200

$1/200 = \text{Focal length} / \text{Distance}$

$1/200 = 28 \text{ mm} / d$

$d \approx 5,5 \text{ m}$

For 1/20 scale:

Negative scale of 1/20 = 1/80

$1/80 = \text{Focal length} / \text{Distance}$

$1/80 = 28 \text{ mm} / d$

$d \approx 2,25 \text{ m}$

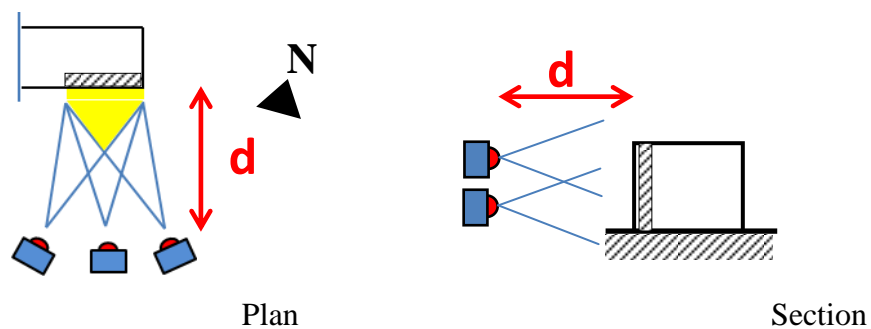


Figure 2.8. Shooting positions

From both distances, each surface piece was documented with 6 photos (Figure 2.7). There are four main surfaces which are necessary to model; viaduct floor plan, arches, walls, and intersection zones. Same photo system was repeated in all these surfaces. Total number of photos was 801.

2) Designing image block:

Three different image blocks were designed in accordance with the forms of the viaduct floor, wall and arches.

- Image block of the viaduct's floor plan (Figure 2.9)

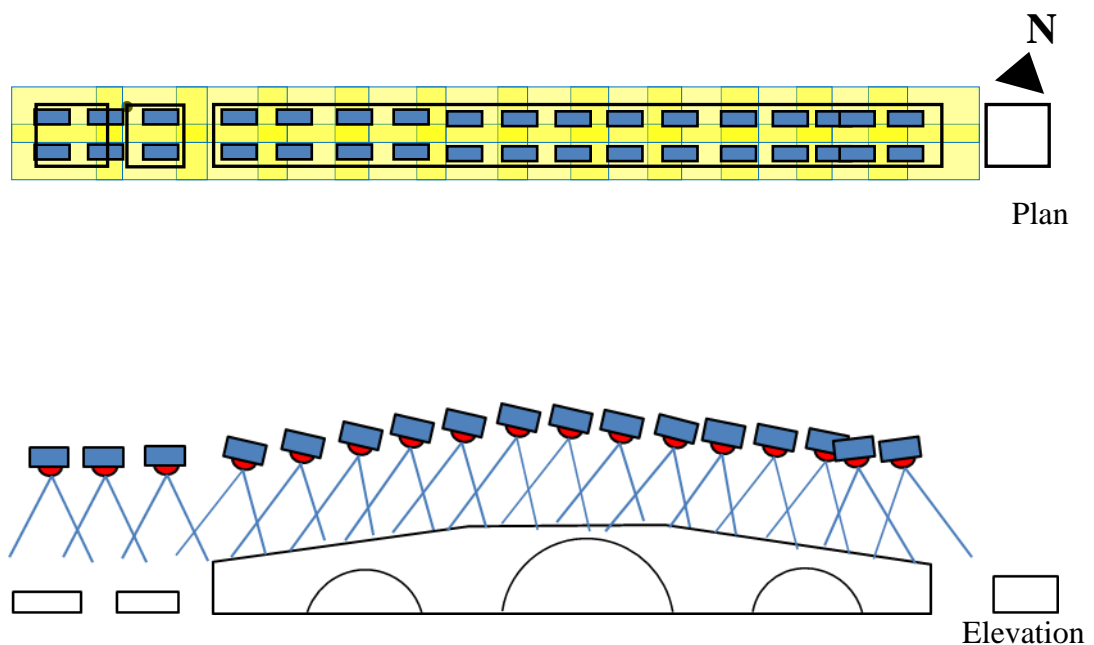


Figure 2.9. Organization of the image block of the plan

Total number of photos was 154 including problematic ones.

- Image block of the facades (Figure 2.10)

For every surface piece documented, six different views of the same surface should be shot from different positions: two taken parallel to the surface with and without ladder, two taken from right side of the parallel position making approximately 45° angle with the bisector's of the central and right views; and two taken from left side of the parallel position making approximately 45° angle with the bisector's of the central and left views (Figure 2.10).

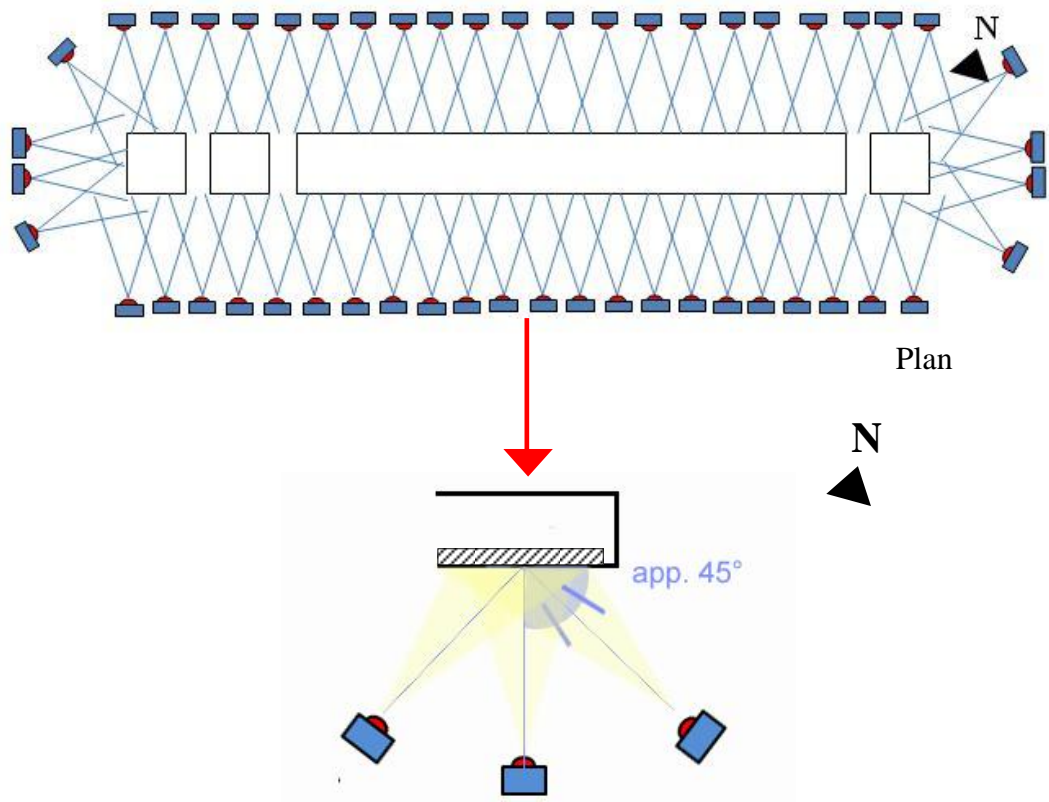


Figure 2.10. Organization of the image block of the facades

Total number of photos of walls was 173 including problematic ones.

- Image block of the arches (Figure 2.11)

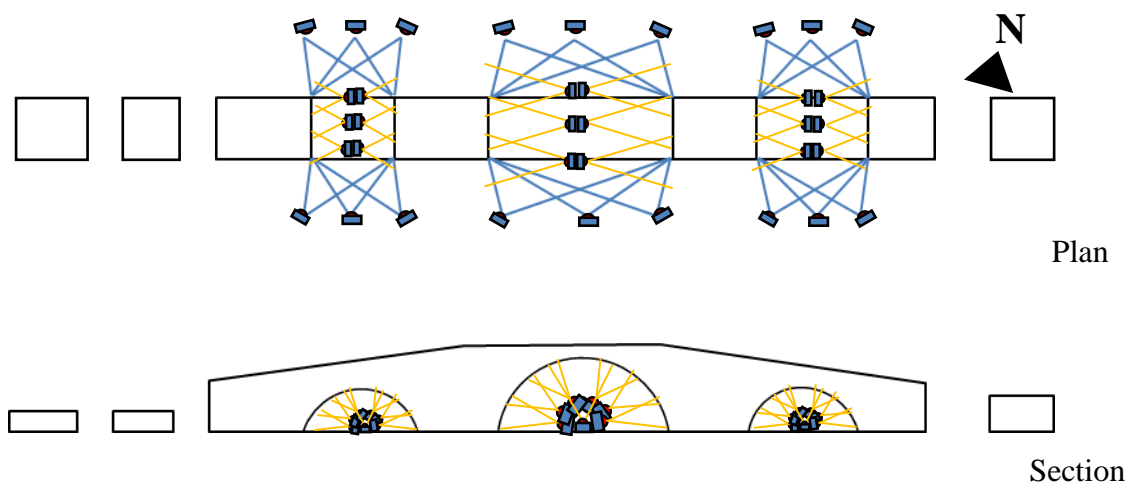


Figure 2.11. Organization of the image blocks of the arches

Total number of the photos of the arches is 261 including problematic ones (Figure 2.12).

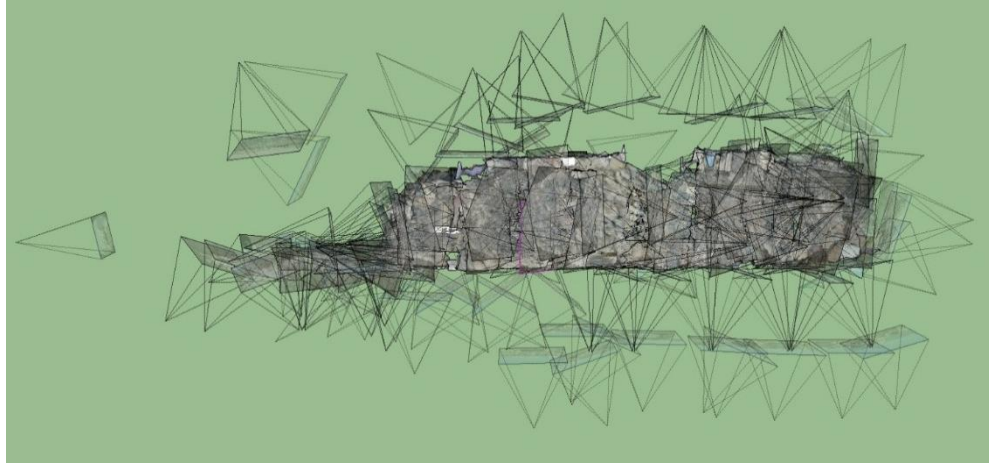


Figure 2.12. Organization of photo positions

- Image block of intersection zones

The zones in which the floor and the wall of the viaduct meet were photographed separately in an overlapping order. Total number of photos was 149, while 91 of them at the northern, 58 of them are at the southern side.

3) Systemization of targets

Targets were positioned in a gridal order. Approximately at least sixteen targets were included in each photo. Each three side targets were also shot in overlapping photos (Figure 2.13).

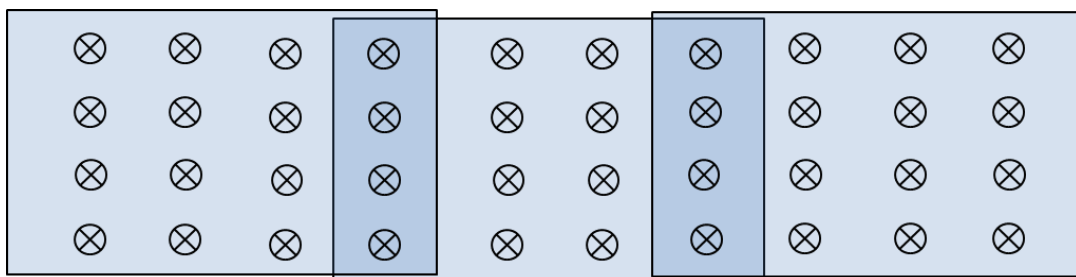


Figure 2.13. Systemization of targets

4) Taking measurement

The distance between two targets was measured to provide scale to the model. The criteria considered in the selection of these two targets was their placement on the same plain and coverage of a distance approximately one third of the length of the whole object (Figure 2.14).

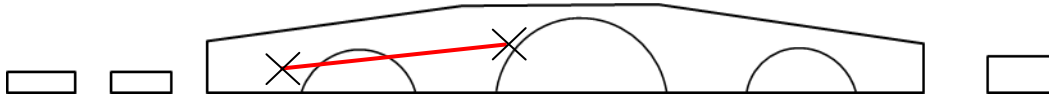


Figure 2.14. Selection of two targets for scaling model

There are some handicaps specific to the field survey of Hypokremnos Viaduct in İçmeler, Urla. The main problem is the disposition of the viaduct in relation with the sea at present. Since the waves splash continuously on the lower surfaces of the viaduct, it was difficult to stick targets here. The surveyors, the camera, and other equipment got wet. It was difficult to shoot on the seaside. Waves gave way to wet and dry surfaces in the facade, therefore, color differences were seen in facades of the viaduct. The brightness problem seen in some of the photographs is related with survey time, which is summer, and lack of clouds.

2.3. Data Processing

Analysis of the photographs taken is the first step of data processing. Different criteria considered in the evaluation of photographs for manual and automatic techniques are pointed out below.

2.3.1. Automatic Photogrammetric Evaluation

Autodesk 123D and Photosynth are software used for automatic evaluation. In all case studies, photos were uploaded to Photosynth and Autodesk 123D; no more

interaction was required. While Autodesk 123D provides both calibration and modeling, Photosynth can just produce point clouds of objects. Meshlab, a free mesh producing software was used for surface construction of point clouds created with Photosynth.

2.3.1.1. Point Cloud Generation

Photosynth can produce just the point clouds of objects. Point cloud is acquired in a few minutes, depending on number of photos. The results are automatically placed at the disposal for the web community. Lastly, point cloud and camera parameters were exported with additional software; Synth Export downloaded from its website. The address on one's synth on the website is copied from browser, pasted in the URL text box of SynthExport. Subsequently, camera parameters and point clouds are exported in ply format (Figure 2.15).



Figure 2.15. Exporting point cloud and camera parameters via SynthExport

For Nysa Library, one photo organization including 105 photos was uploaded. However, Paradiso Aqueduct and Pagos Cistern were studied in a few photo groups due to the limitations in their position and form. The aqueduct was studied with two photo groups including 196 and 202 photos for its each façade, while four photo groups (4x 210 photos) were generated in Pagos Cistern since all parts were not captured in detail

due to their depressed position. Also a different photo group, including surrounding around the cistern, was uploaded to be used for combining these four pieces.

For Hypokremnos Viaduct, one group containing 225 photos was uploaded. However, while exporting, the software automatically divided this photo set in to groups according to their coordinate systems. The point clouds which have the majority of the points (0 and 1) were exported from Photosynth (Figure 2.16).

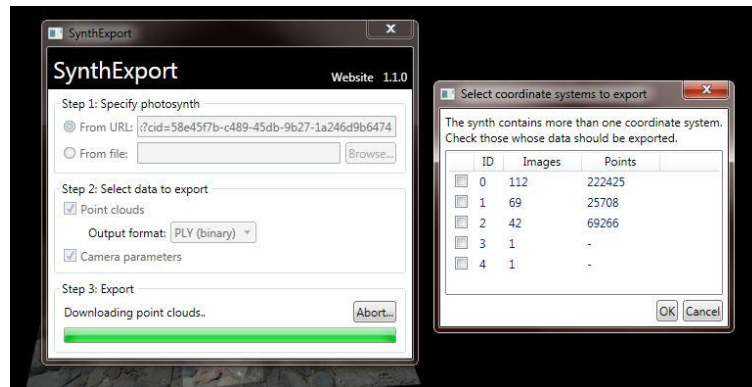


Figure 2.16. Exporting different coordinate system

Autodesk 123D is fully automatic open source software containing both calibration and modeling tools. Also, it has manual calibration opportunity for photos that cannot be calibrated automatically. After appropriate photos were chosen, they were uploaded to Autodesk 123D for automatic calibration, orientation and mesh processing. The model produced can be viewed in wireframe and texture, and only texture formats. Duration processing depended on the number of photos. Unnecessary parts were deleted by selecting rectangular or lasso selection tool. At last, scaling was carried out by defining reference distance.

For Hypokremnos Viaduct, 71 photos were uploaded. However, 9 of them were discarded. These nine photos were calibrated with manual stitching method (Figure 2.17).

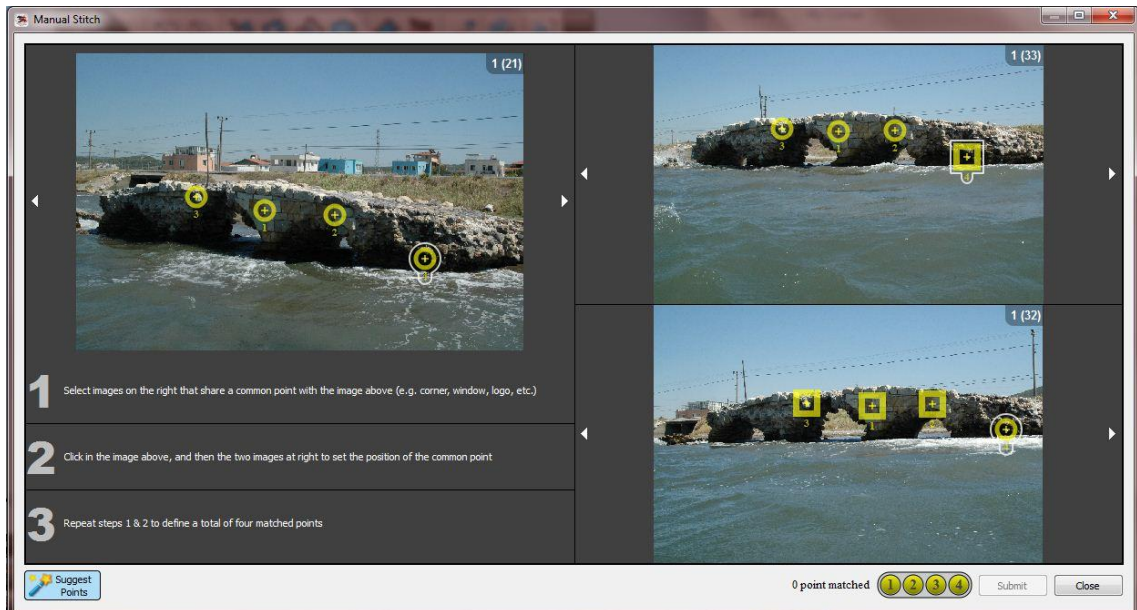


Figure 2.17. Manual stitching in Autodesk 123D

Front facade of Paradiso Aqueduct was just studied with 99 photos, since the software did not accept photos of the rear façade due to the limitations in its position. 50 general photos of Pagos Cistern and 105 general photos of Nysa Library taken from their surroundings were uploaded in Autodesk 123D. The number of photos which were uploaded to Photosynth are more than Autodesk 123D to gain more detailed point clouds. Capacity of Photosynth is higher than Autodesk 123D in respect to uploaded number of photos. However, the models in Autodesk 123D give more satisfactory results with less number of photos (Table 2.1).

Table 2.1. Number of calibrated photos in automatic evaluation

	Nysa Library	Paradiso Aqueduct	Pagos Cistern	Hypokremnos Viaduct
Autodesk 123D	105 photos	99 photos	50 photos	71 photos
Photosynth	105 photos	196+202 photos	210x4 photos	225 photos

2.3.1.2. Modeling

While Autodesk 123D is fully automatic software, point clouds exported from Photosynth have to be modeled. Surface construction of point clouds were carried out in Meshlab. Ball pivoting surface reconstruction filter was preferred for meshing process due to the irregular surfaces of the case studies. By using mesh cleaning and repairing filters, duplicated faces were removed and holes were filled in (Figure 2.18). Then, the mesh model was scaled. First, a distance was measured on the model. The ratio between the real distance and the distance on the model was calculated. This ratio was introduced to Meshlab by choosing the ‘transform: scale’ tool under the heading of filters.



Figure 2.18. Point cloud and mesh construction, Paradiso Aqueduct

Paradiso Aqueduct and Hypokremnos Viaduct, which had two point cloud groups, were tried to be combined in Meshlab. First, each model was scaled, then they were matched with Align Tool by using Point Based Gluing Command (Figure 2.19). However, this application did not give satisfactory results. Pieces were not matched precisely since common points between two pieces were not found due to the ambiguities in the mesh models (Figure 2.19).

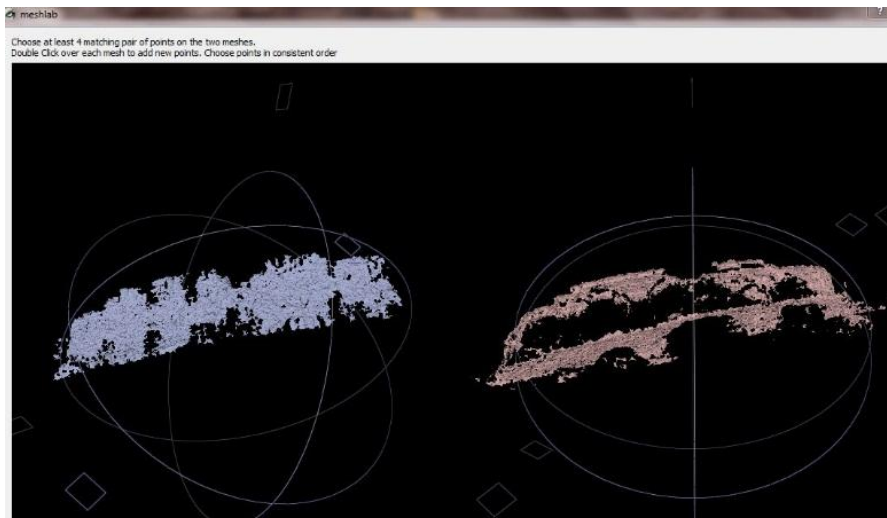
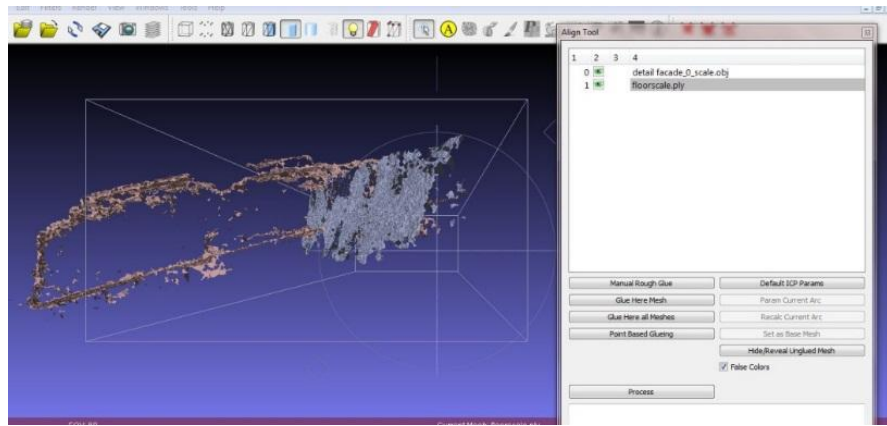


Figure 2.19. Align tool and point based gluing command

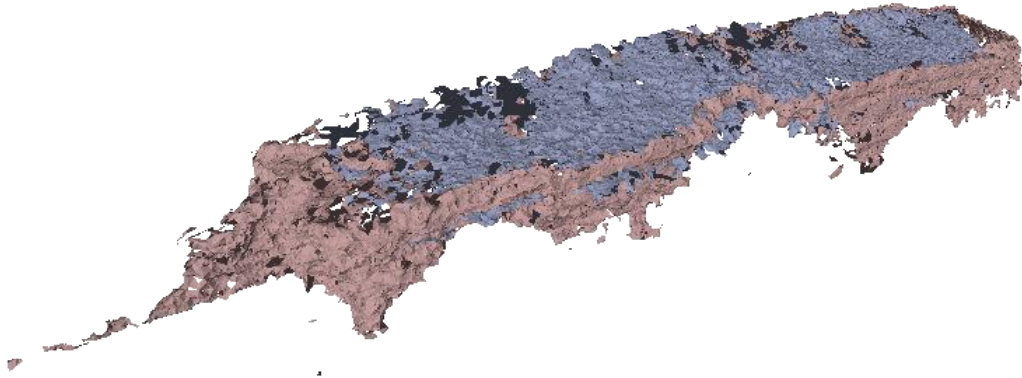


Figure 2.20. Combined pieces, Hypokremnos Viaduct

The model pieces of Pagos Cistern produced by point clouds exported from Photosynth were tried to be combined in SketchUp. A wireframe model was generated with the help of the general point cloud in Autocad. Point clouds were converted to scr format with php parse to use them in Autocad. Base lines were drawn by using the points in Autocad, and then drawing was exported to SketchUp. The pieces whose surfaces construction was completed in Meshlab were also exported to SketchUp. Pieces were combined by using the wireframe model as a base plate in SketchUp (Figure 2.20).

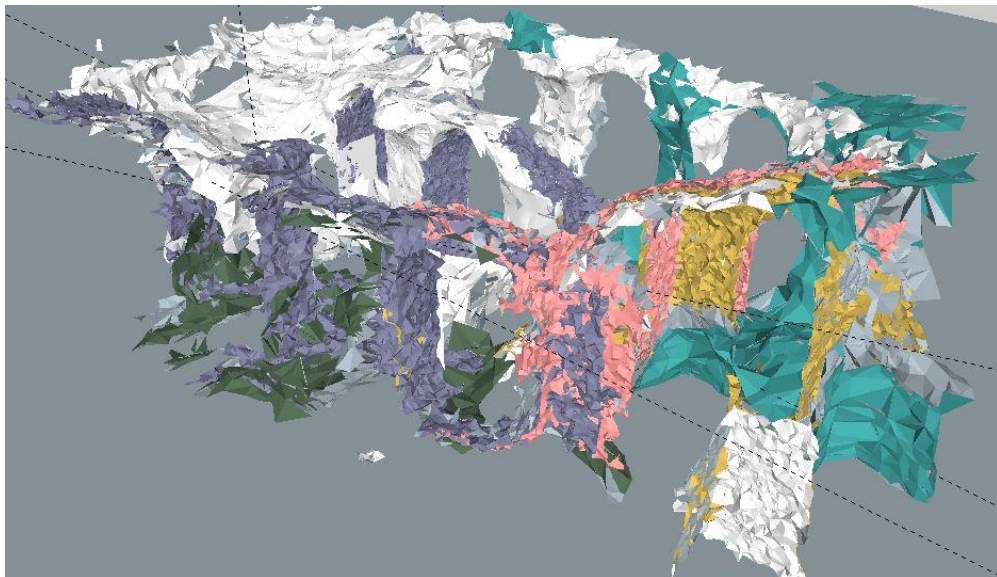


Figure 2.21. Combined mesh model of Pagos Cistern in SketchUp

2.3.2. Manual Photogrammetric Evaluation

The Tgi3D, which includes evaluation, modeling, and texturing tools in a single software package, was used for manual photogrammetric evaluation. After calibration was carried out in Tgi3D, surface reconstruction and texturing processes were completed in Tgi3D which is a plug-in for SketchUp 8 that contains 3D Image-Based Surface Modeler Tool. Modeling can be made in SketchUp 8 with the data exported from Tgi3D Calibration tool.

2.3.2.1. Point Cloud Generation

Image selection, calibration, and scaling were undertaken.

- Image Selection

The photographs of the ancient Viaduct were analyzed. Minimum number of photographs with good photographic quality and best covering the object were selected. This selection was made intuitively and if there were problems observed during the evaluation, the photo set was revised. Nine revisions were made for the documentation of the ancient Viaduct in İçmeler, Urla, İzmir.

However, one more revision was required due to the problems observed at the end of the modeling phase (Figure 2.22). This revision gave way to the repetition of all of the evaluation process which will be discussed below. So, image selection was carried out twice; first with intuition and then with an eye on solving the problems of the 3D model. With this last image set created, number of revisions reached ten.



Figure 2.22. Problematic photos

In the viaduct floor, thirty four images taken from 2.25 meters with a ladder were used. In the short sides of the wall, all of the images taken were used to overcome the problems in the corners. Total number of photos in the short sides is fourteen. The corners were important because they defined the alignment of the long sides of the structure. Any imperfection in their definition gave way to wide angles resulting in wrong alignment of long sides. In the long sides of the wall, thirty four images shot from 5.5 meters taken without a ladder were used. In the edges of the viaduct floor and the wall, seventeen images taken from approximately 100 meters with ladder were preferred. Facades of the arches were taken from 2.25 meter without ladder. Shooting distance of inner side of barrels changed depending on size of the arches. Photos of arch 1 and arch 2 were taken from 100 meters, while arch 3 was taken from approximately 1.90 meters. Sixty images taken without ladder were preferred (Table 2.2).

Table 2.2. Distribution of photos

Viaduct Element	Shooting Distance and Level	No of Photos in the first phase	No of Additional Photos in the final phase
Viaduct floor (max 349 cm)	2.25 meter, with ladder	34 photos	+ 31photos
Short sides of the wall (northeastern facade: 349 cm, southwestern facade: 340 cm)	2.25 meters, without ladder 2.25 meters, with ladder 5.50 meters, without ladder	9 photos 2 photos 3 photos	
Long sides of the wall (northwestern façade: 1431 cm, southeastern façade: 1622 cm)	5.50 meter, without ladder	34 photos, 18 of them at the southern side, 16 of them at the northern side	
Edge of the viaduct floor and the wall	approximately 100 meters, with ladder	17 photos	
Arches Arch1: (189 cm, Arch 2: 197 cm, Arch 3: 395 cm; All ring stones of Arch 3 are missing, so this is not the original size)	For facades of arches: 2.25 meters, without ladder For barrels: Arch 1 and Arch 2; 1.00 meters, Arch 3; 1.90 meters by kneeling down	60 photos, 16 of them for the large arch, 28 of them for the medium one, 16 of them for the small one	
Plan of Ruins (52 cm)	2.25 meters, with ladder	10 photos	
Sides of the ruins (16x280 cm)	2.25 meters, without ladder 5.50 meters, without ladder	8 photos 1 photos	
Total		178 photos	

After selecting the appropriate image sets, the succeeding steps were calibration of the photos and scaling of the point cloud respectively.

- Calibration

The above described image set was loaded to the software, Tgi3D SU PhotoScan Camera Calibration tool V 1.27. Calibration process started with the two images belonging to the east corner of the southern façade. Eight control points were used for calibration. Maximum point error for each point was accepted as smaller than 3.23 pixels (Figure 2.23).

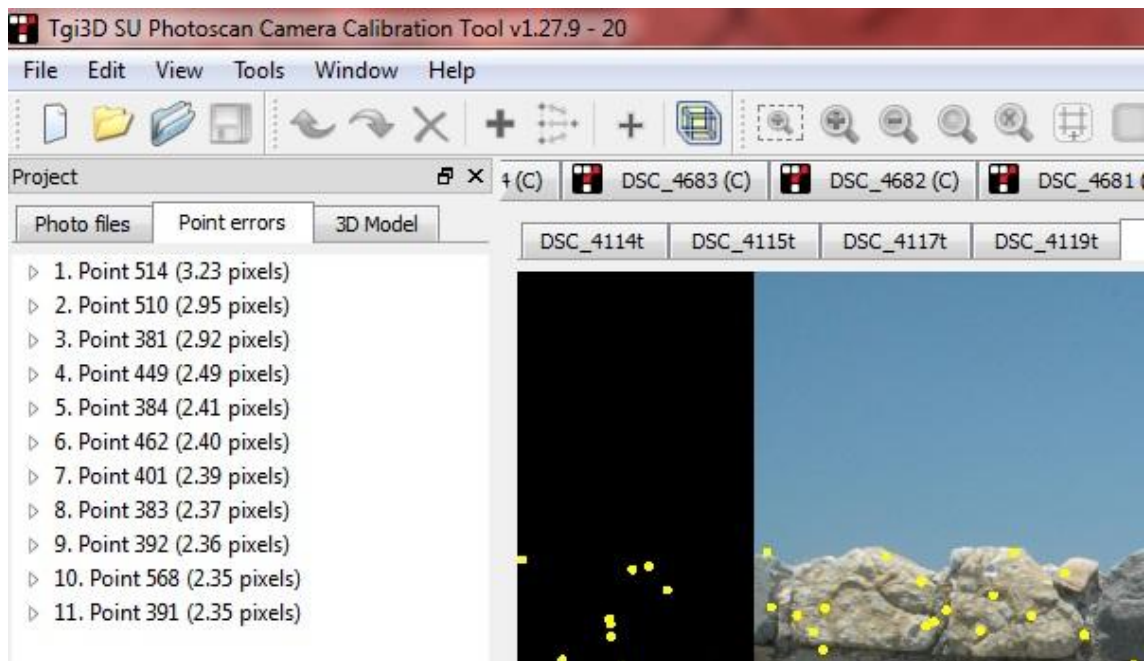


Figure 2.23. Point errors

Then, the other images were calibrated one by one and added to the system. Only three control points were considered sufficient throughout the long sides. Nevertheless, at the corners and at the short sides, four or five control points were used to strengthen the bonding within the system. With the automatic addition of further control points by the software, approximate number of control points per photo on a long side reached six and eight on a short side (Figure 2.24). First, 179 photos were calibrated. Then, thirty one photos of the floor were added to solve problematic parts on the floor of the viaduct.

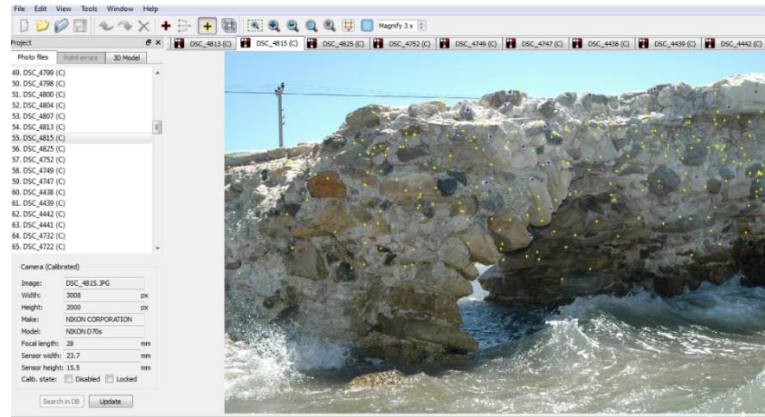


Figure 2.24. Automatic addition of control points

- Scaling

Only one measurement can be entered to the system for providing scale to the model (Tgi3D 2010).

The measurement used was 6.165 meters taken from the southern façade of the wall. This measurement was taken parallel to the façade and it covered nearly one third of the facade.

In turn, the calibration process was completed and the data consisting of the point cloud and images were exported to SketchUp 8 for modeling (Figure 2.25).

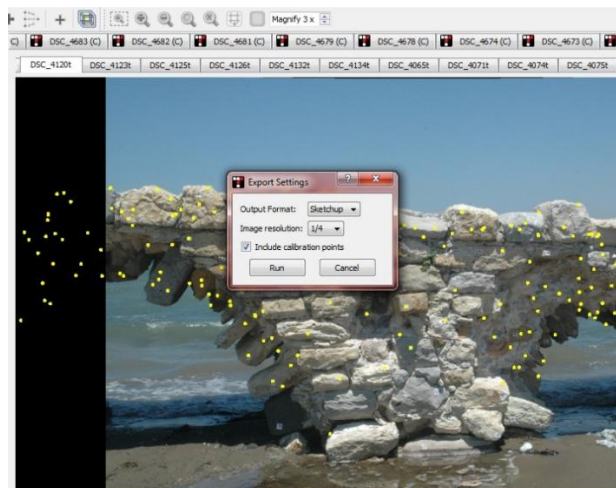


Figure 2.25. Export settings

- Image-Based Surface Modeler toolbar was turned on. After the surface was selected with the up sample mesh command (Figure 2.28) resolution was increased.



Figure 2.28. Upsample mesh and Tgi3D image-based surface modeler toolbar

- With the Multi Segment Surface command (Figure 2.29), the depth differences in 3D face were created. First, twenty iterations, and then the precision 200 iterations were made to increase the roughness effect (Figure 2.30).



Figure 2.29. Multi segment surface command and Tgi3D image-based surface modeler

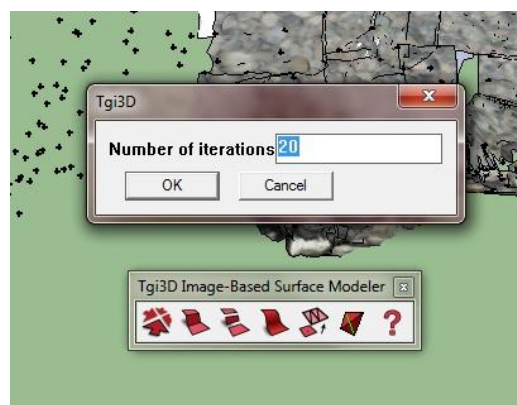


Figure 2.30. Determining number of iterations

- If enough detail is not obtained, number of iterations and resolution can be increased.
- After going back to the first image without tilt, the photo was adopted to the surface with the project photo command in the toolbar activated with right mouse click.
- This textured mesh was made component of the model with the right mouse click (Figure 2.31).

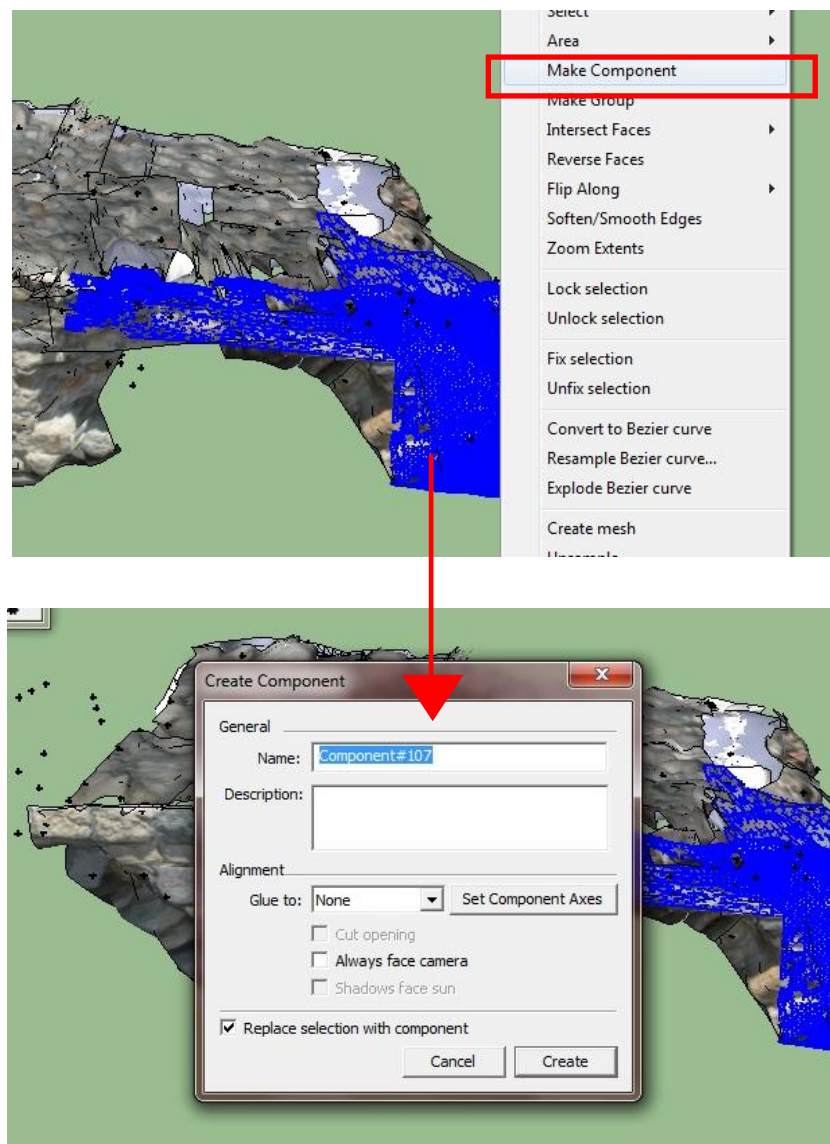


Figure 2.31. Making component

- Then, the neighboring overlapping photo groups were worked on, respectively.

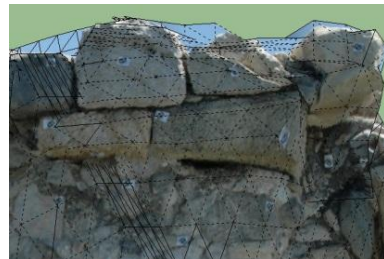
After the long southern façade of the viaduct wall was completed, its two short facades, the long northern facade, viaduct floor, and arches were modeled sequentially.

After finishing the model of every element separately, the parts were combined with each other, however, some problems were observed. These problems are listed in the below:

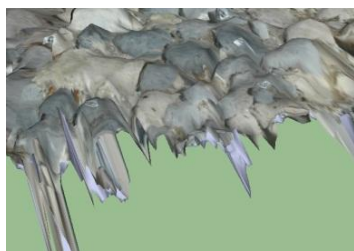
1. Tilt problem: It was seen in the photos which are not taken with the camera lens parallel to the viaduct floor and in the photos of extensively ruined parts of the short sides of the wall (Figure 2.32).
2. Problem of inclusion of sky, water, and ground: It was seen in the borders of the components since sky, ground or water can be adopted to the surface automatically (Figure 2.32).
3. Drooping problem: It was seen generally at the edges of the components (Figure 2.32).
4. Color difference problem: The reasons of the problem are brightness differences between the photos due to the survey time and waves giving way to wet and dry surfaces in the facades (Figure 2.32).



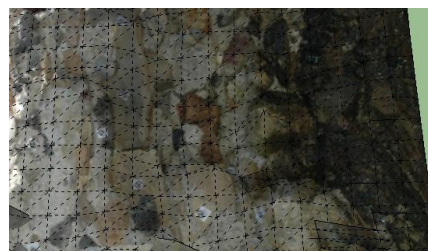
Tilt



Inclusion of Sky



Drooping



Color Difference

Figure 2.32. Problems

The solution developed for the tilt problem was returning to Tgi3D Calibration Tool and adding new photos which were not tilted instead of problematic ones. First, necessary photos were selected, added to former calibration folder of first image set, calibrated, and exported to SketchUp 8. So, calibration and modeling phases were carried out twice; first, with intuitional image set, and then, with expanded image set created to solve the problems of the model. With this last image set, number of revisions reached ten. The problem of color difference can be solved by taking new photos in better conditions and recalibrating these photos; similar to the solution for the tilt problem.

The other two problems have simpler solutions. They were observed generally on the edges of the components. So, this problem had to be solved before combining components. Therefore, parts including sky, water, and ground were deleted with the help of the Eraser command (Figure 2.33). The drooping problem can be solved by pushing and pulling with Tgi3D Su Move Command.



Figure 2.33. Tgi3D toolbar

The drooping parts were repaired by pushing and pulling with Tgi3D Su Move Command (Figure 2.34).



Figure 2.34. Tgi3D Su Move command and Tgi3D toolbar

Then, in the connection zones, meshes connecting components were drawn manually with Create Mesh Command in the toolbar with right mouse click. These meshes were adopted to the appropriate surfaces with Project Photo command in the same toolbar.

The total number of calibrated photos used in this study was 178 in the first phase, and then, it reached 210 in the second phase. This is a high number compared to the so far recorded case studies evaluated with Tgi3D Su (Tgi3D 2010).

In turn, to provide ease in the management of the photographs, 3 groups were modeled one by one and brought together by the help of the origin point and paste in place command (Figure 2.35).

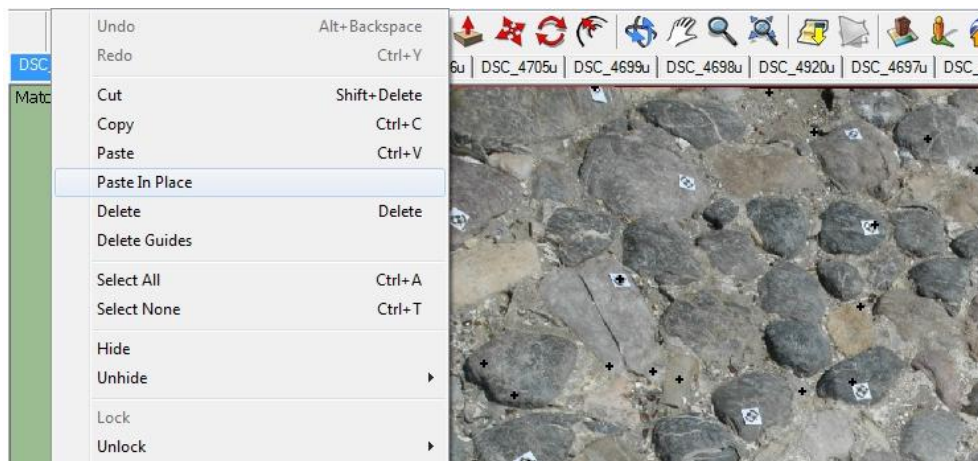


Figure 2.35. Paste in place command

CHAPTER 3

CHARACTERISTICS OF THE CASE STUDIES

In this chapter, historical backgrounds, and site, morphologic and structural characteristics of the case studies are presented. There are four case studies; Hypokremnos (İçmeler) Viaduct, Pagos (Kadifekale) Cistern, Paradiso (Şirinyer) Aqueduct and Nysa (Sultanhisar) Library.

3.1. Hypokremnos (*İçmeler*) Viaduct

Urla, which is a historical settlement on the west of the metropolitan city of Izmir, is an important transition point between Karaburun-Çeşme Peninsula and the mainland of Anatolia (Figure 3.1). İçmeler is about seven km at the west of Urla, and on the southern coast of Gulbahçe. The name comes from a thermal water spring which is today on the skirts of the mountains by the seaside. The hostel by the thermal spring on the coast has been abandoned today. There are a number of inconsiderate buildings and summer houses on the coastline. The case study is a viaduct on the coastline, İçmeler. It is thought to have been constructed in Roman Period as revealed in the history of its vicinity and in its morphologic features. Hypokremnos, meaning the narrowest part of the Peninsula, is the name revealed in the historical sources for the Roman settlement (30 B.C.-300 A.D.) which was present in this region (Foss, et al. 1994)



Figure 3.1. Hypokremnos Viaduct

3.1.1. Historical Background

Hypokremnos was located on the boundary of the Ionian cities Erythrai and Klazomenai (Meriç, et al. 2012) (Figure 3.2). Northern borders of Klazomenai finished with Hypokremnos, while Klazomenai reached to Sığacık Bay on the southern side (Meriç, et al. 2012). On the south of the Hypokremnos, Khersonessos isthmus was situated. Strabo (Strabo 7 BC) mentioned that Erythrai settled on Khersonessos isthmus. South of it was Khalkideis settlement which belonged to Teos, while northern side was Klazomenai settlement known as Hypokremnos. The north of Khalkideis settlement was known as a holy place where Alexander the Great's games were carried out. Briefly, in ancient period, Hypokremnos was located between three Ion Cities; Teos, Klazomenai and Erythrai. There was an ancient road between Klazomenai, Hypokremnos and Erythrai (Bakır and Anlağan 1980).



Figure 3.2. Ancient settlements

Surface investigations have revealed the existence of Archaic, Classic and Roman civilizations in Hypokremnos and its surroundings (Ersoy and Koparal 2008), (Figure 3.3).

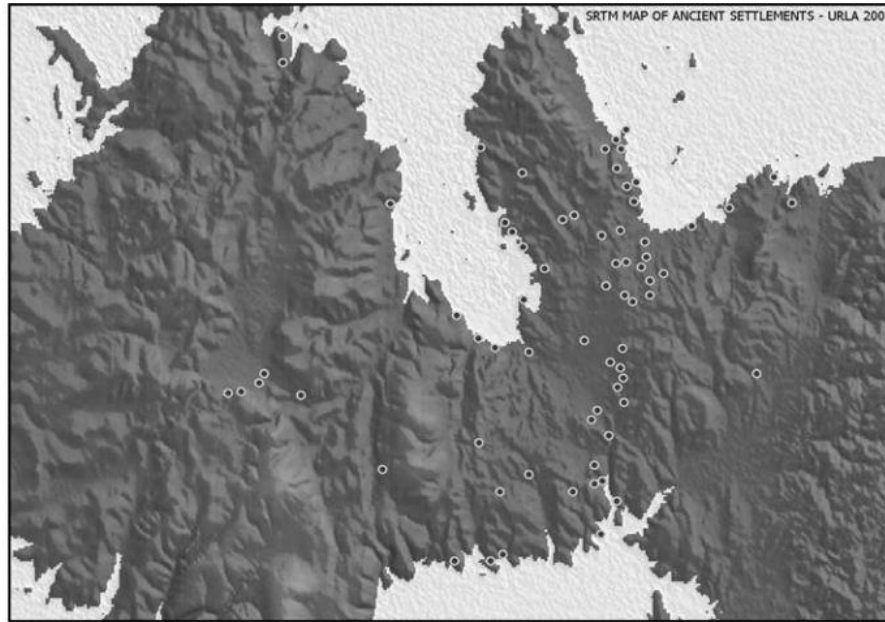


Figure 3.3. Ancient settlements in Urla Region
(Source: Ersoy and Koparal 2008)

The prehistoric Limantepe is located in İskele District of Urla on a mount at the coast of Urla opposite Karantina Island. The city dates from 6000 BC (Neolithic Period) to the end of 2000 BC. It was known for trade of wine and precious metals from its harbor (Erkanal 1997).

Its successor, Klazomenai is one of the twelve Ionian cities which were established between 1050 and 1000 BC. It had overseas commercial relations and known as a production center of olive oil and ceramics (Cadoux 1938). When the city was conquered by the Persians in 499-494 BC, the public moved to the Karantina Island across the harbor (Ersoy 2011). In 404 BC, the mainland was started to be settled again in order to control agricultural areas and sea. In Alexander the Great Period (336 BC-323 BC), a bridge between the island and the mainland was built (Atay 2003). Also, Alexander the Great had an idea to convert the Urla Peninsula to an island with a channel. The most appropriate position for this channel is the valley starting from İçmeler Coast and continuing to the south (Meriç, et al. 2012). This valley was also used for games organized by Alexander the Great (Strabo 7 BC). It is recorded that the valley has been settled since the Prehistoric period, but it became a sanctuary starting with the 6th century BC, as understood from the remains documented eight kilometers at the south of Gülbahçe (Meriç, et al. 2012).

The island was occupied until 4th and 5th century BC. In the 2nd century BC, Urla district was conquered by the Romans (Mater 1982) (Figure 3.4). Hypokremnos was established at the west of Klazomenai in Roman period according to Barrington Atlas (Foss, et al. 1994) (Figure 3.5). The region became a center of episcopacy after Roman Emperor Constantine I accepted Christianity as the state religion. It had continued to be an episcopacy center until the end of the Byzantine Empire (1453) (Milioris 2002). The major church of this period was to the west of Ionian Klazomenai, which is known today as Gülbahçe village (Tok 1997).

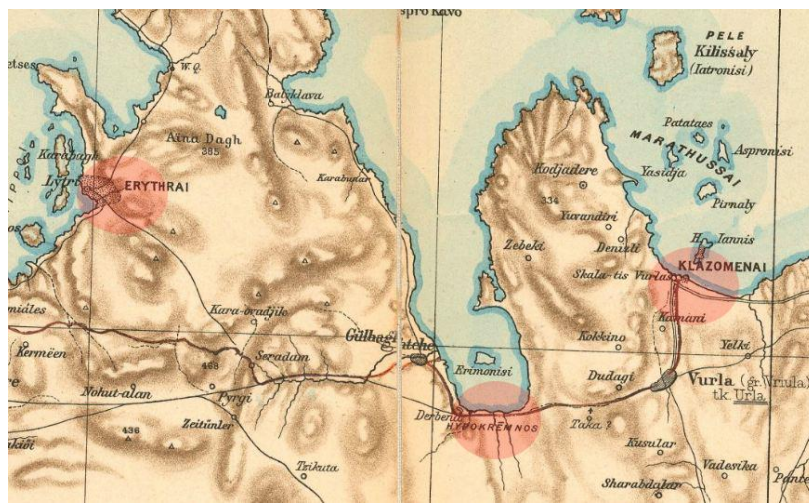


Figure 3.4. Location of Hypokremnos
(Source: Kiepert 1890)

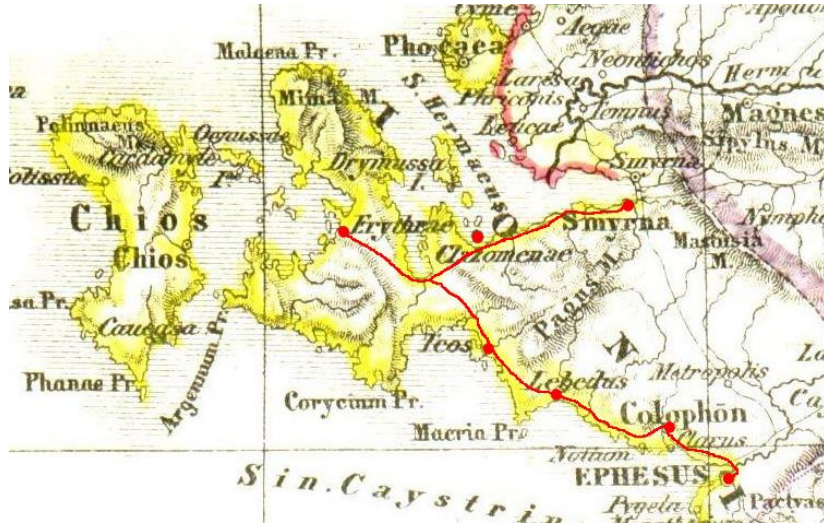


Figure 3.5. Ionia in Roman Period
(Source: Kiepert 1869)

Çaka Bey, who was the commander as as a sailor in Seljuk period, captured Urla in 1080s. Short after, Byzantine Empire took it back again (Atay 2003). At that time, Urla was on the trade way between Chios and Anatolia. It was a control point, so important economic developments took place here. In Emirates Period, Urla was conquered by Aydın Principality in 1330s (Şengün 2007). During the Aydın Principality, coast of Urla was attacked by Venetian and Genoese soldiers (Atay 2003). Agriculture was the main economic activity in the inner zones of Urla in the 15th century. Urla was a district of Aydın City, together with Karaburun, Çeşme, Seferihisar and Izmir (Baykara 1974). In this period, Urla had still been a transfer center between Chios and Anatolia, so it kept on developing. It was also important with its agricultural production; especially Malkoç (İçmeler) came first in olive oil production. Urla was named as Nefs-i Bazaar or Nefs-i Urla due to its leading character in the commercial life of the region (Atay 2003). A population increase was recorded for Urla region in the 16th century. There was a caravan road connecting Çeşme to Cumaovası and Menemen passing through Urla. Remains of this caravan road can be observed in Çeşme, Barbaros, Icmeler and near Çamlıköy (Figure 3.6). Baykara (1976) claims that the central viaduct of Hypokremnos which is studied in this research was part of this Ottoman caravan route leading to Menemen at the north and Cumaovası at the south. However, the glorious times of Urla finished around 1630 s with the increase in the

extent of trade in Izmir. In 17th and 18th centuries, Urla diminished in size and became a rural settlement (Atay 2003).

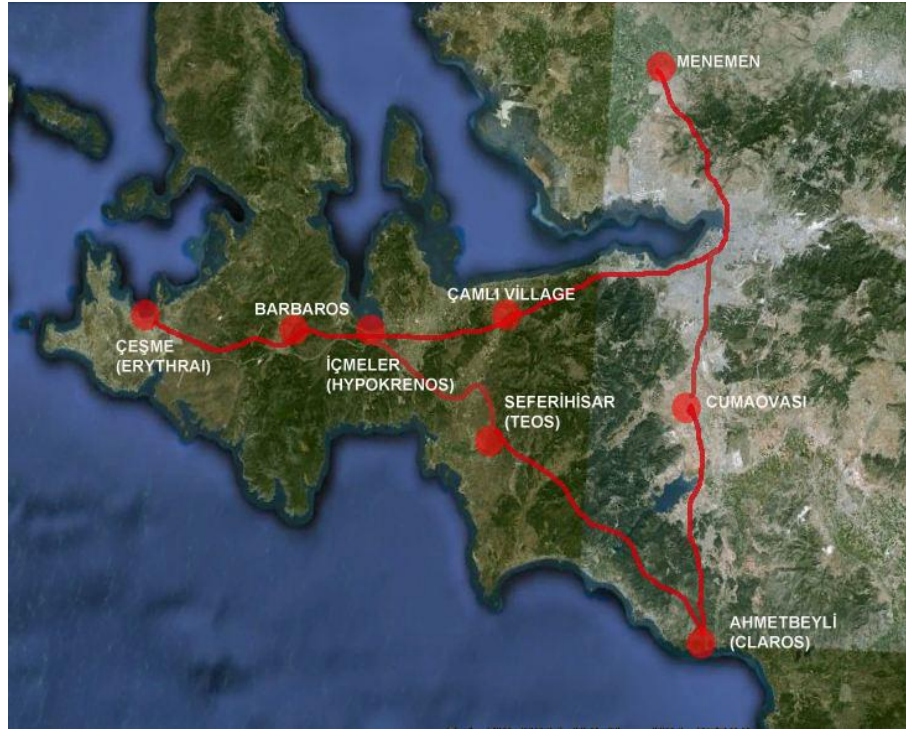


Figure 3.6. The historical caravan route in Ottoman Period

In western Anatolia, Roman roads and Turkish caravan roads either overlap or run nearby one another. The caravan roads passed through the bazaars which people address their needs. All roads followed the most appropriate route from one center to another center (Yapucu Pullukçuoğlu and Özgün 2011). The road passing through Hypokremnos presents the main features of caravan roads in Western Anatolia. In ancient period, it was connecting Erythrai, Hypokremnos and Klazomenai, while in Ottoman period it was a part of the historical caravan way between Chios and Anatolia.

3.1.2. Site Characteristics

The studied viaduct is a part of a series of viaducts crossing the brooks running in south-north direction in Hypokremnos Plateau. Today, Hypokremnos Viaducts are

located on the İçmeler coast which is on the south of the Gülbahçe Gulf. The location of the viaducts indicates that the coastline was further to the northern side in the past. There are four brooks reaching to the Gülbahçe Gulf. One of them is ‘Karapınar Brook’ with two sub-brooks; Tatar Brook and Kapıkaya Brook (Figure 3.7). Tatar Brook runs through the old Söğüt village which was named as Khersonessos isthmus in ancient sources (Figure 3.8).

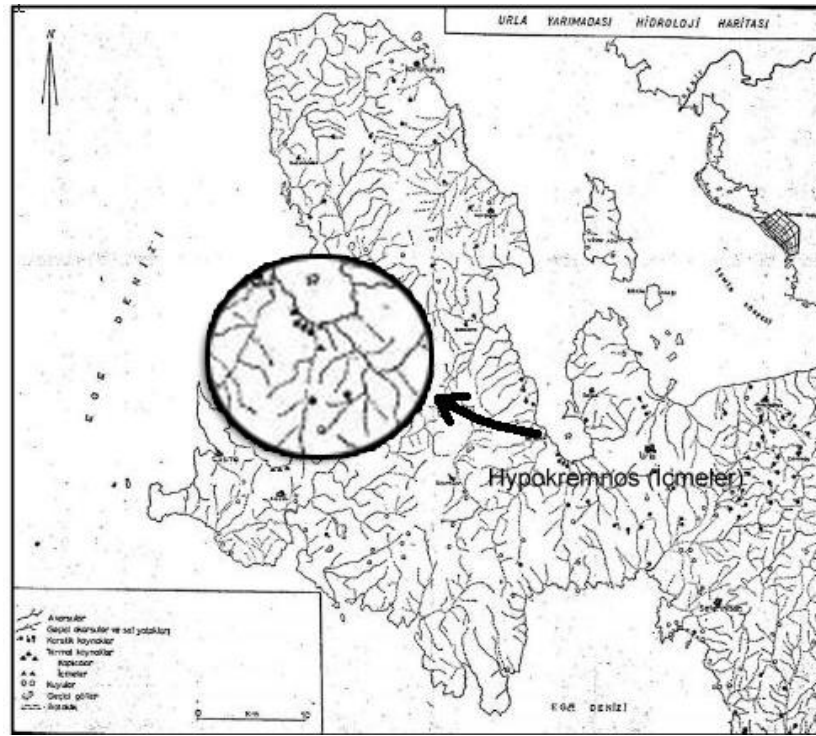


Figure 3.7. Water sources in Çeşme, Karaburun and Urla regions (Source: Mater 1982)



Figure 3.8. Tatar Brook and Hypokremnos (İçmeler)
(Revised from Meriç, et al. 2012)

The double lane traffic way connecting Çeşme to İzmir dates to 1960s. Hypokremnos viaducts are between the seaside and this traffic way and parallel to them. When going to the western direction from the Karapınar Brook through the coastline; three remains of viaducts and remains of a roadway are observed. Today, the brooks run nearby these viaduct remains. This shows that these viaducts were constructed to cross these brooks, of whose routes changed slightly in time (Figure 3.9).



Figure 3.9. Location of the Hypokremnos Viaducts

In this study, the viaduct at the center (number 2 in Figure 3.9) was studied. This middle viaduct is the best preserved among the three. The studied viaduct's northeastern side, which is facing the sea today (the downstream side) is partially under water, while southern side facing the coast (the upstream side) can be easily observed.

The case study is a masonry structure with linear form. The semicircular arches piercing the wall of the viaduct are in different widths; one large in the middle of the viaduct (389 cm, ring stones are missing, so it is not the original span), one medium on the west side (200 cm), and one narrow on the east side (193 cm). The viaduct facades are finished with a cornice on both sides. The wall is crowned with a road way making a crest at its center. The inclination on both sides of the road is around 7%.

3.1.3. Construction Technique

Structural characteristics of Hypokremnos Viaduct were discussed with the data gathered from manual photogrammetric evaluation software, Tgi3D, since the model provided detailed data regarding the structural system (see Appendix B and Appendix C). The model gathered by automatic techniques was not used since they are raw data in comparison to those coming from manual technique.

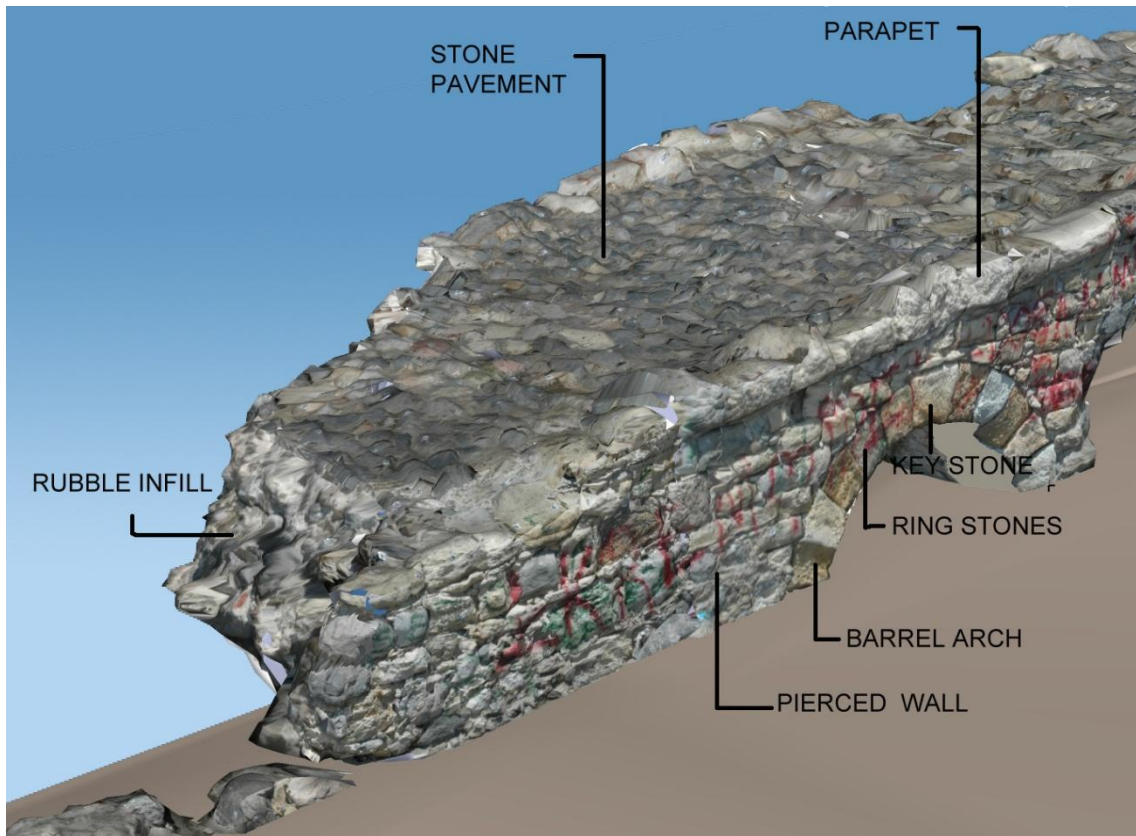


Figure 3.10. Model of structural elements

The Viaduct consists of five structural elements and two architectural elements. The structural elements are pierced wall, three barrel arches and foundation; stone pavements and parapet are the architectural elements (Figure 3.10). In this section, these structural and architectural elements and their materials are analyzed in detail (Table 3.1) (See Appendix B).

Table 3.1. Construction technique and material usage of structural and architectural elements

Element	Element Type	Construction Technique and Material Usage	Recommendation
Pierced wall	Structural element	Dressed stone: rubble laid (<i>opus caementicium</i>) in horizontal beds out of hydraulic lime mortar (app. 25 cm) with a facing of cut stone blocks (app.25 cm) (totally app. 50 cm)	
Barrel Arch 1	Structural element	Semicircular arch, dressed stone (189 cm in width)	
Barrel Arch 2	Structural element	Semicircular arch, dressed stone (197 cm in width)	
Barrel Arch 3	Structural element	Semicircular arch, dressed stone (397 cm in width, all ring stones of Arch 3 are missing, so this is not the original size)	
Foundation	Structural element	Unobserved.	Sampling type excavation necessary.
Pavement (Floor Covering)	Architectural element	Floor covering: Rubble stone and lime mortar (various dimensions, 14x17x12, 11x12x10, etc.)	
Parapet	Architectural element	Cut stone blocks in horizontal lines (various dimensions, 48x52x 25, 37x52x25, etc.)	

Pierced wall: The pierced wall is out of rubble stones laid in horizontal beds in hydraulic lime mortar, *opus caementicium*, with cut stone dressing system on its two sides. The mortar sample taken from Hypokremnos Viaduct showed similar features with mortar used in Roman monuments in terms of raw material composition, basic physical, chemical, mineralogical and hydraulic properties, and pozzolanic activities of aggregates. (See Appendix A). The case study's photos were taken for the model in summer, 2012. At that time, dressing stones were just observed on the southwestern side of the viaduct. However, as a result of the tides of the sea in winter, all double layered dressing stones became visible on the two sides of the viaduct (Figure 3.11).

Dressing stones are composed of two parallel lines of cut stone blocks (approximately 39x25x15) with infill of smaller rubble stones (approximately 10x6x5 cm) (Figure 3.12). While thickness of the wall is approximately 349 cm, double layered dressing system is about 50 cm in width at both facades and rubble in fill in between this system is approximately 249 cm in width.



Figure 3.11. Dressing system of the facades



Figure 3.12. Double layered facing stones of the viaduct

Rectangular cut stone blocks are lined up horizontally in the dressings. However, dressings of the north eastern (sea side) and south western (coast side) façades show different characteristics (Figure 3.13). On the north eastern façade (sea side), larger cut stone blocks are lined up regularly. Between the cut stones, mortar is not observed. Cut stones on the top level of the spandrel wall are curvilinear so as to form the sloping top edge of the viaduct. On the other hand, the south western (coast side) façade is finished with smaller cut stones (15x36, 15x46, 15x56), and between these stones, rubble and lime mortar are observed. To provide the slope of the viaduct, instead of cut stones with curvilinear top edges, small rubble stones (12-25cm) were used. Most parts of the piers are below the ground level. Piers are out of dressed stone.



Upstream (Southwestern) Façade



Downstream (Northeastern) Facade

Figure 3.13. Model of the facing stones

Barrel Arches: Openings are spanned with one centered semicircular arches. There are three arches in different widths (395 cm, 197cm, and 189 cm); however, most of the ring stones and keystones are damaged. Components are observed only in the smallest arch. This arch's keystone and ring stones are out of cut stone blocks (Figure 3.14). The keystone (trapezium form; upper part: 46, bottom part 33, 30, 38) is distinctive and it is larger than the ring stones. Barrels are out of rubble stones positioned in a radial manner.



Figure 3.14. Semicircular arch and keystone in the smallest arch

Stone Pavement: Floor covering is out of rubble stones bonded to spandrel wall's rubble fill with lime mortar (various dimensions, 14x17x12 cm, 11x12x10 cm, etc.), (Figure 3.15).



Figure 3.15. Model of rubble stone pavements

Parapet: Parapet is out of cut stone blocks approximately in the same size lined up above the spandrel wall. Unlike the cut stones of spandrel walls, these cut stone blocks present similar sizes on both facades (various dimensions, 48x52x25 cm, 37x52x25 cm, etc.), (Figure 3.16).



Figure 3.16. Parapet walls

3.2. Pagos Cistern

The ancient Roman Cisterns were fresh water reservoirs commonly set up at the termini of aqueducts and their branch lines, supplying water to urban households, palaces, thermae, etc. The cistern of Philoxenos, Istanbul (5th century), the Theodosius Cistern, Istanbul (5th century) and the Basilica Cistern, Istanbul (6th century) are some famous examples (Wikipedia 2013).

Pagos Cistern (Figure 3.17) and the aqueducts on the Meles River, known as Paradiso Aqueduct and Vezirsuyu Aqueduct, were part of the water installation system providing water to ancient Symrna (İzmir) (Figure 3.18).



Figure 3.17. Pagos Cistern



Figure 3.18. Location of Pagos Cistern and aqueducts

Pagos Cistern, located on Mount Pagos in Izmir, is dated to Byzantine Period. Byzantine Emperor Ioannes III Vatatzes provided funds for its construction in the 13th century (Ersoy 2012). Mount Pagos is located two km far from the eastern coast of the

center of Izmir; Konak. The Cistern was constructed in the castle of Mount Pagos to provide water to the city as an underground chamber (Toksöz 1960).

3.2.1. Historical Background

The new Smyrna (Pagos) was established in 330 BC after Alexander the Great had a dream on Mouth Pagos (Bean 1995). The remains in the citadel belong to Hellenistic, Roman, Byzantine and Turkish Periods. In the Roman Period, the city was the most beautiful of all Ionian cities (Toksöz 1960).

The old city of Symrna was founded 5000 years ago in Tepekule, Bayraklı. Establishment of the new Symrna in ‘Pagos’ was relied on a dream by Pausanias. According to what they write, one day, Alexander the Great fell asleep under a tree by the Temple of Nemesis after hunting at one of the hills of Kadifekale. In his dream, Nemesis came and asked him to build a new city on that site for the people of old Symrna. An oracle interpreted his dream; “People who are to live on the hill of Pagos across the stream of Meles will be three and four times happier than they used to be.” After that, the new Symrna was built on the hill of Kadifekale and its foot in 330 BC (Toksöz 1960).

Strabo states that; some parts of the city were located on Pagos Mountain, but most parts were on the plain between the Mountain and the harbor. Meles River was running by the city wall on the other side (Strabo 7 BC).

After the death of Alexander the Great, Seleucids took the city under their rule. When Pergamon Kingdom started to gain strength in the 3th century BC, Izmir became part of its land together with the other surrounding cities. Izmir had been one of the cities in Pergomon Kingdom until it began to be controlled by the Roman Empire in 133 BC (Baykara 1974).

In Augustus Period, (28 BC- 14AD) Izmir had its most peaceful years. After a damaging earthquake in 178 AD, the city was built more beautiful than its previous state. Between the 395-1081, Byzantine Empire controlled the city.

In the 13th century, when Ioannes III Vatatzes became the Byzantine emperor, Nymphaion (Kemalpaşa) near Smyrna became the administrative center of the Byzantine state. Smyrna became the most important trade and military port and

shipyard. Vatatzes reinforced and repaired the castle walls of Pagos. Pagos Cistern opposite the main entrance of the city was built in the time of Vatatzes in 1225. The cistern had the capability to meet the daily water need of 7000 people. It was understood that rehabilitation of Pagos, where an important part of population of Smyrna lived, was planned in terms of both military and civil needs (Ersoy 2012).

In Seljukid Period, Izmir was conquered by Çaka Bey and Çakır Bey in 1084 (Toksöz 1960). The main Turkish period of Izmir started with the conqurence of Kadifekale by Aydın Emirate in 1317. In 1329, Umur Bey captured the rest of the city (Baykara 1974).

Aydın Emirate had gradually weakened in the second half of the 14th century. In 1389, Ottoman Sultan Yıldırım Beyazıt became the ruler of the city. He could not get control of Port Fortress, but controlled the Turkish settlement at Kadifekale. In these years, the city became the most important port of Western Anatolia (Ersoy 2012). Although it is not mentioned in the sources, the cistern should have continued to be used in the Turkish era.

3.2.2. Site Characteristics

On the south east of the Pagos Mountain, Meles River runs, while Izmir Gulf is located on the northwest. Only the northwestern and southern parts of the ancient castle walls are observed at present. There were three large entrances; at the west, north and east (Toksöz 1960). The Pagos Cistern is located opposite the western entrance (Figure 3.19).



Figure 3.19. Location of Pagos Cistern

The Pagos Cistern is an underground chamber approximately 35.79 meters by 25 meters (about 875 square meters) and 5.20 meters in height at present (Weber 1889) (Figure 3.20).

The crossed-shaped vaults resting on round arches, composing its ceilings, are extensively damaged. They are supported by a forest of 35 stone piers (approximately 2.00 x 2.00 m), whose of 20 are independent at present, and each 3.30 meters high, arranged in six rows, each spaced 4.00 meters a part.

Five stone steps descend down the entrance of the cistern. The cistern is surrounded by a wall with a thickness of approximately 2.5 meters coated with waterproofing mortar.

The cistern's water was carried by Paradiso Aqueduct, which is 2.3 kilometers away and Karapınar Aqueduct, which is 0.65 kilometers north of the cistern. It is empty today with only debris lining the bottom.

As stated in the excavation reports, the ground of the cistern is finished with brick-lime plaster and also the rubble stone walls are covered with two layered brick-lime plaster. A pipe directing usage water to the city is recorded on the southern wall (Ersoy 2012).

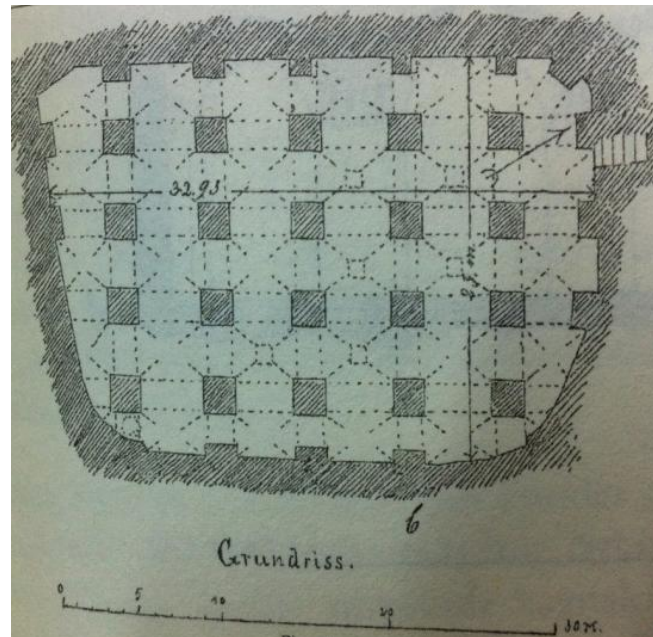


Figure 3.20. Plan of Pagos Cistern
(Source: Weber 1889)

3.2.3. Construction Technique

Structural characteristics of Pagos Cistern were discussed with the data gathered from automatic photogrammetric evaluation software, Autodesk 123D, since the model obtained via Photosynth could not produce useful data to evaluate structural characteristics.

Pagos Cistern is approximately 35 meter by 25 meter in dimension as mentioned in the morphologic characteristics. However, only the part whose superstructure was missing (21x12 m) was photographed and modeled. (Figure 3.21).

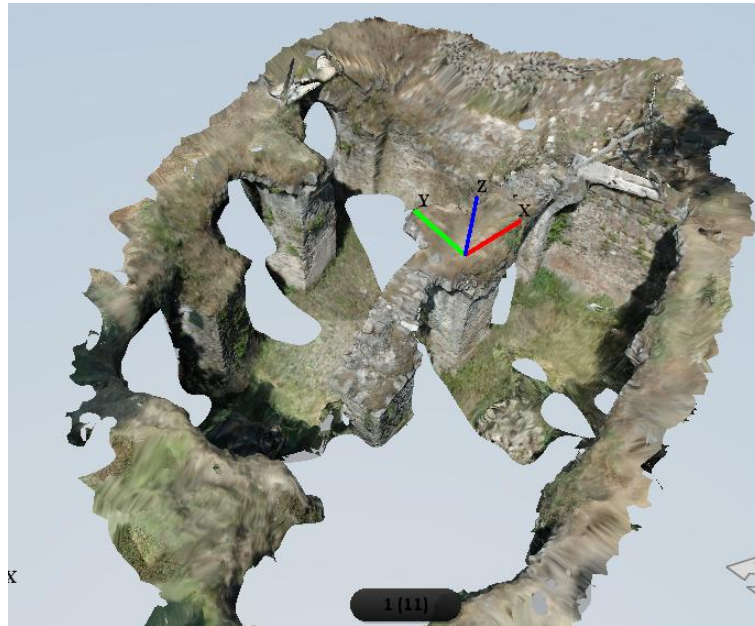


Figure 3.21. Model of partial part of Pagos Cistern

Pagos Cistern consisted of four structural elements: Piers, walls, arches and vaults. In the model, there are two piers in the middle and ten piers around them. Piers are rectangular formed (approximately 200 cm in width and 520 cm in height). The distance between the piers this is in 280-300 cm. At the springing line of the piers, there are systematic holes for the scaffolding system: four rectangular holes (approximately 15x 25 cm) in 300 cm distance to each other.

Walls are composed of rubble stones alternating with bricks, while piers are composed of rubble stones and bricks in an irregular order. At the lower parts of the piers and walls, patches of lime plaster are observed (Figure 3.22).

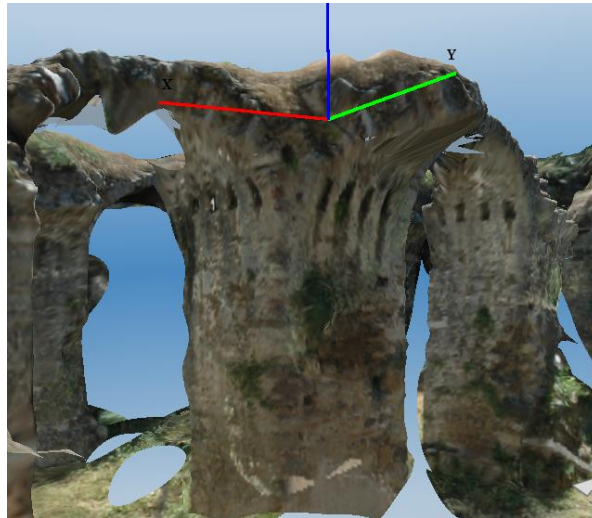


Figure 3.22. Piers, arches, gaps above the piers and plasters

Piers are connected with arches whose thickness is 25 cm. Arches are composed of rubble stones positioned radially. Form of the arches and the cross vaults and dimensions of the rubble stones, bricks, and mortars could not be determined from the model due to its unclear and incomplete details (Figure 3.23).

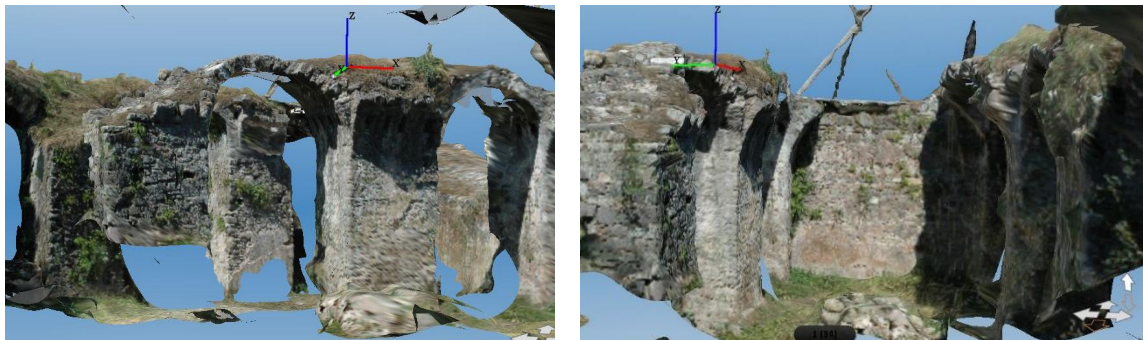


Figure 3.23. Unclear and incomplete structural details

3.3. Paradiso Aqueduct

The Paradiso Aqueduct crossing the valley of Meles Stream is located in Şirinyer, at the south of the city center, Konak. It was a part of the water way supply

channel constructed to convey water to the citadel of Pagos (Weber 1889). It is a late Roman structure dating to 5th A.D. (Hodge Trevor 2005, Weber 1889) (Figure 3.24).



Figure 3.24. Paradiso Aqueduct

3.3.1. Historical Background

Paradiso is 2.5 kilometers from Buca and it is thought as a continuation of the settlement of Buca. In Paradiso, some ancient remains as aqueducts and a castle were encountered. The late Roman aqueduct was constructed in the 5th century A.D. (Hodge Trevor 2005). The purpose of the construction of this aqueduct with Karapınar Aqueduct in Yeşildere was to provide water to Pagos City (Weber 1889).

As Chandler records, calcium carbonate formation on the faces of the stones of the water channel reduced the rate of water flow in the middle ages. Instead of cleaning it, the second Osmanağa aqueduct was built with local materials at the narrow part of the valley. Based on the characteristics on terra cotta pipes, it is thought that the second aqueduct was constructed in Byzantine period (Figure 3.25) (Weber 1889).

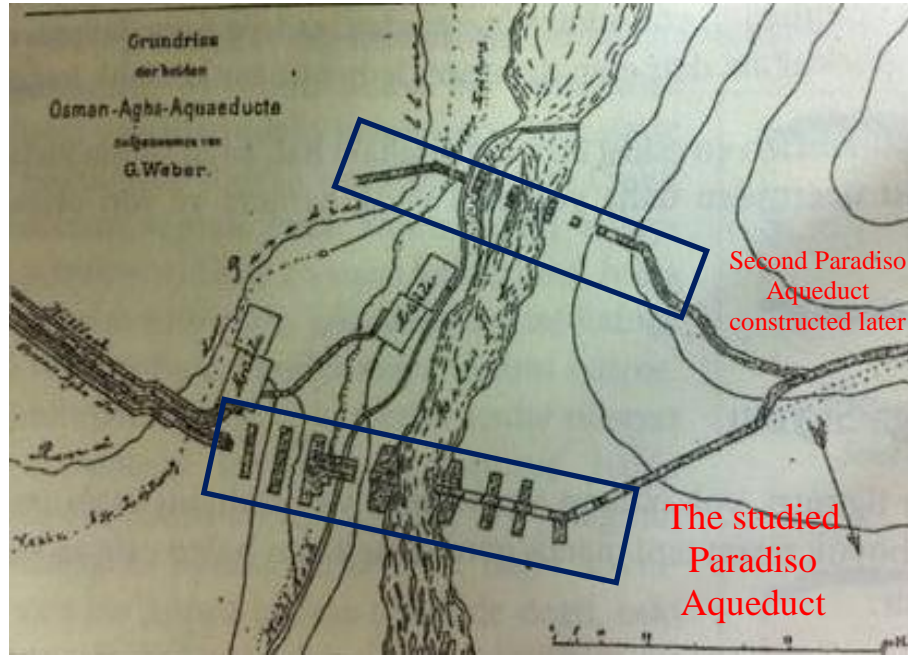


Figure 3.25. Positions of Paradiso Aqueducts
(Source: Weber 1889)

In 1809, the studied Paradiso aqueduct was restored.

The settlement of Paradiso emerged rapidly starting in 1886 as an end result of the establishment of a tobacco plant and systematization of agriculture production in its vicinity. So labor force was required, Greeks who lived in Aegean islands were brought to Izmir. Greek districts were established around Darağacı, Halkapınar, Kızılçullu, Tepecik, Buca and Şirinyer. Greeks named the studied district with the name of the church constructed here: ‘Paradiso Church’. The name ‘Paradiso’ was changed as Kızılçullu in 1922 after the Turkish army ‘Kuvayi Milliye’ conquered the district (Çelenk 2011).

3.3.2. Site Characteristics

Paradiso is located at the south of the city center, Konak, of the modern Izmir. Paradiso is named as Şirinyer today. Şirinyer is a district of Buca. Paradiso aqueduct is located over the Meles Stream; its spring is on Buca Plain at the south of the train station and between the Büyük and Küçük Paradiso. This aqueduct is a part of a water transport system surrounding Pagos and reaching fifty five meters in height with water

channels. At the southeast of the aqueduct, nearly fifty meters away, there is another aqueduct which is parallel to the studied one. These two aqueducts are named as Osmanağa in the historical sources (Weber 1889). Two kilometers away from them in north direction, there is a third aqueduct called Vezirsuyu Aqueduct (Figure 3.26).

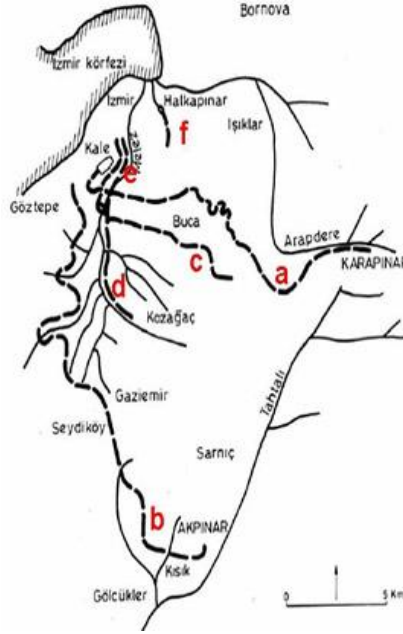


Figure 3.26. Waterways in İzmir (a. Karapınar Waterway)
(Source: Öziş, et al. 1999)

The Paradiso Aqueduct crosses the valley of Meles Stream. Two piers in the middle are located on the stream; the others are at the hills' base. The channel covered with stone carries water from 1.5 m of depth under the train station and reaches Pagos Mountain (Weber 1889).

The aqueduct is 120 meter in length (Weber 1889). The linear water conduit is carried on bridgework composed of 17 arches positioned in rhythmic order at different levels. Where the river had to be crossed, a single span arch with two relieving arches above it was preferred. Piers reinforce this major arch on both sides.

The traveler's route running parallel to the stream was continued underneath the waterway (Figure 3.27, Figure 3.28). However, on the southeastern side, which has the risk of earth sliding; arches were constructed in form of openings (Weber 1889).

Finally, at the two sides of the valley, a single storied arch system was established. The second story was composed of fourteen arches.



Figure 3.27. Travelers' Route underneath the waterway

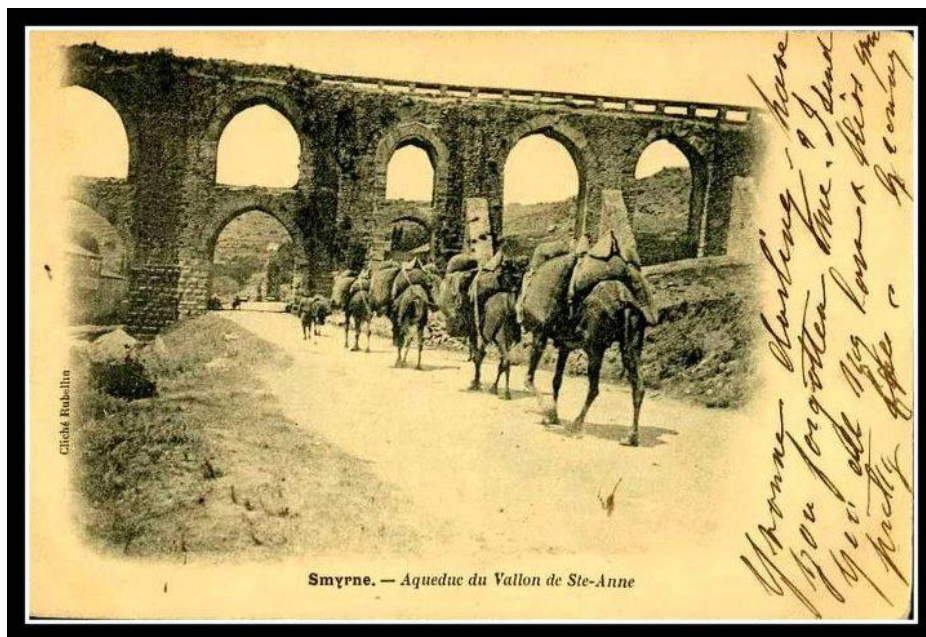


Figure 3.28. Old photo of Ste-Anne (Paradiso) Aqueduct
(Source: Erkmen Senan 2012)

The conduit continuing on the top of the aqueduct has been preserved in a few places.

3.3.3. Construction Technique

Structural characteristics of Paradiso Aqueduct were discussed with the data gathered from automatic photogrammetric evaluation software, Autodesk 123D, since the model obtained by Photosynth did not produce useful data to evaluate structural characteristics.

The length of the Paradiso Aqueduct is approximately 120 meters, however, the model includes just the middle part of the superstructure. The part which was modeled is approximately 28 meters in length. Narrow sides of the aqueduct could not be documented because of trees. The rear façade could not be documented because of the inconvenience for photographing (Figure 3.29).



Figure 3.29. Model of Paradiso Aqueduct

The aqueduct is composed of three main structural elements; wall, arch and buttresses. Walls are out of rubble stones and bricks in random bond and reinforced with cut stones at the corners.

In the modeled part, there are ten arches; however four of them are incomplete (Number 6, 7, 8, 10). Arches numbered as 2, 3, 4, 5, 9 7 are semicircular. The geometry

of the other arches could not be identified due to their ruined form and insufficiency of the model. They are out of brick (Figure 3.30).

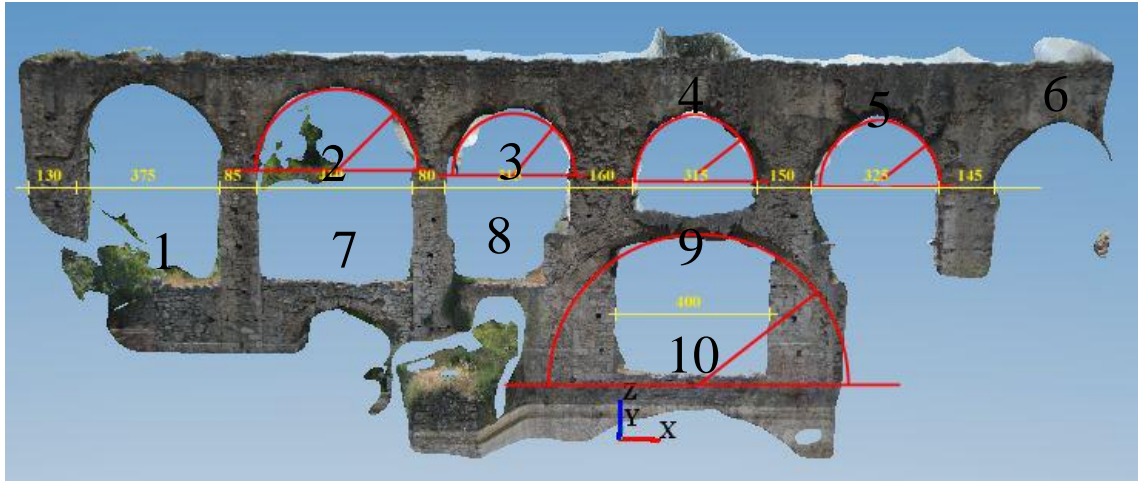


Figure 3.30. Dimensions of piers and arches, type of arches

However, components of the wall and arches as rubble stones, bricks and mortars were not evaluated from the model due to its unclear and incomplete details (Figure 3.31).

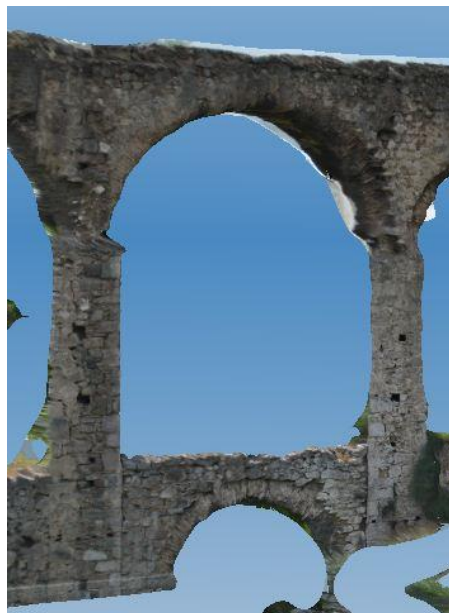


Figure 3.31. Unclear details

Some traces indicating the phases of the construction system were observed in the walls and arches. There are scaffolding holes in square form. Wooden scaffoldings were constructed to mason the higher parts of the wall (Figure 3.32). Also, the stones of the arches at the springing level are slightly projecting to carry the centering used in the construction of the arches.

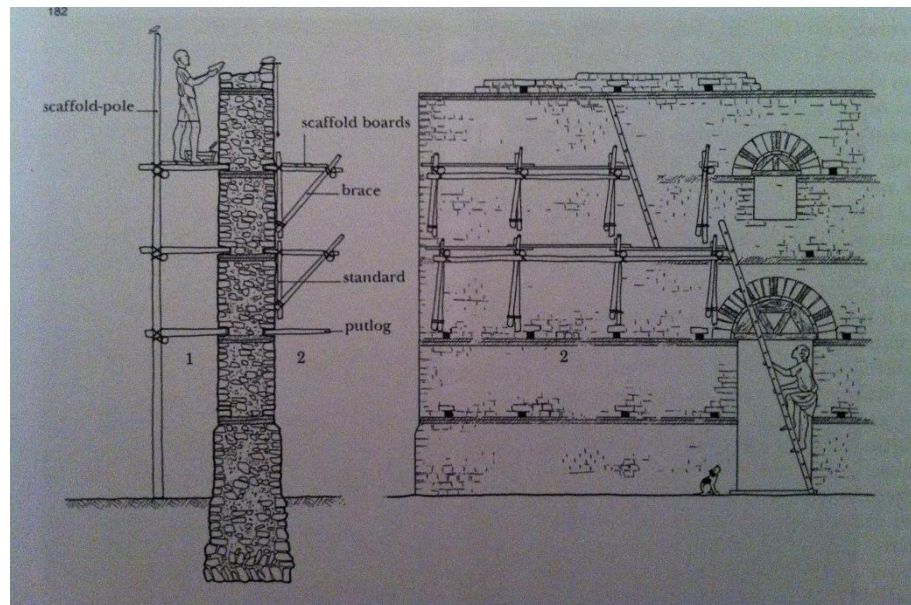


Figure 3.32. Scaffoldings
(Source: Adam 2005)

There are buttresses in front of the piers crossing the valley, but the model is insufficient for interpreting their exact geometric features.

3.4. Nysa Library

The library building is located in Nysa, an ancient city which is 3 km northwest of Sultanhisar and 30 km east of Aydın province of Turkey. It is a Roman Library dated to ca. 130 A.D. taking into consideration its architectural ornaments (Hiesel and Strocka 2006).

3.4.1. Historical Background

Nysa was an ancient city in Caria, in western Anatolia (Figure 3.33). Extant architectural remains and inscriptions as well as small finds prove that the city was inhabited uninterruptedly from Hellenistic to Byzantine times. Nysa Library located near the gymnasium was dated to 130 A.D. It has the typical features of a Roman library feature except its storages (Hiesel and Strocka 2006).



Figure 3.33. Nysa Library

The history of Nysa is mentioned in two antique sources: the Geography of Strabo of Ameseia (Amasya) who describes the Augustus period and the Ethnika of Stephen of Byzantium. According to Ethnika, there were ten cities called Nysa in the ancient world, but only the one founded by Seleucid King Antiochos I (281-261 BC) was named after his wife: Caria. Strabo reported that origins of Nysa lie in the mythical past. Three brothers, Athymbros, Athymbrados and Hydrellos migrated from Sparta in Peloponnese and founded three separate little settlements. Later these three cities joined

and formed the ancient Nysa. Only Athymbros was remembered as the founder of the new city, and it was for this reason the original name of the city was Athymbra, later changed as Antiocheia. The city was known as Nysa at the beginning of the 2nd century BC (İdil 1993).

Nysa was famous in antiquity as an education centre. Strabo studied in the Gymnasium of Nysa. However, it was only after Strabo's death during the Roman imperial period that the city reached to a fully developed state.

The city was captured by Seljuks in the 12th century, however shortly after Byzantines retook Nysa and it remained part of the empire until it became part of Mentese Emirate of Aydın. Nysa fell into a severe decline after despoil of Timurlenk in 1402. Most of the ruins that are seen today date to the Roman and Byzantine periods. The modern town Sultanhisar, lying to the south of the site, was founded in the 14th and 15th centuries (İdil 1993).

The present researches have brought no evidence of the existence of the city before the third century B.C. Extant architectural remains and inscriptions as well as small findings prove that the city was inhabited uninterruptedly from Hellenistic to Byzantine times. The first excavations in Nysa were carried out by the German railroad engineer Walter von Diest between 1907 and 1909. After this first research, further excavation was directed by the Greek archaeologist K. Kourounitios in the 1920s. An interdisciplinary team under the guidance of Vedat İdil from Ankara University has been studying the ancient city since 1990 (Kadioğlu and Kadioğlu 2008).

The Library of Nysa was dated to 130 A.D. typologically, it is similar to the other Roman Imperial libraries, but it seems to include an archive, because of its vaulted rooms on the ground floor. It might have functioned as a court given the presence of an exedra like a tribunal. During the late 4th or early 5th centuries the building was restored without losing its function. The final destruction, whose main reason is most probably an earthquake, couldn't be dated exactly (Hiesel and Strocka 2006).

3.4.2. Site Characteristics

Nysa, an ancient city in Caria, which is a region of western Anatolia, extending along the Aegean coast, is located 3 km north-west of Sultanhisar and 30 km east of

Aydın province of Turkey. The city is close to the main highway between Aydın and Denizli and 70 km east of Ephesus, the capital city of Ionia (Figure 3.34).

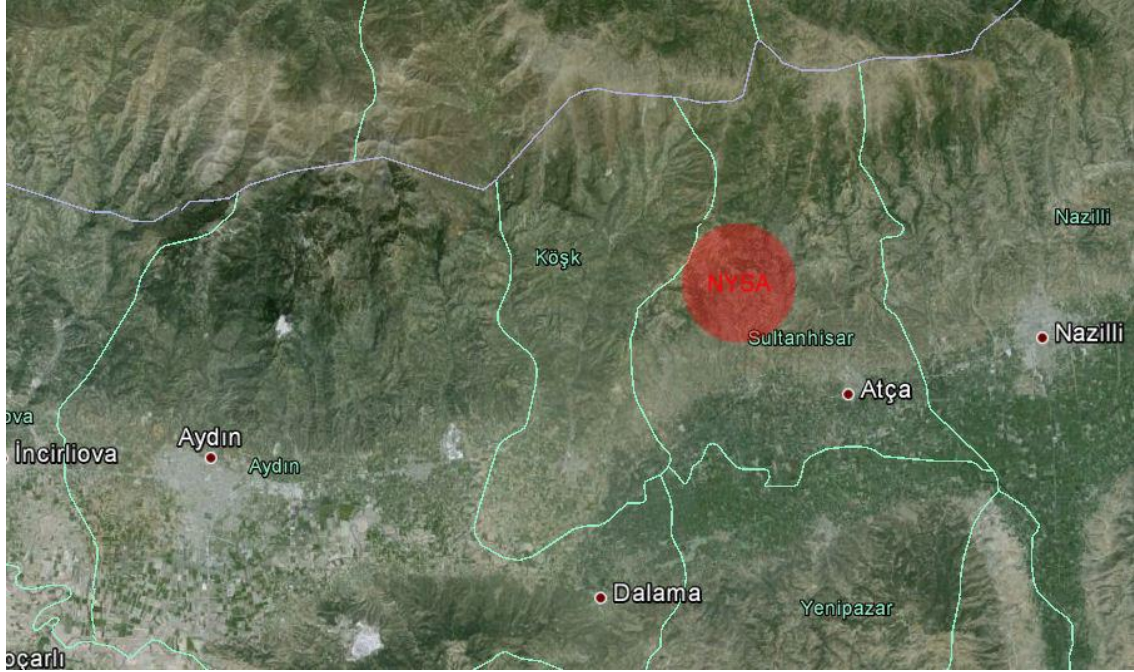


Figure 3.34. Location of Nysa

Nysa lies at the north of the Meander River (Buyuk Menderes) and the ruins of the ancient city are now on the slope of Messogis Mountain Chain (Aydın dağları). The city was settled on two hills on the sides of a stream called Tekkecik. The buildings, streets and public squares of the ancient city were supported by vaulted substructures adapted to the topographic conditions (İdil 1999).

As Strabo states, two sides were connected to each other by a bridge. An amphitheater which has a channel under its ground as precaution for flood was located on one side of the city. There are two hills near the theatre. While a gymnasium for children was located on the slopes of one hill, there is a gymnasium for adults and an agora on the other one (Strabo 7 BC).

The known parts of the city today include several public buildings: The most important surviving buildings include the agora and the Roman public baths in the east, and in the west, the gymnasium, stadium, library, temple, nymphaeum, theatre, bridges, and the Byzantine churches. The remains of the Hellenistic walls have disappeared.

(Kadioğlu and Kadioğlu 2008). The library building is located 150 meters from the gymnasium, because of this reason; it is evaluated as a gymnasium library (Yıldız 2003).

The library is a rectangular planned building (approximately 25x14 m). Its main entrance must have been at the southern side and it had two or three stories (İdil 1993). The spatial elements of the library are the principal room (hall) with its apse where the statue of the god or some defied emperors were put, storages for books, the passages (corridors) for the ventilation of the books and a portico in front of the building. However, the functions of the vaulted rooms on the ground floor were not interpreted. The architectural elements are niches, windows, pilasters and a podium. In the western and eastern walls of the principal room, there are pilasters repeated every 2.5 meters. Three rectangular niches (90x120 cm) were placed between these pilasters (Figure 3.35). On the first floor, between the exterior walls and thick interior walls, the corridors with vaulted superstructure are situated. On the interior walls of the corridors, there are niches for books. The other niches on the exterior walls are evaluated as windows (Yıldız 2003). In front of the eastern internal wall, there is a podium.

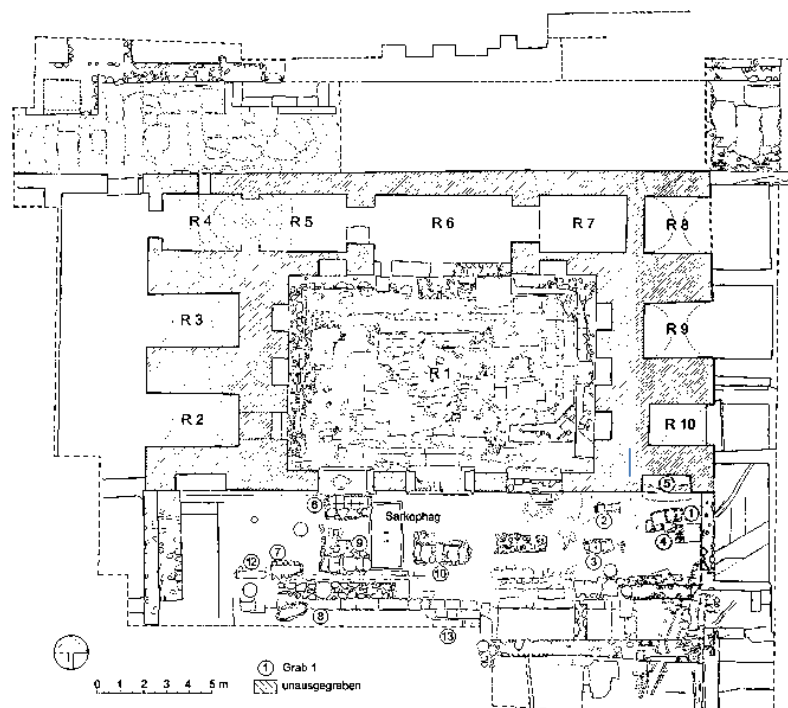


Figure 3.35. Ground floor plan of Nysa Library
(Source: Hiesel and Strocka 2006)

3.4.3. Construction Technique

Structural characteristics of Nysa Library were discussed with the data gathered from automatic photogrammetric evaluation software; Autodesk 123D, since the model obtained by Photosynth did not produce useful data to evaluate structural characteristics.

Nysa Library is a rectangular building composed of two prisms, however just the part located on the east could be modeled. Model of Nysa Library was satisfactory in comparison to Pagos Cistern and Paradiso Aqueduct due to its appropriate form, position, and condition (Figure 3.36).



Figure 3.36. Model of Nysa Library

Nysa Library is a masonry structure composed of three types of structural elements; wall, arch and vault.

Walls of Nysa Library are constructed as dressed stone walls with; rubble infill and mortar surrounded with facing stones. There are three different facing types in Nysa Library.

- First one is the facing composed of rubble stones in different sizes (Figure 3.37).



Figure 3.37. Model of rubble stone facing

- Second one is called *chequer work*: Pilasters between the niches in the inner façade were constructed with this technique. Large cut stone blocks were rested one another, rubble stones were used to fill in the spaces between the cut stones (Adam 2005). Therefore, the main structural element of the system is cut stone blocks (Figure 3.38).

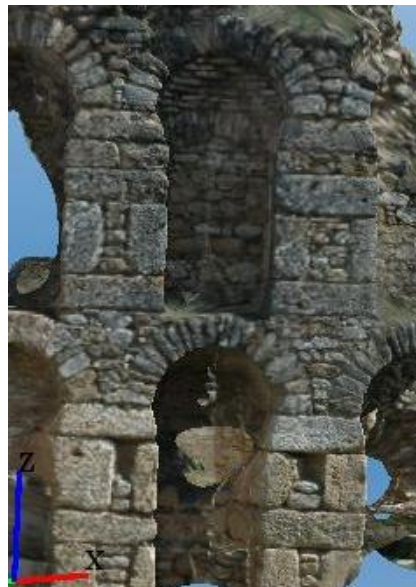


Figure 3.38. Model of *Chequer work*

- Last facing technique is *opus africanum*: Vertical chains of large stone blocks in which upright blocks alternate with horizontal ones (Adam 2005), (Figure 3.39).



Figure 3.39. Model of *Opus Africanum*

The inner wall in the west was composed of niches with semicircular arches. These arches are out of rubble stones approximately 5 cm in width and 26 cm in length (Figure 3.40). Between these arches, there are rubble stones. In the first floor of the library, the same system was repeated, however, relieving arches out of rubble stones approximately, 5.5 cm in width, and 32-33 cm in length were observed under the stone arches. The space in the arches was filled by horizontally laid bricks.

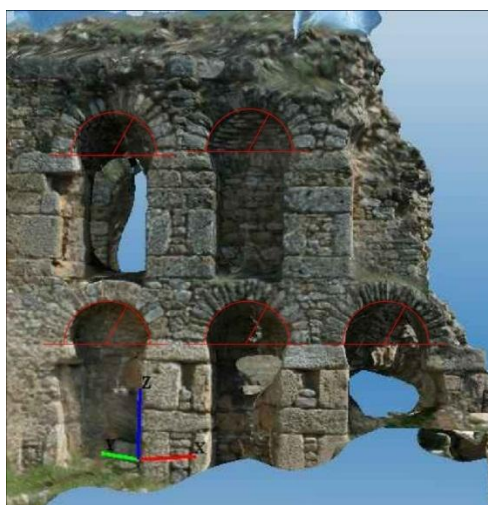


Figure 3.40. Semicircular arches of niches

Barrel vaults are out of rubble stones in different sizes. Thickness of the barrel vault is approximately 25 cm. However, dimensions of the rubble stones could not be measured due to the ambiguity of the model.

CHAPTER 4

HISTORICAL RESEARCH, COMPARATIVE STUDY AND RESTITUTION OF HYPOKREMNOS VIADUCT

In order to identify the place of the case study viaduct with in other Anatolian viaducts and to evaluate its alterations, comparative study was carried out. The Anatolian viaducts in Roman (70 BC -5th century), Byzantine (4th -15th century), Seljukid (11th-13th century) and Ottoman (14th -18th century) periods were compared in terms of their forms, compositions, structural and architectural elements and construction techniques.

4.1. History of the Site

Except the case study viaduct, there are two viaduct remains and remains of a road way found on the coastline with visual analysis in the site survey. Near all viaduct remains, brooks flowing through Icmeler plateau were encountered. Narrow streams or deep valleys were spanned with one arched viaducts, while wide rivers with low flow required a series of arches, whose direction could vary in accordance with the stability of ground. If the rivers are flowing on a wide area, the structure is composed in pieces (Tanyeli 2000).

As revealed from historical research and old maps, there was an ancient road between Klazomenai and Hypokremnos (Bakır and Anlağan 1980). In Kiepert's map (1869) indicating Roman period in Ionia, a road between Erythrai, Klazomenai and Teos passing from Hypokremnos was drawn (Figure 4.1). The geographic boundaries of Klazomenai are determined with a number of nodes known as Dubatepe, Akçahisar, Sivricetepe, Cindersesi, Hacıgebeş and Yarentepe. Dubatepe, Akçahisar and Sivricetepe are castles and Cindersesi, Hacıgebeş and Yarentepe are settlements. Hacıgebeş was also used as a control point between Klazomenai and Erythrai (Koparal 2012).

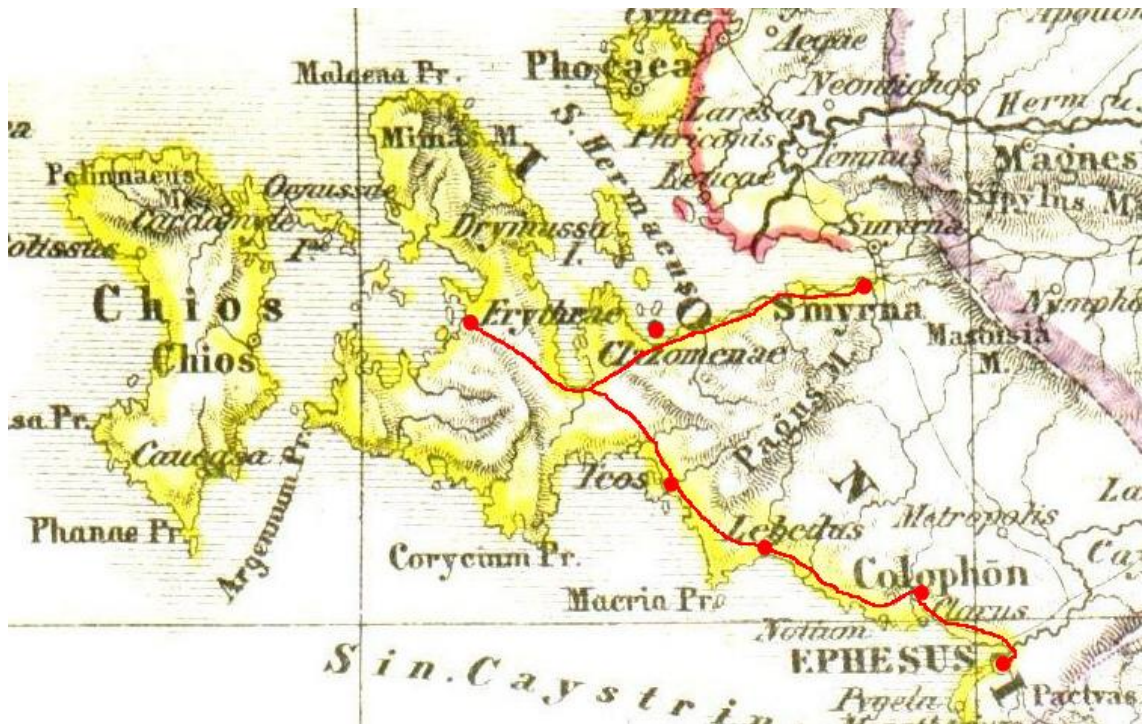


Figure 4.1. Ionia in Roman Period
(Source: Kiepert 1869)

4.2. History of Ancient Viaducts in Anatolia

The characteristics of the site and the date of construction are the primary parameters that determine the form and construction techniques of Anatolian Viaducts. In Roman, Byzantine, Seljuk and Ottoman periods, masonry structures in linear forms carried with one or series of arches was the basic theme of the viaducts. Narrow streams or deep valleys were spanned with one arched viaducts, while wide rivers with low flow required a series of arches, whose direction could vary in accordance with the stability of the ground (Tanyeli 2000).

Similar construction techniques presented consistency throughout periods. Since Roman period, viaduct walls and piers constructed as masonry structures composed of rubble stone infill surrounded with stone blocks and foundations are out of timber piles (Tanyeli 2000, Tunç 1978).

Roman viaducts are generally rectangular formed structures with one semicircular arches or series of semicircular arches; however triangular façades are sometimes encountered in Anatolia (Tunç 1978). If the roadway of the viaduct rises

from two sides to the middle, the viaduct has inclined road way, so it has triangular facades. The wall is crowned with the road way making a crest at its center. However, if the roadway of the viaduct is flat and parallel to ground, the viaduct has rectangular facades. Taş Viaduct, Seyhan, Adana, Gazimihal (Hamidiye) Viaduct, Edirne and Kırkgöz Viaduct, Afyon (Figure 4.3) are rectangular formed Roman Viaducts, while Aspendos (Belkıs) Viaduct, Antalya, Aizonai Viaduct (Figure 4.2), Çavdarhisar and Misis Viaduct, Adana have triangular façade (Karayolları Genel Müdürlüğü 2008). The keystone of the arches is generally visible (Aizonai Viaduct, Çavdarhisar) (Doğangün and Ural 2007). Masonry walls and piers were constructed with rubble stone infill surrounded with large cut stone blocks infill (Tunç 1978, Eyüce 1992, Tanyeli 2000). The viaducts mentioned in Karayolları Genel Müdürlüğü Yapı Onarım Envanteri (2008); Taş Viaduct, Seyhan, Adana, Aspendos Viaduct, Antalya and Gazimihal Viaduct, Edirne was constructed with cut stone blocks and rubble stone.



Figure 4.2. A Roman Viaduct; Aizonai, Penkalas Brook
(Source: Define Gizemi 2013)



Figure 4.3. A rectangular formed Roman Viaduct; Taş Viaduct, Seyhan, Adana
(Source: Tanyeli 2000)

Byzantine viaducts are generally similar to Roman Viaducts according to their form, composition and construction techniques (Kırkgöz Viaduct, Afyon, Çobançeşme Viaduct, İstanbul, Beşköprü Viaduct, Sakarya) (Figure 4.4). However, facings of patterns and choice of material show sometimes differences in the construction of walls and piers. They sometimes used bricks in alternating rows between the cut stone blocks (Tunç 1978).

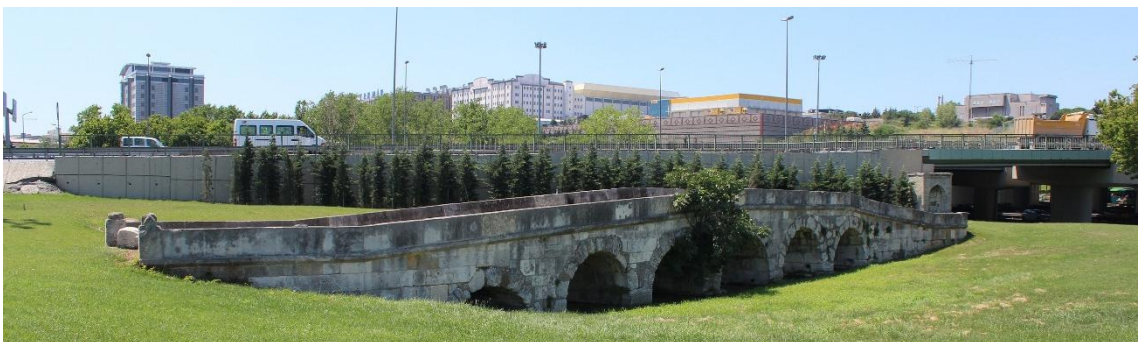


Figure 4.4. A Byzantine Viaduct; Çobançeşme Viaduct
(Source: İstanbul Tv 2013)

Seljukid and Ottoman viaducts have generally triangular formed facades. They are composed of one arch or series of arches, but series of arches are common due to geographic features of Anatolia. Two types of arches are generally observed; pointed or depressed (Tunç 1978, Eyüce 1992, Tanyeli 2000). The Seljuk and Ottoman viaducts mentioned in the study of Tanyeli have the characteristics features; Seljuk Viaducts; Hıdırlık Köprü, Tokat, Çokgöz Viaduct, Kayseri, Hoşap Viaduct, Van and Ottoman Viaducts; Sinanlı Viaduct, Alpullu, Meriç Viaduct, Edirne and Uzun Viaduct, Kırklareli.

Flood control arches are more common in Turkish period in comparison to Roman and Byzantine viaducts (Tunca Viaduct, Edirne, Fatih Viaduct, Edirne, Sinanlı Viaduct, Alpullu), (Tunç 1978). Some architectural elements are generally observed as belts and kiosks. Kiosks are generally used in Ottoman viaducts as a traditional element to give information about the construction date of viaduct or watch around (Meriç Viaduct, Edirne, Tunca Viaduct, Edirne, Babaeski Viaduct, Kırklareli) (Tanyeli 2000). Main principles of construction technique of Roman era continued in Seljukid and Ottoman viaducts, however, these viaducts can present differences in terms of material usage and pattern of facing. Seljuks sometimes used different colored and sized cut stone blocks in a regular order (Figure 4.5) (Bayramiç Viaduct, Çanakkale, Selçuk Viaduct, Ağrı, Hoşap Viaduct, Van), Ottomans preferred small cut stone blocks as opposed to Roman viaducts composed of large cut stone blocks (Meriç Viaduct, Edirne, Tunca Viaduct, Edirne, Babaeski Viaduct, Kırklareli, Sinanlı Viaduct, Alpullu) (Tunç 1978) (Figure 4.6).



Figure 4.5. Different coloured and sized cut stone blocks in a Seljukid Viaduct; Bayramiç Viaduct (Source: Çanakkale İli Private Website 2009)



Figure 4.6. Ottoman Viaduct; Sinanlı Viaduct (Source: Bozkurt 1952)

4.3. Comparison of Ancient Anatolian Viaducts with the Case Study

Characteristics features of the case study viaduct are evaluated with reference to comparative study (Figure 4.7).





CONSTRUCTION PERIOD																											
FORM		COMPOSITION		STRUCTURAL ELEMENTS										ARCHITECTURAL ELEMENTS			CONSTRUCTION TECHNIQUE				EXAMPLE						
RECTANGULAR	TRIANGULAR	SINGLE WIDE ARCH	SERIES OF ARCHES	TIMBER PILES CLOSE TO EACH OTHER	GROUND INFILL (RAFT)	PIERS	FLAT SPANDREL WALLS	PROJECTED SPANDREL WALLS	FLOOD CONTROL ARCH	POINTED + DEPRESSED ARCH	SEMICIRCULAR ARCH	RELIEVING ARCHES	KEY STONE	BREAK WATERS IN FRONT OF THE PIERS	ELEMENTS IDENTIFYING ENTRANCES	KIOSK	FLOOR COVERING	BELT	PARAPET	MASONRY							
																				FACING: BIG CUT STONE BLOCKS MORTAR: NOT SEEN IN THE INFILL INFILL: RUBBLE STONE INFILL		FACING: BIG CUT STONE BLOCKS AND SOMETIMES BRICK IN ALTERNATING ROWS MORTAR: NOT SEEN IN THE INFILL INFILL: RUBBLE STONE INFILL	FACING: SMALL CUT STONE BLOCKS IN ALTERNATING ROWS MORTAR: SEEN IN THE INFILL INFILL: RUBBLE STONE INFILL	FACING: SMALL CUT STONE BLOCKS MORTAR: SEEN IN THE INFILL INFILL: RUBBLE STONE INFILL			
OTTOMANS (15.-18. Century)	Rarely observed.	Generally observed.	Rarely observed.	Generally observed.	Generally observed.	Not observed.	Always observed.	Not observed.	Generally observed.	Generally observed.	Generally observed.	Rarely observed.	Generally observed.	Not distinctive.	Sometimes observed.	Not observed.	Generally observed.	Always observed.	Generally observed.	Generally observed.		Not observed.	Not observed.	Not observed.	Always observed.		
SELJUKIDS (11.-14. century)	Rarely observed.	Generally observed.	Rarely observed.	Generally observed.	Generally observed.	Always observed.	Not observed.	Generally observed.	Generally observed.	Generally observed.	Rarely observed.	Generally observed.	Not distinctive.	Sometimes observed.	Not observed.	Always observed.	Generally observed.	Generally observed.	Generally observed.	Generally observed.	Not observed.	Not observed.	Sometimes observed.	Generally observed.			
BYZANTINES (4th-15th century)	Generally observed.	Rarely observed.	Generally observed.	Generally observed.	Rarely observed.	Always observed.	Always observed.	Not observed.	Not observed.	Not observed.	Always observed.	Always observed.	Not observed.	Sometimes observed.	Not observed.	Always observed.	Not observed.	Always observed.	Not observed.	Not observed.	Not observed.	Not observed.	Always observed.	Not observed.			
ROMANS (-70 BC and 5th century)	Generally observed.	Rarely observed.	Generally observed.	Generally observed.	Rarely observed.	Generally observed.	Always observed.	Always observed.	Not observed.	Not observed.	Not observed.	Always observed.	Distinctive.	Sometimes observed.	Sometimes observed.	Not observed.	Always observed.	Not observed.	Generally observed.	Always observed.	Not observed.	Not observed.	Not observed.	Always observed.			

Figure 4.7. Characteristics of ancient viaducts in Anatolia

4.3.1. Façade Composition

Firstly, geometric features of Anatolian viaducts are compared. There are two façade types observed in Anatolian viaducts; rectangular and triangular facades. If the roadway of the viaduct rises from two sides to the middle, the viaduct has inclined roadway, so it has triangular facades. The wall is crowned with the roadway making a crest at its center. However, if the roadway of the viaduct is flat and parallel to ground, the viaduct has rectangular facades. Roman Viaducts are generally rectangular formed in Rome, while triangular formed viaducts are observed in Anatolia in Roman Period (Tunç 1978). Taş Viaduct, Seyhan, Adana, Gazimihal (Hamidiye) Viaduct, Edirne and Kırkgöz Viaduct, Afyon are rectangular formed Roman Viaducts, while Aspendos (Belkıs) Viaduct, Antalya, Aizonai Viaduct, Çavdarhisar and Misis Viaduct, Adana have triangular façade (Karayolları Genel Müdürlüğü 2008). These two façade types are also observed in Byzantine Viaducts in Anatolia. Kırkgöz Byzantine Viaduct, Afyon has rectangular form, while Çobançeşme Byzantine Viaduct, İstanbul has triangular form. However, triangular form is generally basic preference in Seljukid and Ottoman periods (Sinanlı Viaduct, Alpullu, Fatih Viaduct, Edirne), (Tanyeli 2000). The case study is a triangular formed viaduct (Figure 4.8). So, it can belong to any period according to façade form.



Figure 4.8. Façade form of case study viaduct

In Roman, Byzantine, Seljukid and Ottoman periods, viaducts were carried with one or series of arches. Viaducts composed of series of arches can be discussed under two headings: viaducts with same sized arches and viaducts whose middle arch is wide and side arches are narrow. Roman and Byzantine viaducts with series of arches have generally same sized arches in Rome (Taş Viaduct, Seyhan, Adana, Gazimihal (Hamidiye) Viaduct, Edirne and Kırkgöz Viaduct, Afyon), while middle arch can be

rarely wider than side arches in Anatolia (Aspendos (Belkıs) Viaduct, Antalya, Aizonai Viaduct, Çavdarhisar and Misis Viaduct) (Tunç 1978). In Seljukid and Ottoman viaducts, middle arch is generally wide and sides are narrow (Sinanlı Viaduct, Alpullu, Fatih Viaduct, Edirne), (Tanyeli 2000). The case study viaduct has series of arches which have different sizes; the middle one is wide and sides are narrow (Figure 4.8). So, it can belong to any period according to organizations of arches.

4.3.2. Architectural Elements

Architectural elements can be discussed in five groups; elements identifying entrances to the viaduct, kiosk, floor covering, belt and parapet. Architectural elements emphasizing entrances are only used in some of Roman Viaducts (Cendere Viaduct, Kahta), (Tanyeli 2000). The entrances of the case study viaduct are not seen today, because they are slightly damaged and the ground level has risen.

Kiosks are typical elements enriching Ottoman caravan routes. They are located on the highest part of the viaduct as a projected element. They have two different functions; kiosks providing information on the history of the viaduct with inscription panels “Tarih Köşkü” and kiosks for enjoying the vista “Seyir Köşkü” (Figure 4.9), (Meriç Viaduct, Edirne, Tunca Viaduct, Edirne, Babaeski Viaduct, Kırklareli), (Tanyeli 2000). There is no kiosk in the case study as in Roman examples.

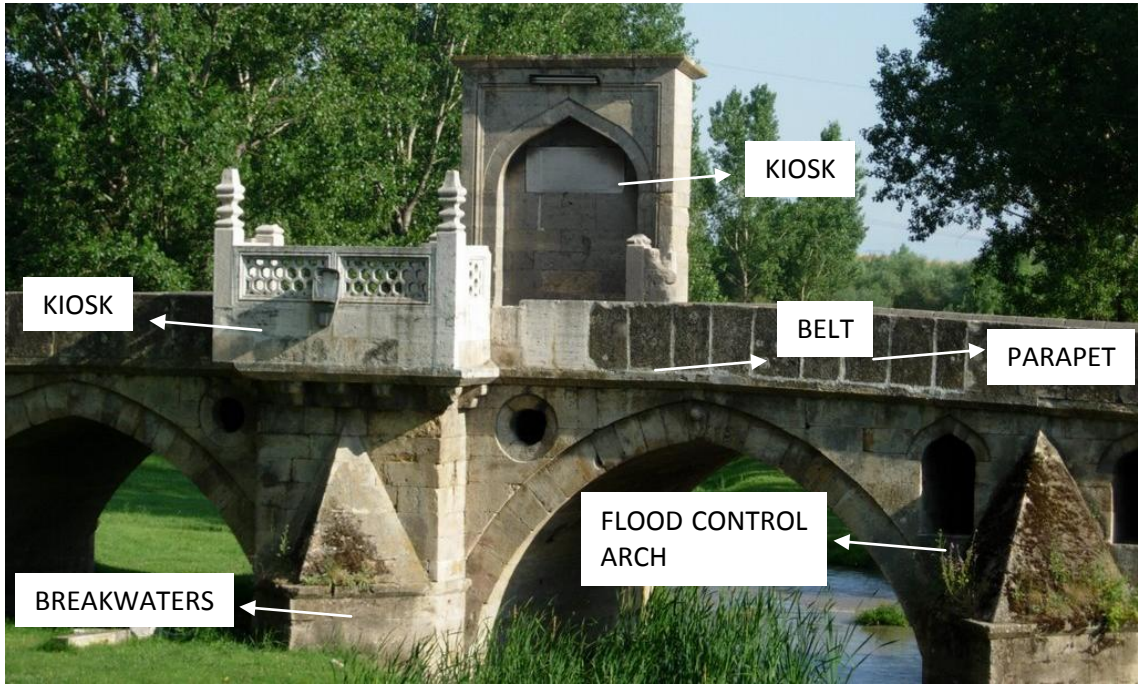


Figure 4.9. Babaeski Viaduct with its kiosks
(Source: Panoramio 2007)

Floor covering out of rubble and cut stones are always used on the roadways in all periods. The case study viaduct's roadway is paved with small rubble stones (Figure 4.10).



Figure 4.10. Floor covering of Hypokremnos Viaduct

Belt stones are generally observed between spandrel walls and parapet in Seljukid and Ottoman Viaducts, however they are not preferred in Roman and Byzantine Viaducts (Tunç 1978) (Figure 4.9). In the study of Tanyeli (2000), Seljuk and

Ottoman Viaducts; Altıgöz Viaduct, Afyon, Uzun Viaduct, Kırklareli, Meriç Viaduct, Edirne have belts, but Aspendos Viaduct, Antalya, Taş Viaduct, Seyhan, Adana constructed in Roman period do not have belts. They are in form of a single row of stones under the parapet stones. The case study viaduct does not have belt stones under its parapet as in Roman and Byzantine cases.

Parapets near the two sides of the roadway of the viaducts are generally observed in all periods (Roman Viaduct; Aizonai, Çavdarhisar, Byzantine Viaduct; Çobançeşme, İstanbul, Seljuk Viaduct; Altıgöz, Afyon and Ottoman Viaduct; Fatih, Edirne), (Figure 4.9). The case study has projected parapet stones above its spandrel wall.

4.3.3. Structural Elements

Structural elements of viaducts can be discussed under eleven subtitles from ground to top; timber piles, ground infill (raft), piers, disposition of spandrel walls as flat or projected, form of the main arches as semicircular, pointed and depressed arches, relieving and flood control arches, breakwaters in front of the piers and keystone (Figure 4.11).

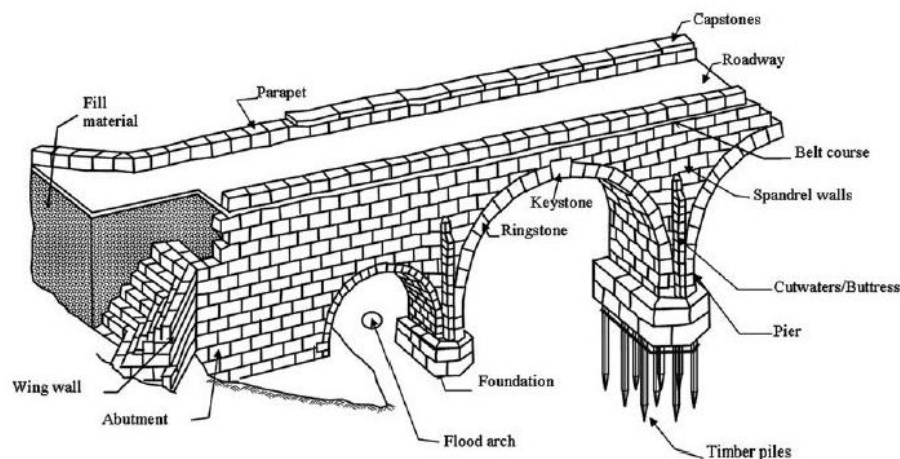


Figure 4.11. Structural elements of a Viaduct
(Source: Ural, et al. 2008)

There is limited information on the foundation systems of viaducts. Most of the information in literature is on Roman foundations and some on Ottoman ones. It is stated that closed timber piled foundation was generally preferred in Roman and Ottoman viaducts in Anatolia (Tanyeli 2000). In Roman period, timber piles were employed, when it was necessary to stretch the foundation level below the deep water table (Cowan 1977) (Figure 4.12).

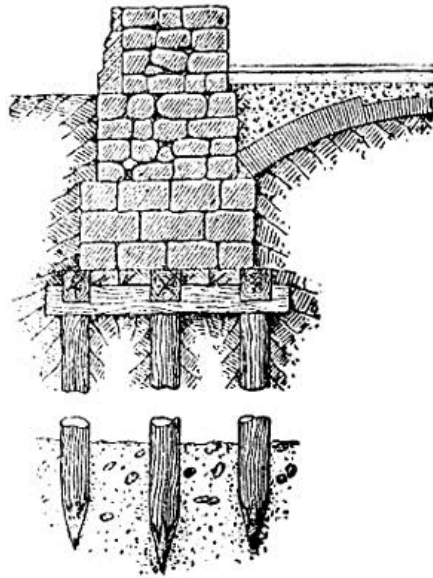


Figure 4.12. Timber piled foundation system
(Source: Santos 2000)

Cofferdam (batardo) was used as a temporary support for construction work carried under water in Roman period. Construction of a Roman cofferdam consists of three simple phases: A double ring of wooden stakes was driven into the river bed around the planned location of a viaduct pier by a manually operated pile driver. Clay was packed into the division between the two circles, and then the water was emptied from the enclosed space. After that, timber pile foundations were installed (Brown 2001), (Figure 4.13).

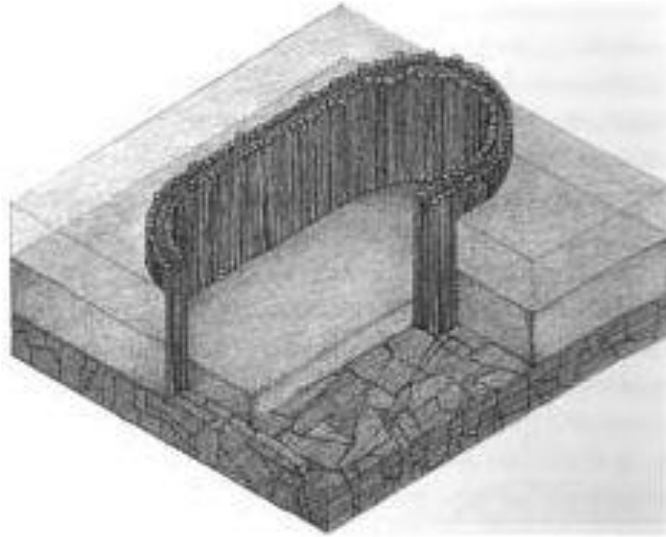


Figure 4.13. The principle of a Roman cofferdam
(Source: Brown 2001)

Ground infill (raft) was only used in Roman viaducts to give rectangular form to the viaducts; however this application was not repeated in Ottoman viaducts. The ground level has increased in time with accumulation of debris in the case study, but the form is triangular; so, the presence of such an infill is not expected (Tunç 1978).

Piers and spandrel walls are observed in all periods. There are two different types of spandrel walls; flat and projected spandrel walls. Flat spandrel walls are always used in Roman and Byzantine periods (Taş Viaduct, Adana, Aspendos Viaduct, Antalya, Kırkgöz Viaduct, Afyon) while projected spandrel walls are more common than flat ones in Seljukid and Ottoman periods (Altıgöz Viaduct, Afyon, Uzun Viaduct, Kırklareli, Meriç Viaduct Edirne), (Tanyeli 2000, Karayolları Genel Müdürlüğü 2008). The case study viaduct has flat spandrel walls, as in the majority of the Roman and Byzantine examples (Figure 4.14).



Flat spandrel walls; Hypokremnos Projected spandrel walls; Babaeski Viaduct Viaduct (Seljukid Period)

Figure 4.14. Spandrel walls
(Source: Panoramio 2007)

The form of the main arches presents characteristics specific to periods. Semicircular arches are generally preferred in Anatolian Roman and Byzantine viaducts (Karaköprü, Diyarbakır, Aizonai Viaduct, Çavdarhisar, Tekkeboğazı Viaduct, Bergama), however, depressed and pointed arches are generally preferred in Seljukid and Ottoman Viaducts (Fatih Viaduct, Edirne, Sinanlı Viaduct, Alpullu, Meriç Viaduct, Edirne), (Tunç 1978, Tanyeli 2000). The case study viaduct has semicircular three arches, as in Roman and Byzantine examples (Figure 4.15).

In a semicircular arch, more of the thrust goes directly downwards. They do not need strong side bracing at the abutments. This means that if the piers were wide enough, (one third of the span) any two could support a complete arch without further propping from the sides (Brown 2001).



Figure 4.15. Semicircular arches

Centering was used in the construction of arches of viaducts. The centering which forms the profile of the intrados of an arch remains in place until the arch is completed. There are two types; centering supported by timber studs resting on the ground or centering supported by buttresses resting on piers. The second type is especially common for viaduct construction, if there is continuous water flow (Figure 4.16) (Mark 1993).

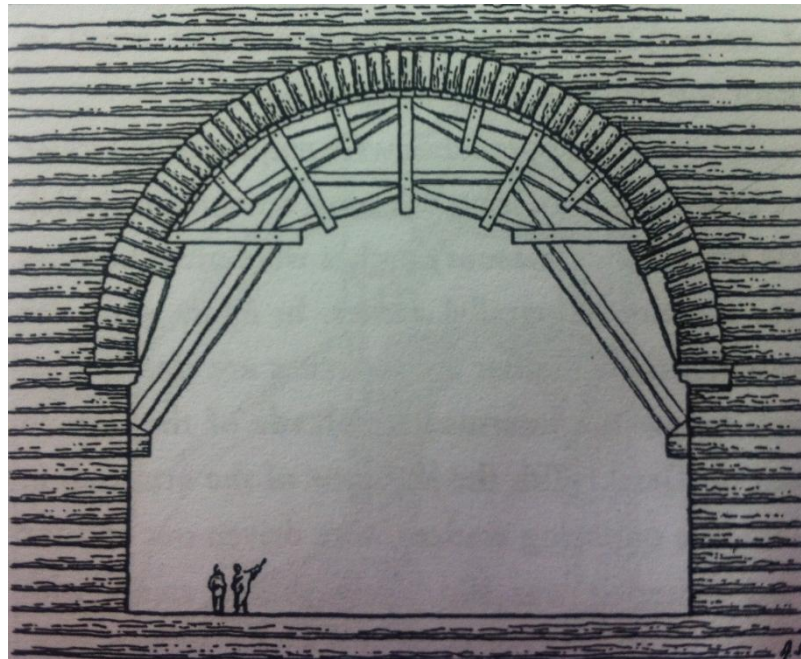


Figure 4.16. Centering
(Source: Mark 1993)

Flood control arches are generally observed in Seljukid and Ottoman viaducts (Tunca Viaduct, Edirne, Fatih Viaduct, Edirne, Sinanlı Viaduct, Alpullu), (Tunç 1978, Karayolları Genel Müdürlüğü 2008). The case study viaduct does not have flood control arches, as in Roman and Byzantine examples (Figure 4.11).

A relieving arch is an arch built over a main arch to relieve or distribute the weight of the wall and the main arch. They are common in Seljukid and Ottoman periods, but they are rarely used in Roman period Viaducts (Tunç 1978). There is no relieving arch in the case study viaduct, as in Roman examples.

The keystone is generally distinctive in Roman period (Aizonai Viaduct, Çavdarhisar), while in Seljukid and Ottoman Periods, it is not emphasized (Fatih

Viaduct, Edirne), (Doğangün and Ural 2007). In the case study, the preserved keystone at the northwest of the upstream facade is larger than other ring stones of the arch. So, the viaduct can be interpreted as a Roman period example (Figure 4.17).

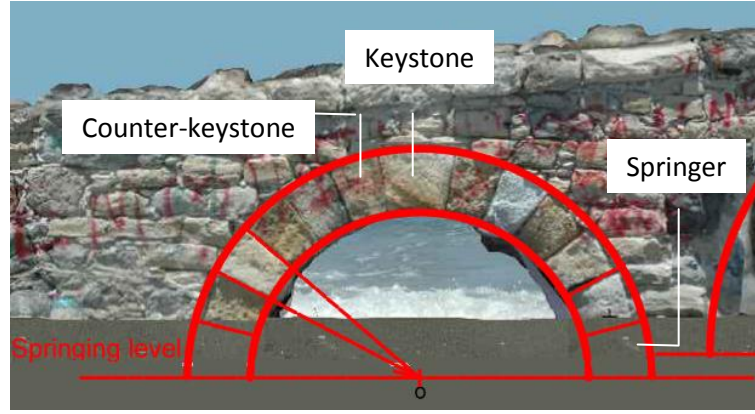


Figure 4.17. Keystone of the arch of Hypokremnos Viaduct

Breakwaters juxtaposing the upstream façade of the piers are constructed to protect the viaduct from floods and waves (Figure 4.9). They are preferred in all periods, if there is a necessity in relation with the stream characteristics (Roman Period; Karaköprü, Diyarbakır, Ottoman Period; Fatih Viaduct), (Karayolları Genel Müdürlüğü 2008). The case study viaduct does not have breakwaters in front of its piers. This should be related with the low speed of stream water running on the flat plateau of Hypokremnos.

4.3.4. Construction Technique and Material Usage

Due to the vulnerable characteristics of timber, historical viaducts out of this material have not reached today. Nevertheless, masonry viaduct examples from all periods can be observed in Anatolia (Tanyeli 2000). They can present differences in terms of material and pattern of facing and infill. Rubble stone infill was covered with large cut stone blocks in Roman Viaducts. Mortar was not exposed in the joints (Tunç 1978, Tanyeli 2000), (Gazimihal Viaduct, Edirne). In Byzantine period, rubble stone infill with large cut stone facing were continued to be used (Kırkgöz Viaduct, Afyon),

however, bricks in alternating rows were sometimes observed. Mortar was exposed in the narrow joints (Tunç 1978). Viaducts constructed in Turkish period were generally different from Roman and Byzantine ones in terms of facing material. Facing material was generally small cut stone blocks. Mortar was exposed in narrow joints (Meriç Viaduct, Edirne, Tunca Viaduct, Edirne, Babaeski Viaduct, Kırklareli, Sinanlı Viaduct, Alpullu), (Tanyeli 2000). Sometimes small cut stone blocks in alternating rows were preferred in Seljukid Viaducts (Bayramiç Viaduct, Çanakkale, Selçuk Viaduct, Ağrı, Hoşap Viaduct, Van), (Tunç 1978).

The case study viaduct is out of rubble stone infill covered with cut stone blocks. However, upstream (southern) and downstream (northern) facades of the viaduct show different characteristics. There are large cut stone blocks without mortar between them on the sea side, while there are smaller cut stone blocks with mortar in narrow joints on the other. So, the seaside façade resembles Roman order, while the coast side resembles Turkish examples. It may be claimed that the sea side had to be designed strong against splashing waves and salty water carried with northern wind. So, cheaper and less durable material was utilized on the coast side. Period alteration of facades cannot be discussed since there is no trace of intervention (Figure 4.18).



Upstream (Southern Facade)



Downstream (Northern Facade)

Figure 4.18. Facing materials and patterns of facades

4.3.5. Historical Evaluation

Briefly, the case study has a triangular façade form with series of semicircular arches in different sizes; the middle one is wide and sides are narrow. The keystones are visible in the arches. It has flat spandrel walls. It does not have relieving arches above the main arches, breakwaters in front of the piers and flood control arches. It has projected parapet stones, while it does not have belt under the parapet. It is a masonry structure out of rubble stone infill and cut stone blocks. According to these features, the case study is thought to be a Roman Period Anatolian viaduct (Table 4.1). This is also supported by laboratory analysis. The mortar sample taken from Hypokremnos Viaduct showed similar features with mortars used in Roman monuments in terms of raw material composition, basic physical, chemical, mineralogical and hydraulic properties, and pozzolanic activities of aggregates (see Appendix A).

Table 4.1. Dating of Hypokremnos Viaduct

Characteristic Features of Viaduct	Roman Period	Byzantine Period	Seljukid Period	Ottoman Period
Triangular form	✓	✓	✓	✓
Series of arches in different size	✓	✓	✓	✓
Visible keystone	✓			
Semicircular arches	✓	✓		
Flat spandrel walls	✓	✓		
Without relieving arch	✓			
Without flood control arch	✓			
Without belt	✓			
Parapet	✓			✓
Facing: Large cut stone blocks Infill: Rubble stone	✓	✓		
Facing: Small cut stone blocks Infill: Rubble stone			✓	✓
Mortar: Not seen in the joints (sea facade)	✓			
Mortar: Seen in the joints (coast facade)			✓	✓
Characteristics of the mortar	✓			

4.4. Restitution of Hypokremnos Viaduct

The characteristics of the site and the date of construction are the primary parameters that determine the form and construction technique of Anatolian Viaducts. Main aim of this section is restitution of the case study viaduct and determination of its structural details and construction phases with the help of the detailed photogrammetric 3D model (see Appendix B and C) and comparative study results presented in the previous sections of this study. Restitution of the site and the morphological characteristics need to be carried out before identifying structural details and construction phases.

4.4.1. Restitution of Site Characteristics

The necessity of connecting various ancient centers in the vicinity of Hypokremnos and the geographic characteristics of the site are the basic reasons behind the construction of the case study viaduct.

Site survey, comparative study and historical research were realized to solve restitution problems at site scale (see Section 4.1).

Based on the historical development of the region and comparative study results; the viaduct was thought to be constructed in Roman Period as a part of a series of viaducts passing the plateau of Hypokremnos as a part of the ancient road connecting Klazomenai, Teos and Erythrai (Figure 4.19, Figure 4.20).

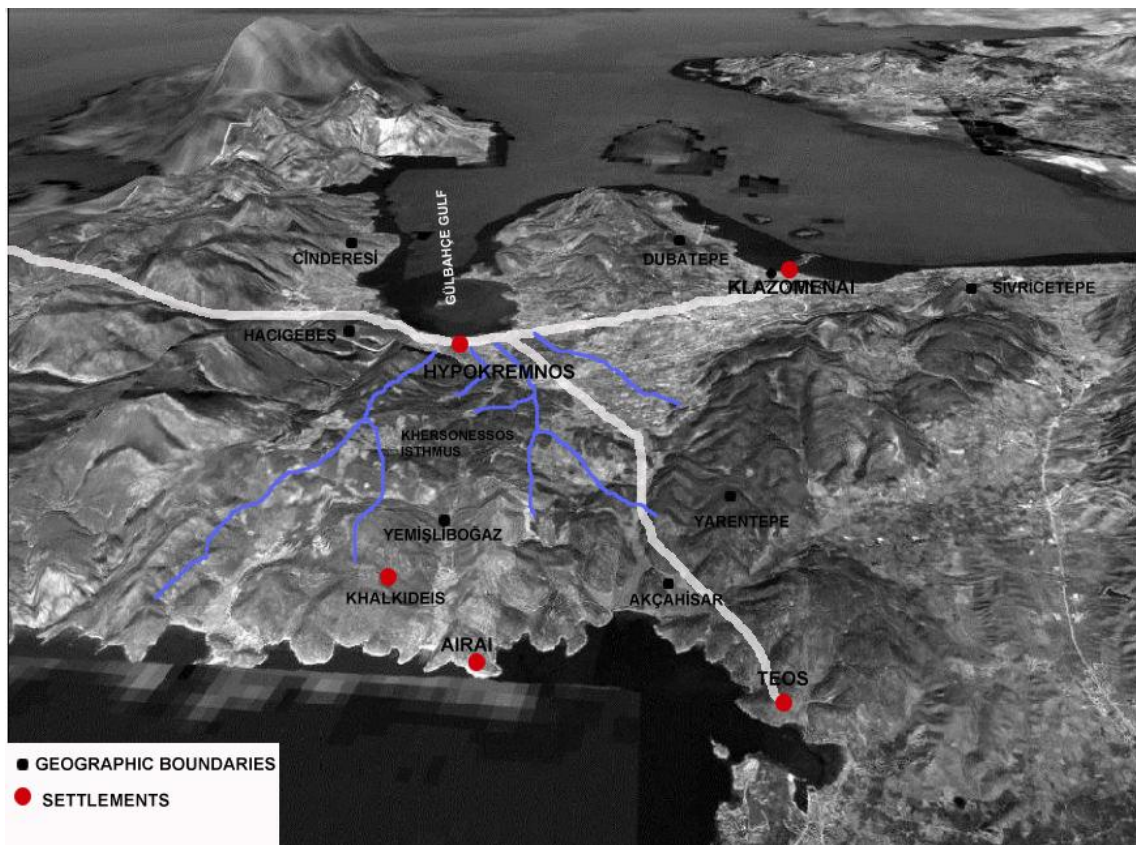


Figure 4.19. Ancient road passing through Hypokremnos
(Revised from: Koparal 2012)

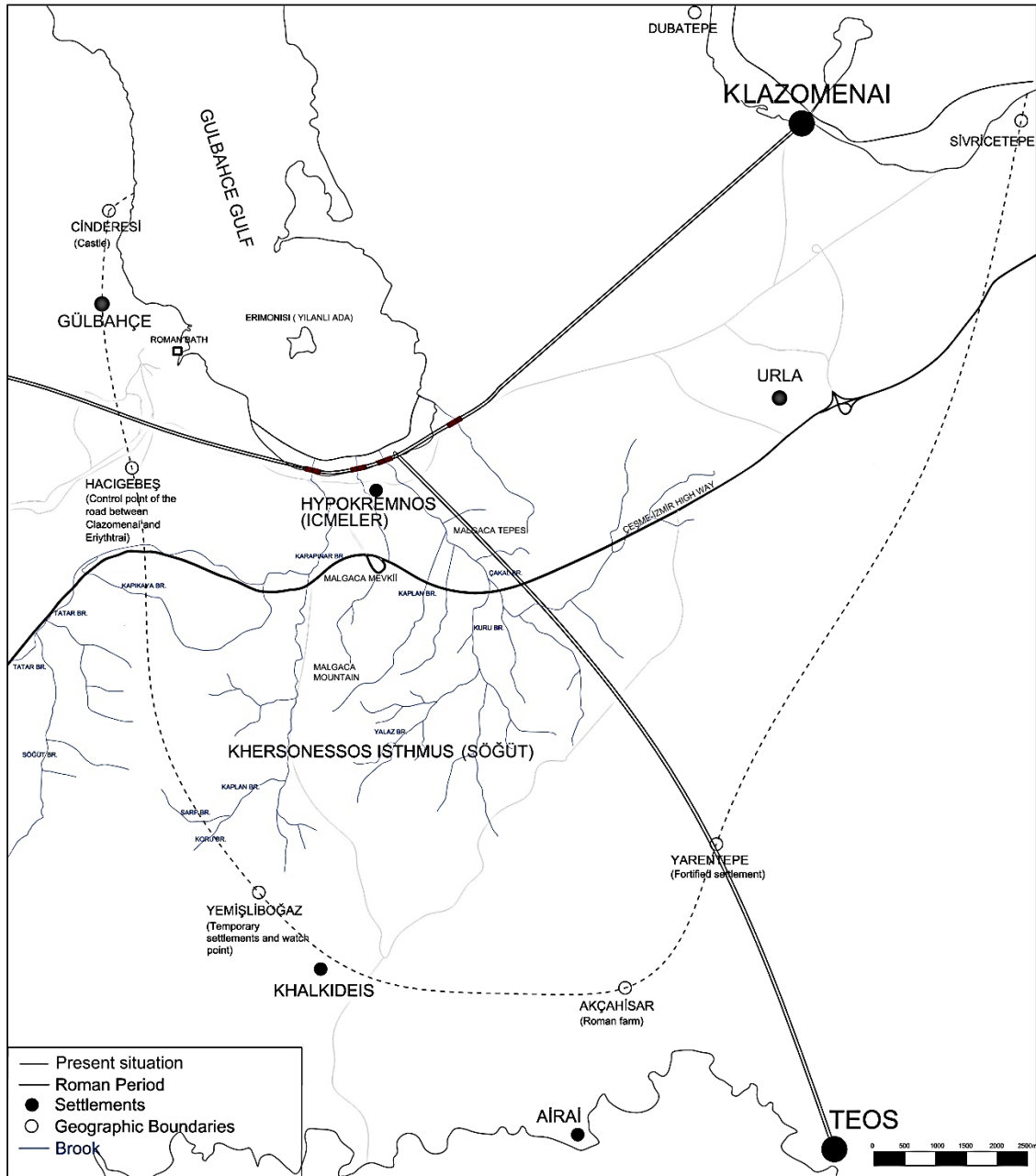


Figure 4.20. Hypokremnos Region in Roman Period

4.4.2. Restitution of Morphologic Characteristics

In Roman, Byzantine, Seljukid and Ottoman periods, masonry structures in linear forms carried with one or series of arches was the basic theme of viaducts.

Some parts of the studied viaduct were damaged due to the probable factors such as coast line change, ruining effects of waters of brooks and the sea and weathering. Both southeastern and northwestern sides are in ruined condition. Piers and some parts of the wall are underground. Main source for morphological restitution is the traces coming from the case study; second source is comparative study. If the wall remains on the ground and slope of the roadway are completed, the original form of the viaduct can be revealed. For underground parts, excavation is necessary. Within the limits of this study, an optimum height is determined based on the comparative study results on piers (Figure 4.21).

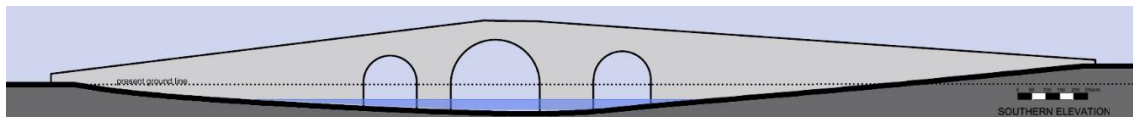


Figure 4.21. Restitution of southern facade

4.4.3. Restitution of Structural Characteristics

The aim of the restitution of structural characteristics is to identify structural system detail and possible sequence of the construction of the viaduct.

Comparative study was utilized for the structural restitution. This study was composed of two part; comparative study within the building and comparative study with other examples. Comparative study within the building was based on the detailed reality based 3D model.

4.4.3.1. Structural System Detail

3D measured survey includes 3D point clouds and 3D surfaces, which are visible, rather than their invisible structural components. Therefore core of the structural elements are not documented. The related representation is a reality based 3D model.

Restitution drawings are not directly produced from this 3D representation, but the irregular parts of the survey model representing the failures and deteriorations are made use of for extraction of information regarding the core of the structural elements (Figure 4.22).

In turn, data of the core of the structural elements were collected from the observable damaged parts distributed in the object (Table 4.2). These collected data from different parts of the object were brought together for restitution of structural system detail (Figure 4.23). Actually, this process, which is a conventional way for restitution, was referred as comparative study within the building. The second source of the restitution was comparative study with other examples for unobservable parts. The same type objects constructed in the same period were explored: Roman Bridges. In turn, the end result system detail includes data both from measured survey, which requires a reality based representation language, and also from historical research, which requires a virtual reality based representation language. A structural system detail that mixes the concepts of reality based and virtual reality based representations was produced (Figure 4.24).

Properties of main structural elements as piers, arches, walls, and components of these elements as cut stone blocks, rubble stone infill and floor coverings, mortars and architectural elements were taken from the different parts of the 3D model showing relations and dimensions of these elements (Figure 4.23). Then, unobserved parts, especially foundations, were completed with the data coming from comparative study with ancient Roman viaducts (see 4.3.4) (see Appendix D).

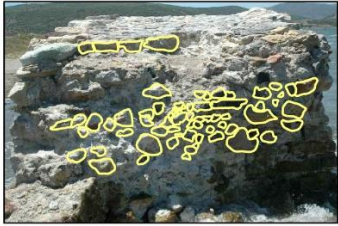


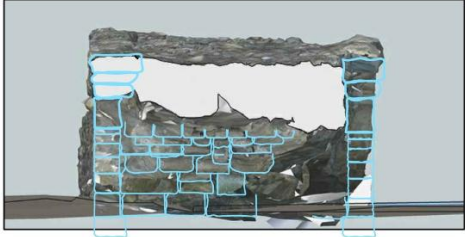


a	
b	
c	
d	
e	
f	

Figure 4.22. Data gathering positions

Table 4.2. Characteristics of Hypokremnos Viaduct

Element	Analyzed spot	View	Data	Graphic
Pierced wall	Cross section of northeastern arch	Section	Rubble stone (32x9, 19x9, 8x6, etc. cm) infill put together with lime mortar	a
Pierced wall	Longitudinal section of pier wall at the southeastern corner	Section	Rubble stone (9x18, 6x9, etc. cm) infill put together with lime mortar	b
Pierced wall	Southeastern façade of pier wall at the northwestern corner	Facade	Rough cut stone (46x13, 54x15, etc. cm) + thin mortar	c
Pierced wall	Northwestern façade of pier wall at the southwestern corner	Facade	Cut stone (44x25, 39x32, etc. cm) without mortar in the pointing	e
Pierced wall	Top view	Section	Rough cut stone (54x30, 46x30. etc. cm) put together with lime mortar	f
Arch	Longitudinal section of northeastern arch	Section	Vertical rough cut stone (14x34 cm)	b
Arch	Southeastern façade of northeastern arch	Facade	Cut stone (30x36 cm) without mortar in the pointing	c
Arch	Cross section of northeastern arch	Facade	Rough cut stone (14x61, 24x55 cm) without mortar in the pointing	d
Arch	Cross section of northeastern arch	Section	Ring stone (27x30, 30x36, etc. cm)	d
Arch	Cross section of northeastern arch	Facade	Ring stone (34x30 cm)	d
Pavement	Top view	Facade	Rubble stone (7x8, 6x13, etc. cm)	f
Pavement	Cross section of northeastern façade	Section	Rubble stone (13x14, 12x8, etc. cm)	a
Parapet	Cross section of northeastern arch	Section	Rough cut stone (20x48 cm)	d
Parapet	Eastern side of southeastern façade	Facade	Rough cut stone (20x38, 20x52, etc. cm)	c
Parapet	Top view	Facade	Rough cut stone (48x38, 48x52, etc. cm)	f

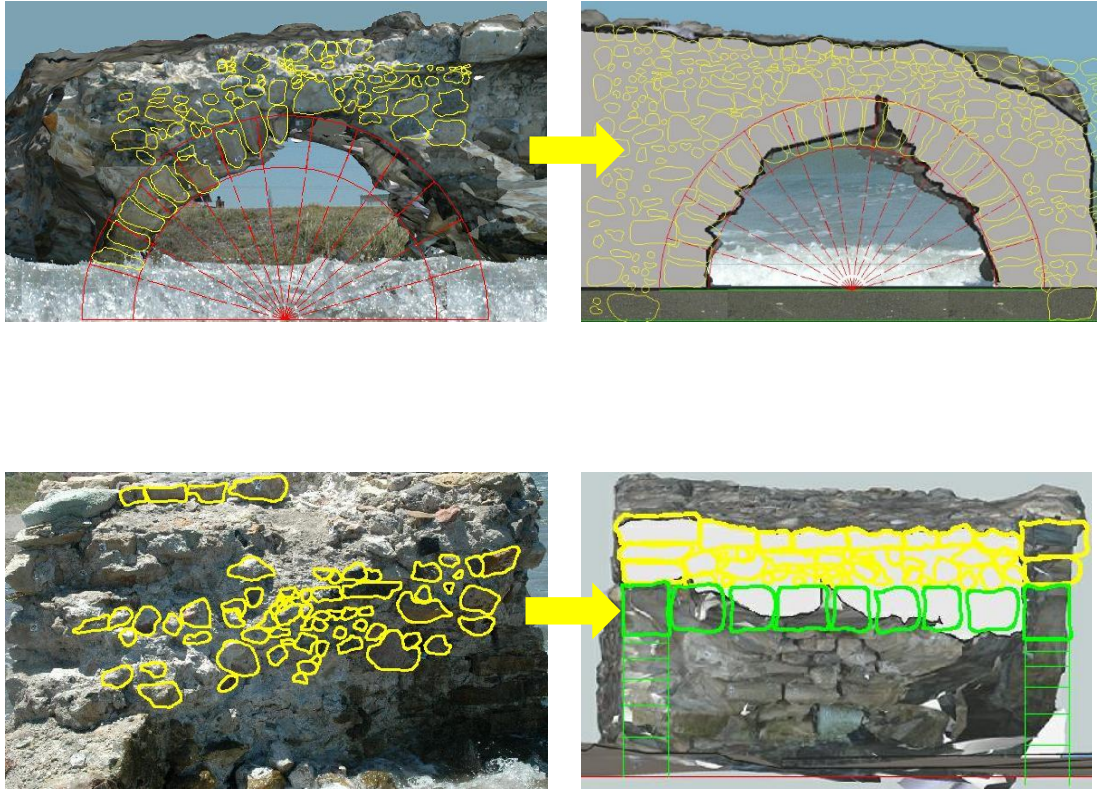


Figure 4.23. Bringing together data gathered from different parts of the object

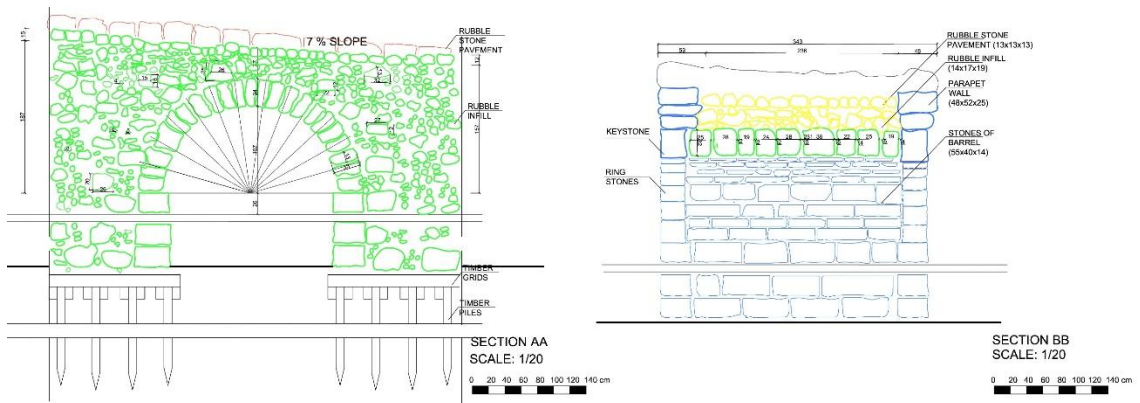


Figure 4.24. Structural system detail

4.4.3.2. Construction Phases of the Viaduct

Restitution model of the case study was based on the mixed structural system detail produced with comparative study within the building based on reality based 3D model (photogrammetric 3D model) and comparative study with Roman viaducts. Reality based 3D modeling technique was combined with virtual reality technique for the restitution model to present the construction phases of the viaduct. In turn, a mixed 3D model was produced.

These data are not sufficient for the decision of the construction phases of the viaduct. Phases are identified by supporting additional data coming from comparative study with Roman Viaducts. Twelve phases including construction of cofferdam, timber piled foundation, pier with facing and infill, centering and arch, spandrel wall, parapet and pavement could be identified. These are the twelve phases:

- Construction of wooden cofferdams (1)
- Emptying of water from the enclosed space (2)
- Construction of timber piled foundation system (3)
- Construction of double layered facing wall (4)
- Construction of rubble stone infill (5)
- Removal of wooden cofferdams (6)
- Construction of wooden centering and starting of the construction of ring stones of barrel arch (7)
- Construction of stone barrel arch (8)
- Placing of keystones of barrel arch (9)
- Completion of facing stones and rubble infill, removal of wooden centering (10)
- Construction of parapet walls (11)
- Covering of rubble stone pavement (12)

In accordance with these phases, the mixed model was structured with producing each structural element starting from ground to top in Archicad with constructive solid geometry technique. Each element was produced as a solid geometry; boundary representation technique was not used.

After the phases of the model composed of solid structures were completed by adding previous phase in Archicad, phases were transferred to Artlantis Studio

respectively. Artlantis Studio was used for the texturing phases. The appropriate textures and colors which were selected similar to original features of the material were added. Each photo of phases was captured with the same camera properties (Figure 4.25)

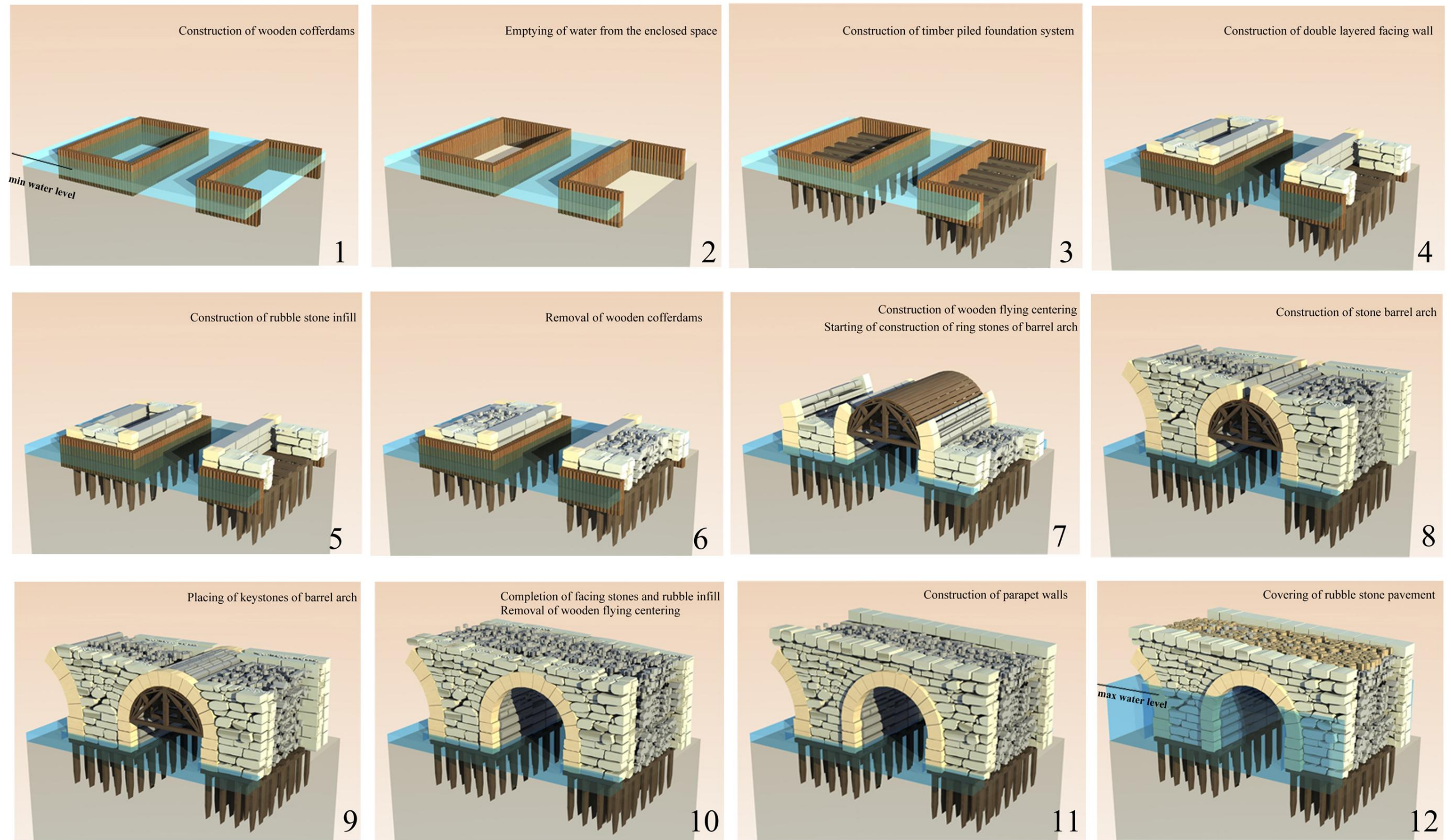


Figure 4.25. Construction phases of Hypokremnos Viaduct

CHAPTER 5

DISCUSSION

This thesis has focused on 3D modeling of ancient monuments based on photogrammetric documentation. Full automatization and manual operation of the documentation process was taken as a parameter defining the quality of the documentation. Four cases, all ancient structures in Western Turkey, were studied. One, the Hypokremnos Viaduct in Icmeler, Urla, Izmir was documented with manual and automatic photogrammetric techniques, whereas the other three were documented with only automatic ones. The Hypokremnos Viaduct is a 16.22 m long linear object with 3.49 m width and 1.93 m maximum height. It is an independent structure. The Paradiso Aqueduct, Buca, Izmir, is also a linear object (app. 120x3x20 m), whereas it is surrounded by shrubs and trees and a brook. The Pagos Cistern, Kadifekale, Izmir (app. 35.79x25x5.2 m) is a cubical object at a depressed position. The Nysa Library, Aydın (app. 25x14x4m) is a mass composed of two prisms which are independent, excluding some shrubs and debris. The variation in the form, size and displacement of the objects has been defined as the second parameter effective on the quality of the documentation. Another consideration of this thesis has been to develop a three dimensional way of documenting an ancient monument so that its structural characteristics can be interpreted. This aim was fulfilled with a set of experiments carried on the three dimensional model of the viaduct. In fact, automatic evaluation results are insufficient for providing data leading to structural evaluation. A 1/20 scale aimed for the viaduct in its manual documentation has produced a rich information set on its structural characteristics.

The results of the automatic and manual documentations for objects with different forms, sizes, and displacements are discussed below. Then, the efficiency of the manual method developed for interpreting of structural characteristics of an ancient monument is discussed with emphasis on the Hypokremnos Viaduct in Icmeler, Urla, İzmir.

5.1. Advantages and Disadvantages of Automatic Photogrammetric Evaluation Software

In this study, the performances of the automatic photogrammetric evaluation software Autodesk 123D and Photosynth were tested on a number of historical structures presenting different architectural characteristics. As a result of these studies, advantages and disadvantages of the automatic softwares are discussed. Two automatic softwares were compared with each other.

The major advantage of automatic techniques is the reduction they provide in data gathering and processing time. Sticking of targets on the surface of the monument is not necessary at the site. Taking photos parallel to the surface with surrounding around the building is the only process for the data gathering without the necessity of any further survey (Figure 5.1). In the office, calibration and orientation phases and surface construction phase depending on the software were carried out by the software automatically. This increases the processing speed and prevented extra labor at the site and the office.

The models produced with Photosynth and Autodesk 123D can be useful for overall decisions about the historical structures. They illustrate a reconstruction of the form of the monuments at 1/50 and 1/100 scale.

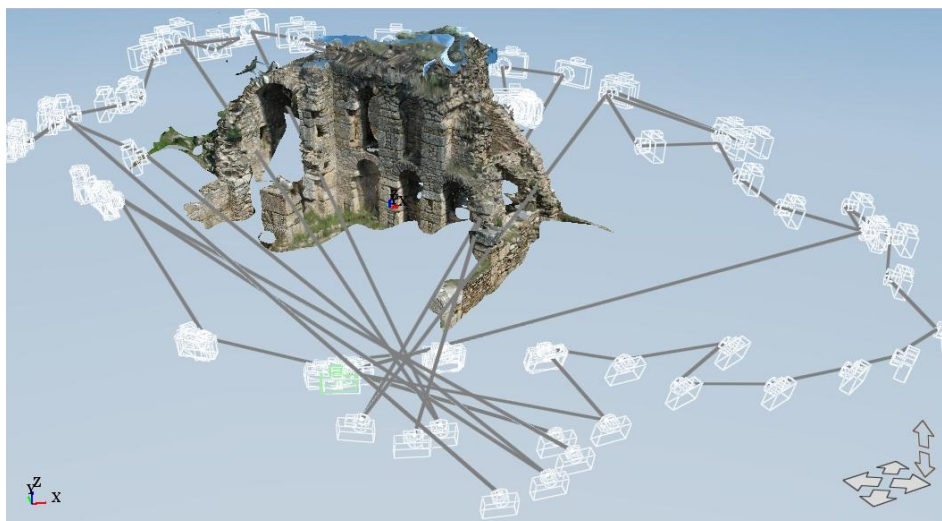


Figure 5.1. Model and photo positions by Autodesk 123D in Nysa Library



Figure 5.2. Unclear details by Autodesk 123D, in Nysa Library

As well as the advantages of automatic softwares, they have more drawbacks for the documentation of antique monuments. First, the automatic softwares do not provide an opportunity for viewing the accuracy of the measured point clouds, the related reality based models cannot be regarded as reliable sources for guiding the interventions.

The second drawback is lack of detail in the reality based model. Since the scales of the models cannot be reconstructed beyond the content of 1/50 scale, detail information including the amorphous surfaces of building material cannot be extracted from the models. In turn, structural intervention details cannot be planned based on the related documents (Figure 5.2)

The reality based models which were gained by automatic techniques have incomplete surfaces and holes, so the presentation of models is not satisfactory. If the shooting position is not parallel to the building or there are some occlusions blocking the building, software cannot orient the photos, and some parts of the model are discarded. Filling these holes with surfaces is not preferred since these parts do not represent the original surface of the monument (Figure 5.3).

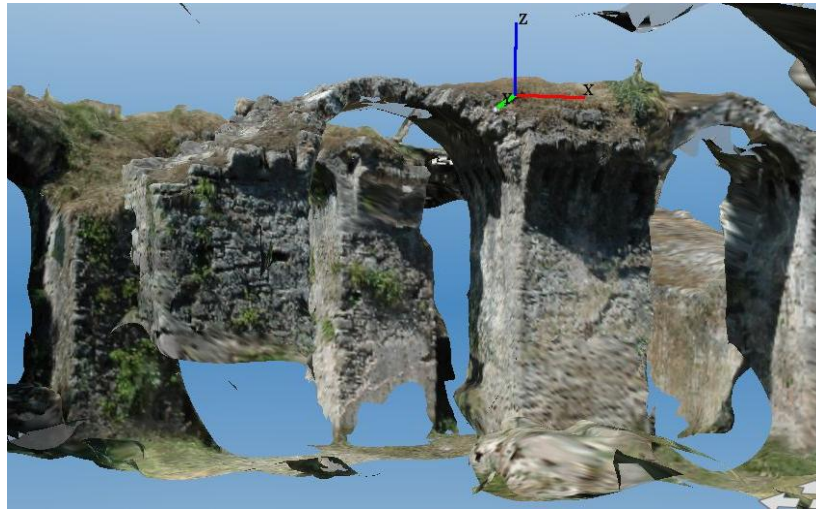


Figure 5.3. Incomplete surfaces by Autodesk 123D, in Pagos Cistern

If these two automatic approaches are compared with each other, Autodesk 123D produces more detailed models from Photosynth. Models with Autodesk 123D may be useful for guiding emergency interventions in 1/50 scale, while models produced with Photosynth and Meshlab complicate understanding of the form of the building (Figure 5.4).

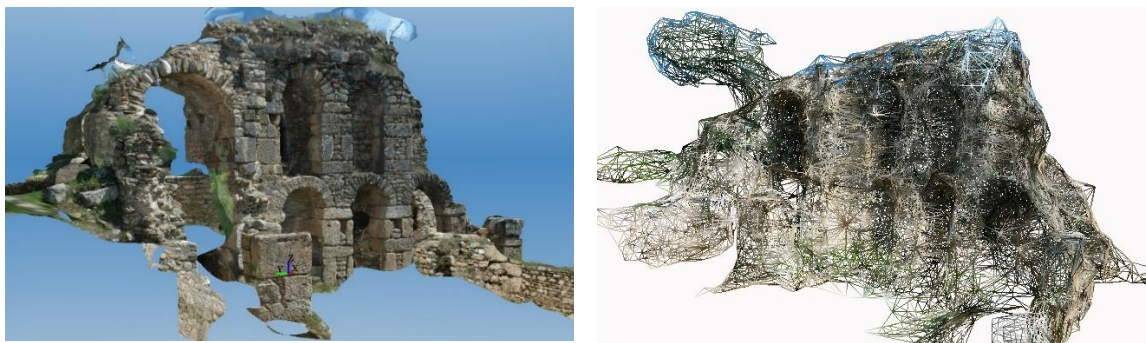


Figure 5.4. Comparison of models gained by Autodesk 123D and Photosynth+Meshlab in Nysa Library

When the reality based models of case studies which have different geometries, positions and restrictions produced with Autodesk 123D were compared, it is understood that Autodesk 123D requires all general photos, parallel shots and optimum shooting distance to give more satisfactory results.

- Reality based model of Pagos Cistern is unsatisfactory due to its depressed position. In turn, photos are not taken parallel to the object surface. With objects in depressed positions, shooting process is relatively difficult. The photographs of lower parts of the object present limited number of points, because they can be covered in less number of photographs, taken in more distance and with more tilt (Figure 5.5).

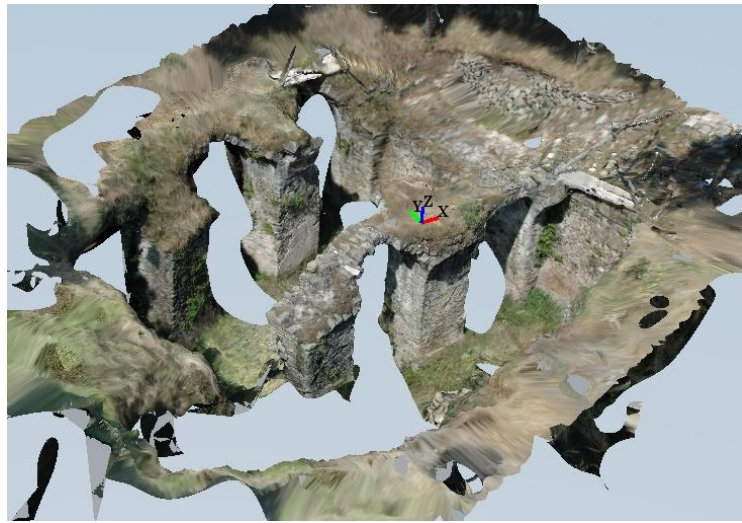


Figure 5.5. Model of Pagos Cistern by Autodesk 123D

- Reality based model of Paradiso Aqueduct is unsatisfactory due to its long and high form and shrubs, brook and trees restrictions (Figure 5.6). In turn, the restrictions just in front of the surface to be documented such as trees, shrubs, brook, etc. give way to long shooting distances (approximately 28 m). This problem was tried to be coped with choosing a different focal length, 55 instead of 28 in the case study. But, still, less detailed results were achieved compared to surfaces documented from shorter distances. The highness becomes a negative input because the photographs of the upper parts can be taken with more tilt.



Figure 5.6. Model of Paradiso Aqueduct by Autodesk 123D

- The reality based model of Hypokremnos Viaduct is moderately satisfactory since the roadway and the vaults cannot be shot parallel to their surfaces within general shots. Facades have photos taken parallel to their surfaces and modelled quite well. But the vaults and the roadway are problematic (Figure 5.7).

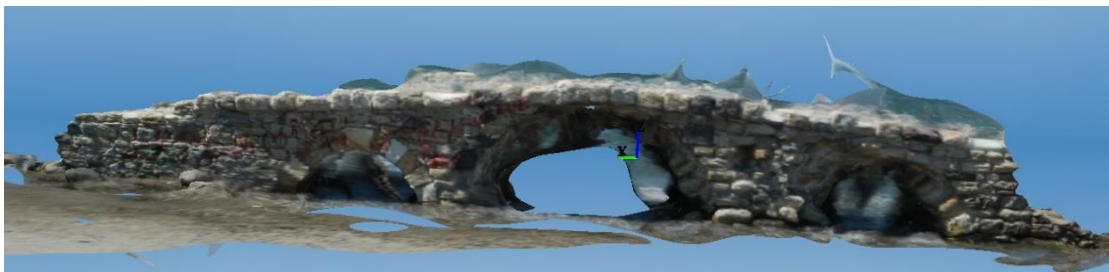


Figure 5.7. Model of Hypokremnos Viaduct by Autodesk 123D

- The reality based model of Nysa Library is relatively satisfactory due to its prismatic form and suitable site conditions. Parallel shots of exterior surfaces and general views can be taken by surrounding the monument (Figure 5.8).



Figure 5.8. Reality based model of Nysa Library by Autodesk 123D

5.2. Advantages and Disadvantages of Manual Photogrammetric Evaluation Software

Advantages and disadvantages of the manual evaluation; Tgi3D are discussed below according to its performance of documentation of Hypokremnos Viaduct.

The major advantage of manual technique is the opportunity of viewing the point errors of the point clouds. A list of point errors is presented by the software, since point error of each calibrated photo is calculated one by one. Two error values found according to this list were used in the calculation of the error of the model; maximum (max) error; the highest value and global error; the average value. When the maximum error value is high, calibration of the problematic photos has to be redone.

At last, by using these point errors (max and global), the error in the reality based model can be calculated. Therefore, the reality based model can be regarded as a reliable source for guiding the interventions.

Error is calculated considering the shot length of the object at the site and in the image. It is calculated according to formula in the below.

L = Shot length of the object at the site

N = Shot length of the object in the image

Error $\sim L/N \times$ pixel error

- Maximum error: 3.33 pixel

Error (max) $\sim L/N \times \text{pixel error (max)}$

Error (max) $\sim 345/3000 \times 3.33$

$\sim 0.38 \text{ cm}$

When 0.5 cm error is accepted for 1/20 scale for an architectural heritage, if the image size is 3000 pixels, object size in the image is 345 cm, point error is accepted as max 4.31 pixels. The end product model's max error is under this value, so model can be reliable for 1/20 scale structural detail drawings (Figure 5.9).

- Global error: 0.47 pixel

Error (global) $\sim L/N \times \text{pixel error (global)}$

Error (global) $\sim 345/3000 \times 0.47$

$\sim 0.05 \text{ cm}$

The error amount in the 1/1 scale presentation is around half of a millimeter which human eye can hardly detect. Therefore, the end product model's global accuracy is very high. In turn, this model can be used for 1/1 scale detail drawings (Figure 5.9).

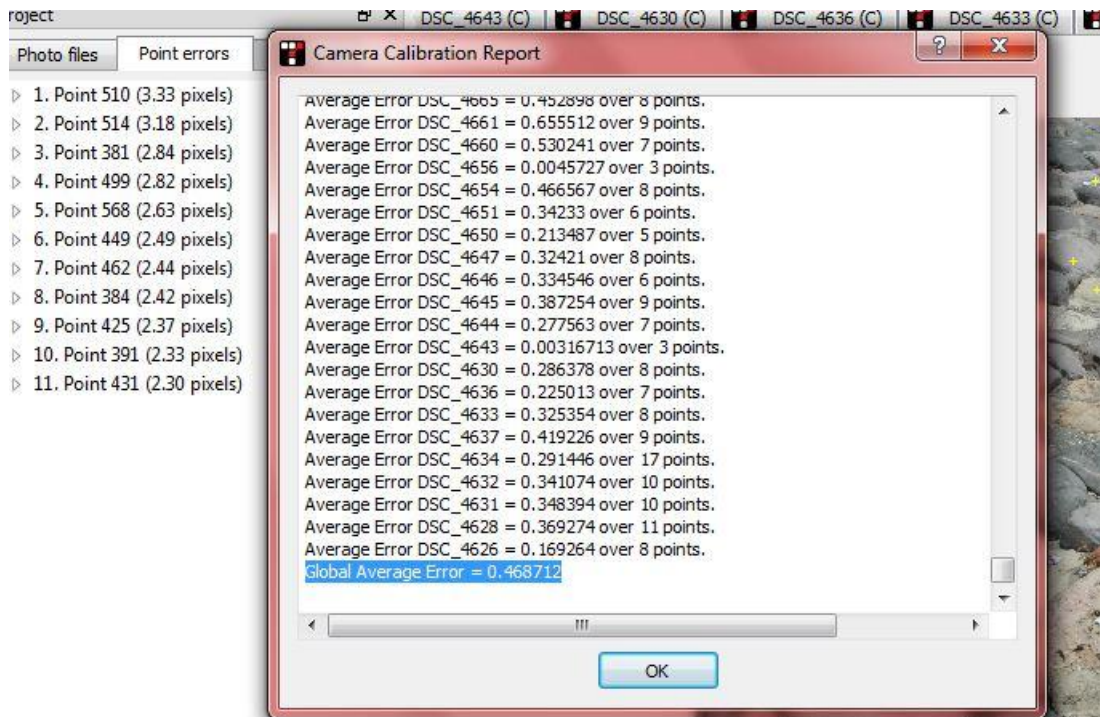


Figure 5.9. Maximum and global point error

The reality based model produced with manual software is sufficient for documentation of both overall shape of the monument and also structural elements in

detail (Figure 5.10). It was appropriate for especially 1/20 scaled system details and of course 1/50 scaled application drawings. It can be regarded as an important source for structural intervention decisions.

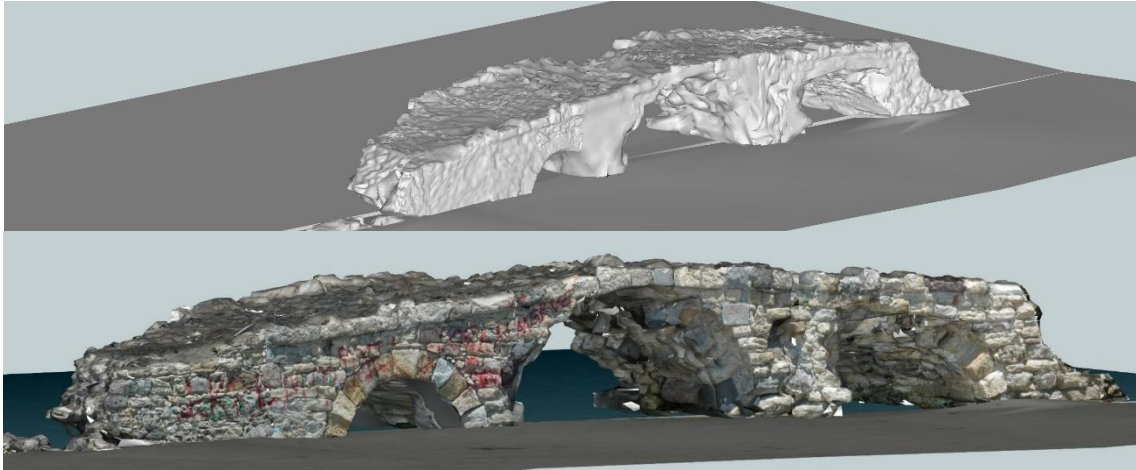


Figure 5.10. Models of Hypokremnos Viaduct by Tgi3D

All components and their amorphous surfaces of the case study are modeled in detail by Tgi3D. Features of both major structural elements such as arches, piers, and walls and their materials such as cut stone blocks, rubble stones, and mortar are documented. Reality based models can be regarded as important sources to produce structural system details (Figure 5.11).

Restitution model of the structural characteristics of the case study were produced based on mainly reality based 3D model (photogrammetric 3D model) and secondarily comparative study with Roman viaducts. Restitution model was developed by combining of virtual reality technique with reality based 3D modeling technique to present the construction phases of the viaduct. In turn, reality based 3D model provided production of a mixed 3D model of structural characteristics.

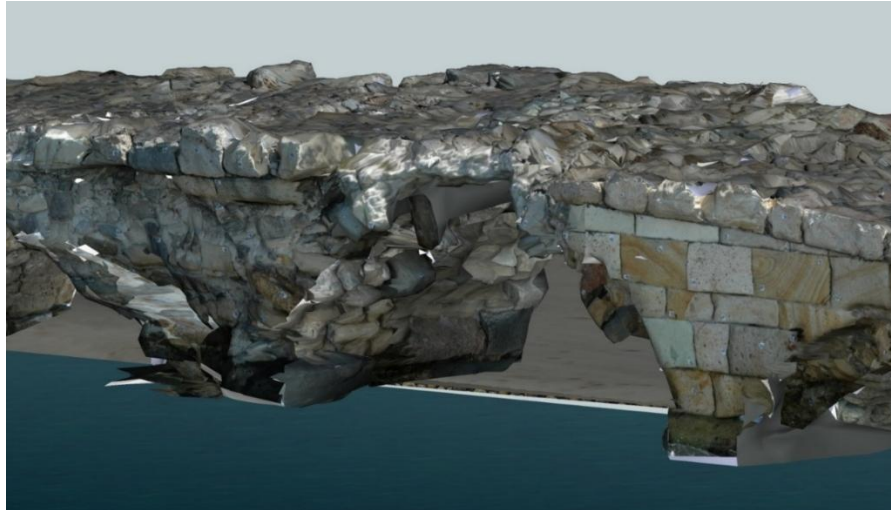


Figure 5.11. Detailed 3D model of Hypokremnos Viaduct by Tgi3D

The reality based model does not have incomplete surfaces and holes in comparison to automatic evaluations, since these missing parts can be filled by creating meshes. Then mesh surfaces are textured by using appropriate photos. This is the advantage of software directed by a human operator manually (Figure 5.12).



Figure 5.12. Orthographic view of the model without incomplete surfaces and holes

However, producing this detailed, satisfactory model takes a relatively long time. While working time at the site is short, data processing composed of calibration and modeling phases at the office is time consuming in comparison to automatic ones (Table 5.1).

Table 5.1. Duration of calibration and modeling

		Nysa Library	Paradiso Aqueduct	Pagos Cistern	Hypokremnos Viaduct
Autodesk 123D	Calibration+	40 minutes	35 minutes	20 minutes	30 minutes + 15 min (manual stitching time)
	Modeling Time				
Photosynth	Calibration Time	15 minutes	60 minutes	120 minutes	20 minutes
	Modeling Time	20 minutes	60 minutes	120 minutes +time of combining in SketchUp	20 minutes
Tgi3D	Calibration Time	-	-	-	420 hours
	Modeling Time	-	-	-	600 hours

In the calibration phase, each photograph was added one by one and calibrated. Firstly, 179 photos were calibrated. Then thirty one photos of floor were added to solve problematic parts on the floor of the viaduct. In the first ten photos, calibration time was two seconds. Then calibration time increased in direct proportion to number of photos; twenty four seconds in the fortieth photo, one minute and four seconds in the sixty third photo, seven minutes and thirty seconds in the 100th photo, forty five minutes twenty seconds in the 140th photo and one hour and thirty minutes in the 180th photo. Last calibration took one hour and thirty four minutes in the 210th photo (Table 5.2).

Table 5.2. Calibration time

Photo number	Calibration Time
10. photo	2 seconds
15. photo	4 seconds
40. photo	24 seconds
65. photo	1 minutes 4 seconds
100. photo	7 minutes 30 seconds
140. photo	45 minutes 20 seconds
180. photo	1 hour 30 minutes
210. photo	1 hour 34 minutes

According to these data, if all calibrations were carried out without any problems, all photos can be calibrated in approximately 170 hour. However, calibration of some photos was redone more than once due to the point errors recorded greater than 3.5 pixels. Therefore calibration time lasted approximately 420 hours.

Surface construction phase is also time-consuming. Meshes created with textures in SketchUp 8 have some problematic parts which should be edited.

- Problem of inclusion of sky, water and ground in the mesh due to the pixels illustrating the surroundings (Figure 5.13).
- Drooping problem due to the depth differences within the object surfaces (Figure 5.14).

While problem of inclusion of sky, water and ground in the mesh solved by deleting these parts by Eraser command, drooping problem was solved by repairing these parts by push-pull tool. Each part was deleted one by one not to damage the original surface of the model of the case study, and all drooping parts were pushed and pulled until reaching their original position. These editing processes extend the modeling phase twice.

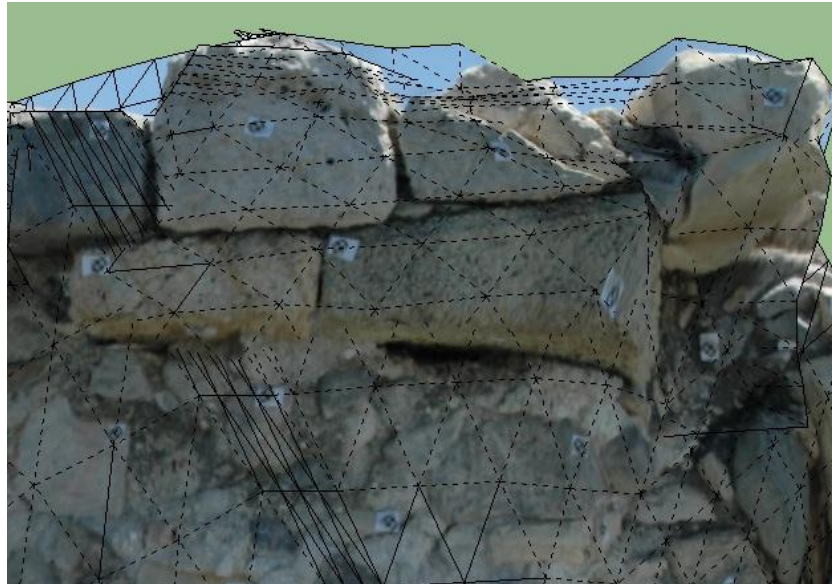


Figure 5.13. Problem of inclusion of sky

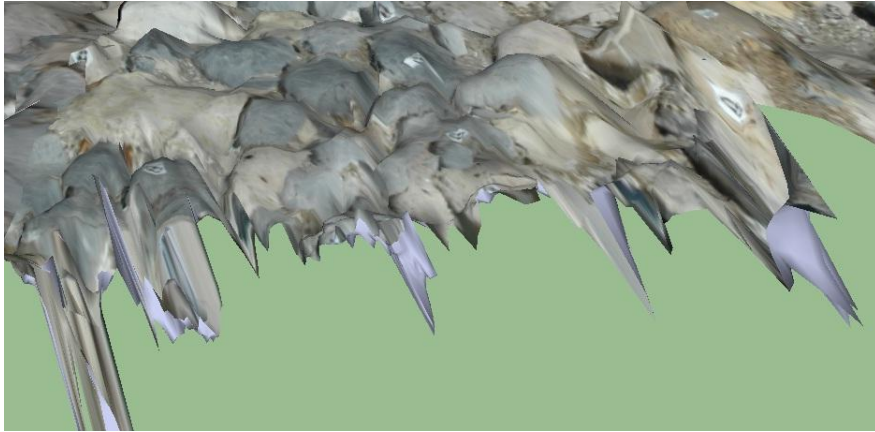


Figure 5.14. Drooping problem

CHAPTER 6

CONCLUSION

If guiding of construction details regarding restoration of an ancient structure is considered, manual photogrammetric technique, Tgi3D; is more sufficient than traditional and automatic photogrammetric documentation techniques in terms of accuracy control, level of geometric detail, working time and documentation of surfaces (Table 6.1).

With the help of manual photogrammetric software; Tgi3D, features of both major structural elements such as arches, piers, and walls and their materials such as cut stone block, rubble stone, mortar were documented in detail. If conventional techniques were preferred, sketches of small components would be necessary and they would be measured one by one. This means extra time and labor at the site. In spite of all these efforts, the results would be relatively less satisfactory. Since dimension of components are just measured as their width, length and height in a conventional survey, the produced drawing does not give any information about the amorphous surfaces of elements.

In comparison to a point cloud generated with a total station, results of automatic photogrammetric techniques are more promising in terms of documentation of amorphous surfaces. In a total station survey combined with traditional techniques, working time at the site and the office is relatively long. The general forms of the building elements can be documented.

Table 6.1. Evaluation of documentation techniques

	Total station documentation supported with traditional techniques	Automatic photogrammetric documentation	Manual photogrammetric documentation
Working time	-	++	+
Accuracy control	+	-	++
Level of geometric detail	+	-	++
Documentation of surfaces	-	+	++

Some problems can be observed in the manual evaluation due to the lack of experience of the operator. These problems are; clearness depending on tilted photos, brightness differences depending on the sun position and color differences between wet and dry surfaces (Figure 6.1). These problems are derived from inappropriate photos taken at the site. Solution of them is the main reason extending the working time at the office. To solve these problems, appropriate photos were chosen instead of problematic ones, and then recalibrated and modeled. Calibration and modeling phases were carried out twice. However, if the photos are taken by taking precautions for these problems at the beginning, working time can be decreased relatively in Tgi3D.

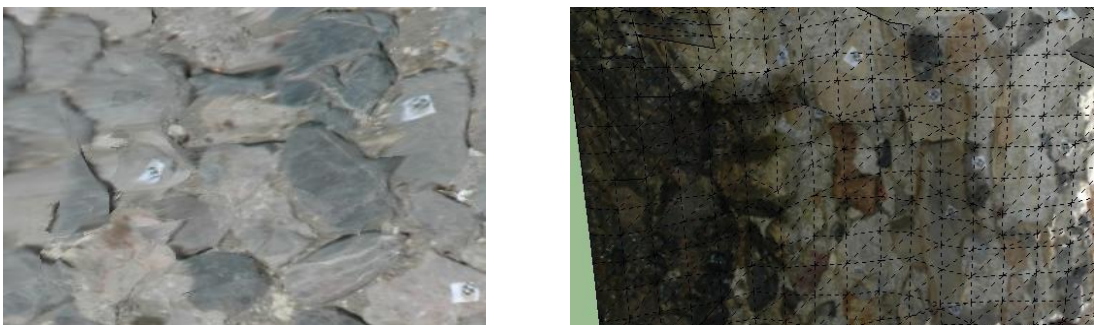


Figure 6.1. Tilted photos and color differences

Results gained from manual evaluation are sufficient for documentation of both overall shape of the monument in 1/50 scale and structural elements in 1/20 scale. In

addition to 1/50 and 1/20 scales, results of accuracy indicate that this model can be guided for 1/1 scale detail drawings.

This detailed reality based model facilitates to conceive the structural system detail and guides intervention decisions. Reality based models are also useful to prepare a step-by-step project for restoration following conservation principles.

By means of features mentioned in the above, reality based documentation technique enriches the content of documentation of a historical structure. Mixed structural system detail to be used in intervention decisions of structural system is produced with the help of the reality based 3D model (see Appendix B and C) without the necessity of any further documentation (Figure 6.2). In the development of this mixed system detail, not just a specific part of the viaduct is studied, data is collected from different parts of the object which have some deformations (Figure 6.3).

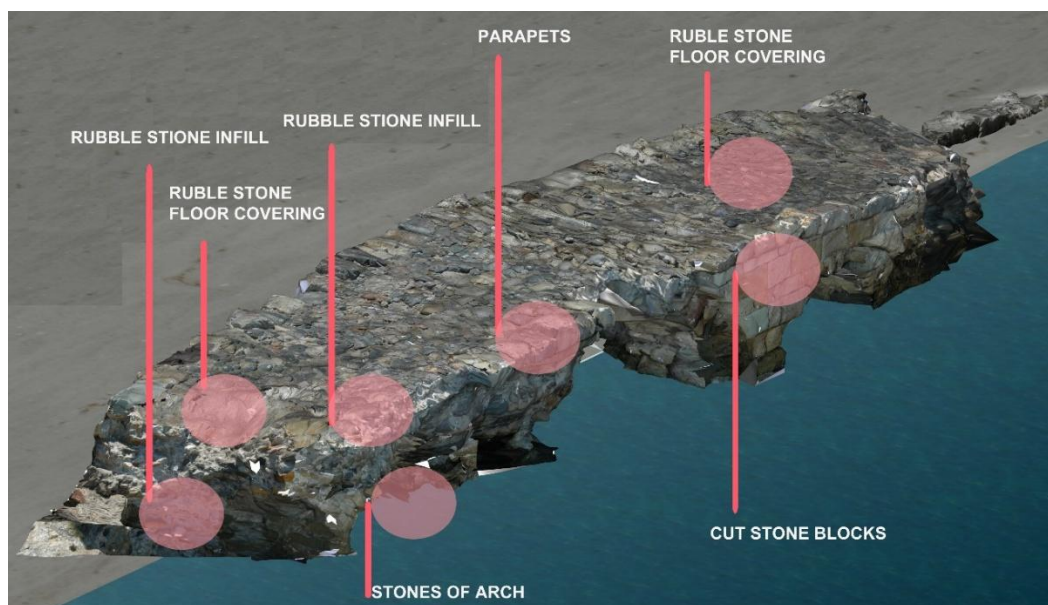


Figure 6.2. Analyzed spots on the reality based 3D model for system detail

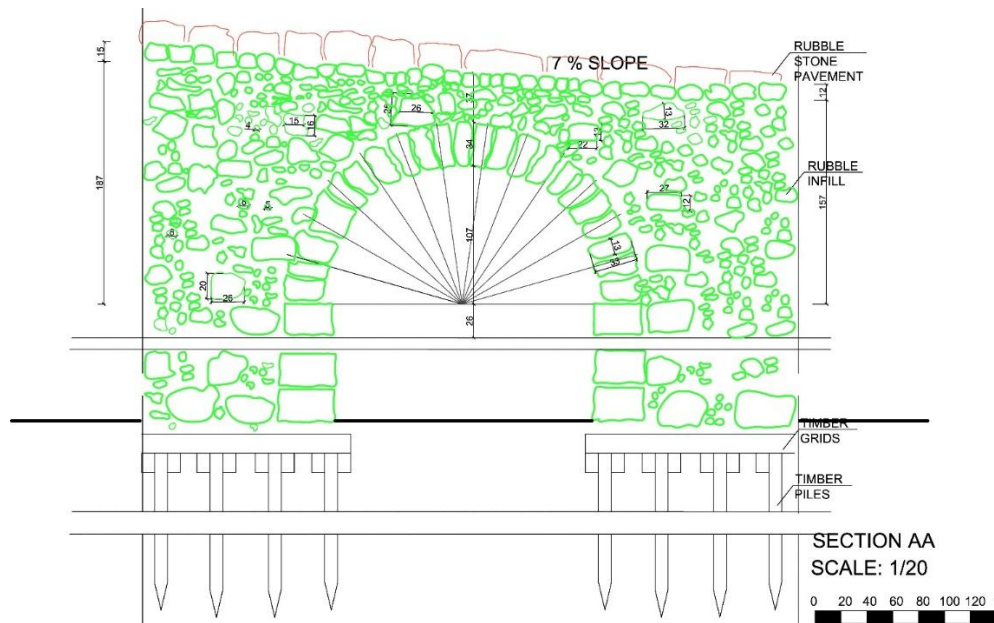


Figure 6.3. Structural system detail

Construction phases of the historical structure has been interpreted and presented in the mixed 3D model with reference to the mixed detail drawing based on reality based (photogrammetric) 3D model combined with virtual reality technique (Figure 6.4).

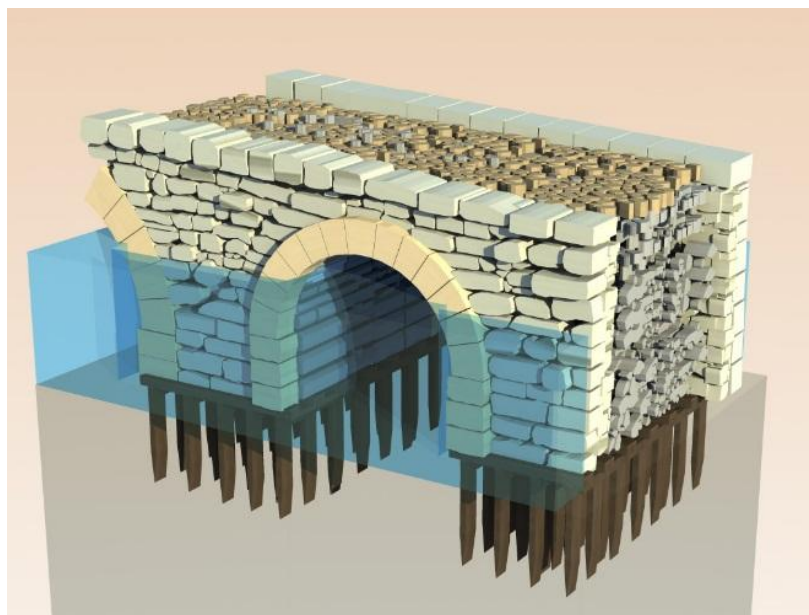


Figure 6.4. Structural system detail as view on the mixed 3D model

REFERENCES

- Adam, J. P. 2005. *Roman Building, Materials, and Techniques*. Translated by Anthony Mathews. London and Newyork: Routledge. 76-85, 119-145, 174-176.
- Annibale, E. 2011. *Image Based Modeling From Spherical Photogrammetry And Structure For Motion. The Case of the Treasury, Nabatean Architecture in Petra*. Proceedings of the 23rd International Symposium of the International Scientific Committee for Documentation of Cultural Heritage CIPA 2011. Prague, Czech Republic.
<http://cipa.icomos.org/fileadmin/template/doc/PRAGUE/038.pdf>.
- Arias, P., Herra'ez, J., Lorenzo, H. and Ordonez, H. 2005. *Control of Structural Problems in Cultural Heritage Monuments Using Close-Range Photogrammetry and Computer Methods*. Computers and Structures 83. 1754–1766.
- Atay, Ç. 2003. *Kapanan Kapılar İzmir Hanları*. İzmir: İzmir Büyükşehir Belediyesi Kültür Yayını. 32-39.
- Bakır, G. and Anlağan, G. 1980. *1979 Yılı Klazomeani Kazısı*. II. Kazı Sonuçları Toplantısı. 90.
- Barazzetti, L., Scaioni, M. and Remondino, F. 2010. *Orientation and 3d Modelling from Markerless Terrestrial Images: Combining Accuracy with Automation*. The Photogrammetric Record 25 (132). 356–381.
- Barazzetti, L., Binda, L., Scaioni, M. and Taranto, P. 2011. *Photogrammetric survey of complex geometries with low-cost software: Application to the 'G1' Temple in Myson, Vietnam*. Journal of Cultural Heritage 12. 253–262.
- Baykara, T. 1974. *İzmir Şehri ve tarihi*. İzmir: Ege Üniversitesi Matbaası. 26-31, 69-71.
- Baykara, T. 1976. *Urla Yarımadasın'da Bir Kervan Yolu*. II. Milletler Arası Türkoloji Kongresi Tebliğ Özetleri. İstanbul. 5-6.
- Bean, G. E. 1995. *Eski Çağda Ege Bölgesi*. İstanbul: Arion Yayınevi. 21-31, 108-126.
- Blachut, T.J. and Burkhardt, R. 1988. *Historical Development of Photogrammetric Methods and Instruments*. American Society for Photogrammetry and Remote Sensing, Falls Church, Va.

- Blais, F. 2004: *A Review of 20 Years of Range Sensors Development*. Journal of Electronic Imaging. 13(1). 231-240.
- Böhler W. and Heinz G. 1999. *Documentation, surveying, photogrammetry*. XVII CIPA Symposium. Recife, Olinda. Brazil. 1999. <http://www.i3mainz.fh-mainz.de/publicat/cipa99/cipa99.pdf>.
- Brown, D. J. 2001. *Bridges: The Thousand Years of Defying Nature*. USA: MBI Publishing Company. 19-21.
- Cadoux, C. J. 1938. *Ancient Smyrna; a History of the City from the Earliest Times to 324 A.D.* Oxford: Basil Blackwell. 38. 86-201.
- Callieri, M., Cignoni P., Dellepiane M., Ranzuglia G. and Scopigno R. 2011. *Processing a Complex Architectural Sampling with Meshlab: The Case of Piazza Della Signoria*. Proceedings of 4th International Workshop 3D-ARCH'2011 3D Virtual Reconstruction and Visualization of Complex Architectures. Trento. Italy.
- Cignoni, P., Callieri, M., Corsini, M., Dellepiane, M., Ganovelli, F. and Ranzuglia, G. 2008. *MeshLab: an Open-Source Mesh Processing Tool*. Proceedings of Eurographics Italian Chapter Conference.
- Cowan, H. J. 1977. *The Master Builders: A History of Structural and Environmental Design from Ancient Egypt to the Nineteenth Century*. New York: John Wiley & Sons.
- Çanakkale İli Private Website. 2009. <http://www.canakkaleili.com/bayramic-tas-kopru.html>.
- Çelenk, S. 2011. *Paradiso'dan Kızılçullu'ya*. İstanbul: Heyamola Yayınları. 13-17.
- Çulpan C. 2002. *Türk Taş Köprüleri; Ortaçağdan Osmanlı Devri Sonuna Kadar*. Ankara: Türk Tarih Kurumu Basım Evi. 1-17.
- Define Gizemi. 2013. <http://www.definegizemi.com/forum/tarihe-yolculuk/aizanoi-antik-kenti-cavdarhisar-kutahya-t19085.html>. (accessed June 16, 2013).
- Doğangün, A. and Ural, A., 2007. *Characteristics of Anatolian Stone Arch Bridges and a Case Study for Malabadi Bridge*. ARCH'07 – 5th International Conference on Arch Bridges. Madeira. Portugal. September 12-14. 179-186.
- El-Hakim, S.F., Beraldin, J.A., Picard, M. and Godin, G. 2004. *Detailed 3D Reconstruction of Large-Scale Heritage Sites with Integrated Techniques*. IEEE Computer Graphics and Application. 24(3). 21-29.

- Erkanal, H. 1997. *Liman Tepe: New Light on Prehistoric Aegean Cultures*. Proceedings of International Symposium: The Aegean in the Neolithic, Chalcolithic and the Early Bronze Age. Research Center for Maritime Archaeology (Anküsam). Ankara University. 179-190.
- Erkmen Senan. 2012. http://erkmensenan.blogspot.com/2012_09_23_archive.html.
- Ersoy, A. 2010 *Ancient Smyrna: Archeology in İzmir and Stratigraphy in Ancient City Centre*. Urban Historical Stratum: from Smyrna to İzmir, 132-137. The Scientific and technological research Council of Turkey.
- Ersoy, A., Çelik, G. and Yılmaz, S. 2011. *2010 Yılı Smyrna Antik Kenti Kazısı Raporu*. 33. Kazi Sonuçları Toplantısı 2. Cilt. 189-192.
- Ersoy, Y. 2011. *Urla – Klazomenai Kazısı, 2011 Yılı Çalışmaları, Sonuç Raporu*. <http://www.ttk.gov.tr/templates/resimler/File/Kazilar/2012/40-klazomenai.pdf>. (accessed June 16, 2013)
- Ersoy, A. 2012. *Smyrna (Izmir) History and Archeology*. International Earth Science Colloquium on the Aegean Region. IESCA-2012, 1-5 October 2012. Izmir. Turkey.
- Ersoy, Y. and Koparal, E. 2008. *Klazomenai Khorası ve Teos Sur İçi Yerleşim Yüzey Araştırması 2006 Yılı Çalışmaları*. 25. AST 3. Cilt. 28 Mayıs-01 Haziran 2007. Kocaeli. 47-70.
- Eyüce, Ö. 1992. *Köprüler*. İzmir: İzmir Yüksek Teknoloji Enstitüsü.
- Fellbaum, M., 1992. *Low-Cost Systems in Architectural Photogrammetry*. International Archives of Photogrammetry and Remote Sensing. XXIX. Part B5. Washington DC. 771-777.
- Foss, C. Mitchell, S and Reger, G. 1994. *Map 56 Pergamum*. Barrington Atlas of the Greek and Roman World: Map by Map Directory, Volume 1. Princeton University. 847.
- Goodman, B., Reinhardt, E., Dey, H., Boyce, J., Schwarcz, H., Sahoglu, V., Erkanal, H., and Artzy, M. 2008. *Evidence for Holocene Marine Transgression and Shoreline Progradation Due to Barrier Development in Iskele, Bay of Izmir, Turkey*. Journal of Coastal Research. Vol.24 No.5: 1269-1280.
- Grimm, A. 2007. *The Origin of the Term Photogrammetry*. The Photogrammetric Week 2007. Stuttgart. Germany.

- Gruen, A., Remondino, F. and Zhang, L. 2004. *Photogrammetric Reconstruction of the Great Buddha of Bamiyan*. The Photogrammetric Record 2004. 19. 177-199.
- Grussenmeyer, P., Hanke, K., Streilein, A., 2002. *Architectural photogrammetry*. Digital Photogrammetry. Edited by M. Kasser and Y. Egels, Taylor & Francis. 300-339.
- Guidi, G., Remondino, F., Russo, M., Rizzi, A., Voltolini, F., Menna, F., Fassi, F., Ercoli, S., Masci, M. E. and Benedetti B. 2008. *A Multi-Resolution Methodology for Archeological Survey: The Pompeii Forum*. Proceeding of 14th International Conference on Virtual Systems and Multimedia. Limassol, Cyprus.
- Hiesel, G. and Strocka, V. M. 2006. *Die Bibliothek von Nysa am Mäander, Vorläufiger Bericht über die Kampagnen 2002–2006*. Originalbeitrag erschienen in: Archäologischer Anzeiger 2. 81-97.
- Hodge Trevor, A. 2005. *Roman Aqueducts & Water Supply*. London: Gerald Duckworth & Co. Ltd. 136.
- Honkavaara, E. 2008. *Calibrating Digital Photogrammetric Airborne Imaging Systems Using a Test Field*. Ph.D. Thesis. Finland: Helsinki University of Technology, Espoo, Finland.
- Horn, B. K. P. and Brooks, M. J. 1989. *Shape from Shading*. Cambridge: MIT Press. 577.
- İdil, V. 1993. *Nysa Kazısı 1992 yılı Çalışmaları*. XV.Kazı Sonuçları Toplantısı. Ankara. 115-120.
- İdil, V. 1999. *Nysa and Acharaca*. İstanbul: Yaşar Eğitim ve Kültür Vakfı. 95-124.
- İstanbul Tv 2013. <http://www.iamistanbul.tv/haber/cobancesme-koprusu.html>. (accessed June 16, 2013).
- Jedrzejewska, H. 1981. *Ancient Mortars as Criterion in Analysis of Old Architecture*. Proceedings of Symposium on Mortars. Cements and Grouts Used in the Conservation of Historic Buildings. Rome. (1981). 311-329.
- Kadioğlu, M. and Kadioğlu, Y. K. 2008. *Native of the marble in ancient city, Nysa on the Meander of Hellenistic and Roman Period, Aydin, Western Anatolia, Turkey*. Donald D Harrington Symposium on the Geology of the Aegean IOP Publishing IOP Conf. Series: Earth and Environmental Science 2. 2-7.

- Karayolları Genel Müdürlüğü. 2008. *Tarihi Köprüler Müdürlüğü Çalışmaları, Yurt İçindeki Onarım Envanteri*. Köprüler Dairesi Başkanlığı. Tarihi Köprüler Şubesi.
<http://www.kgm.gov.tr/SiteCollectionDocuments/KGMdocuments/MerkezBirimler/SanatYapilariDairesiBaskanligi/Calismalar/TarihiKopruler/Calismalar.pdf>. (accessed June 30, 2013).
- Kiepert, H. 1869. *Map of Asiatic Interior*. Atlas Antiquus: Zwölf Karten zur Alten Geschichte. Berlin: D. Reimer.
- Kiepert, H. 1890. *Map of the Western Part Asia Minor*. Berlin: Dietrich Reimer. 1890-1892.
- Koparal, E. 2012. *Klazomenai Khora'sında Savunma Sistemi*. İsmail Fazlıoğlu Anı Kitabı. Edirne: Trakya Üniversitesi Sosyal Bilimler Enstitüsü. 2012/3. 139-146.
- Lensch, H.P.A., Kautz, J., Goesele, M., Heidrich, W. and Seidel, H.P. 2003. *Image-Based Reconstruction of Spatial Appearance and Geometric Detail*. ACM Trans. Graph. 2003. 22. 234-257.
- Luxan, M.P., Madruga, F. and Saavedra, J. 1989. *Rapid Evaluation of Pozzolan Activity of Natural Products of Conductivity Measurement*. Cement and Concrete Research. Vol. 19. 63-68.
- Manferdini, A. M. and Remondino F. 2012. *Reality-Based 3D Modeling, Segmentation and Web-Based Visualization*. International Journal of Heritage in the Digital Era. Volume 1. Number 1. 103-124.
- Mark, R. 1993. *Architectural Technology up to Scientific Revolution*. England. London: MIT Press. 68-69.
- Mater, B. 1982. *Urla Yarımadasında Arazinin Sınıflandırılması ile Kullanılışı Arasındaki İlişkiler*. İstanbul: İstanbul Üniversitesi Edebiyat Fakültesi Matbaası.
- Meriç, A. E, Öz, A.K. and Uhri, A. 2012. *Urla Söğüt Kutsal Alanı Seramik Buluntularının Değerlendirilmesi*. Edebiyat Fakültesi Dergisi. 1/1: 40-54.
- Meydenbauer, A. 1912. *Handbuch der Messbildkunst*. Wilhelm Knapp. Halle, Saale.
- Milioris, N.E. 2002. *1922 Öncesinde Urla*. Translated by Caymaz, T. Bilim Ofset Basım Yayın ve Tic. Ltd. Şti. Konak. İzmir.

- Özbay, F. 2006. *Klazomenai'deki M.Ö. 4.yy Yerleşimi*. Doktora Tezi. Ege Üniversitesi. İzmir.
- Öziş, Ü. Özdemir Y., Kosova A. and Çördük, A. 1999. *İzmir'in Tarihi Su Getirme Sistemleri*. İzmir Su Kongresi Bildirisi. 4-5 Haziran 1999. İzmir. Pg.
- Panoramio. 2007. <http://www.panoramio.com/photo/638013>. (accessed June 16, 2013).
- Pomaska, G. 2009. *Utilization of Photosynth Point Clouds for 3D Object Reconstruction*. Proceedings of the 22nd International CIPA Symposium, October 11-15. Kyoto, Japan.
- Remondino, F. and El-Hakim, S. 2006. *Image -based 3D Modeling: A Review*. 21 (115). 269-291.
- Remondino, F. 2011. *Heritage Recording and 3D Modeling with Photogrammetry and 3D Scanning*. Remote Sensing 3. 1104-1138.
- Rosnell, T. and Honkavaara E. 2012. *Point Cloud Generation from Aerial Image Data Acquired by a Quadcopter Type Micro Unmanned Aerial Vehicle and a Digital Still Camera*. Sensors. 2012, 12. 453-480.
- Salonia P., Bellucci V., Scolastico, S., Marcolongo, M. and Leti Messina, T. 2007. *3D Survey Technologies for Reconstruction, Analysis and Diagnosis in the Conservation Process of Cultural Heritage*. Proceedings of Cipa 2007 XXI International Symposium. Anticipating the Future of the Cultural Past. Athens.
- Salonia, P., Scolastico, S. Pozzi, A., Marcolongo, A. and Messina, T. L. 2009. *Multi-scale cultural Heritage Survey: Quick Digital Photogrammetric Systems*. Journal of Cultural Heritage 10S (2009). 59-64.
- Santos, M. H. R. 2000. *Lisbon Downtown of Pombal, Past and Future*. Livros Horizonte. Portuguese.
- Strabo, 7 BC. *The Géographica*. Translated by Hamilton, H.C. Geography of Strabo, Volume III. Book XVI. 1854-1857. 17-24.
- Streilein, A., 1994. *Towards Automation in Architectural Photogrammetry: CAD-Based 3-D Feature Extraction*. ISPRS Journal of Photogrammetry and Remote Sensing. 49 (5). 4-15.
- Swallow, P., Dallas, R., Jackson, S. and Watt D. 2004. *Measurement and Recording of Historic Buildings*. United Kingdom: Donhead Publishing. 142-163.

- Şengün, B. 2007. *Urla Tarihi Kent Merkezindeki Konut Mimarisinin İncelenmesi ve Cumhuriyet Döneminde Meydana Gelen Değişimlerin Koruma Bağlamında İrdelenmesi: Zafer Caddesi Örneği*. MS.C. Thesis. Dokuz Eylül University. İzmir. 22-42.
- Tanyeli, G. 2000. *Türkiye'nin Köprüleri*. Türkiye'nin Köprüleri. İstanbul: Koç Allianz Hayat Sigorta A.Ş.
- Texier, C. 2002. *Küçük Asya; Coğrafyası, Tarihi ve Arkeolojisi*. Ankara: Enformasyon ve Dokümantasyon Hizmetleri Vakfı. 139-148, 247-249.
- Tgi3D. 2010. <http://www.Tgi3D.com>. (accessed June 16, 2013).
- Tok, E. 1997. *Türkiye'de Orta ve Son Bizans Dönemi Kiliselerinde Cephe Düzeni*. İzmir: Ege Üniversitesi, Edebiyat Fakültesi, Sanat Tarihi Bölümü.
- Toksöz, C. 1960. *İzmir Tarih ve Arkeoloji*. Ankara: Ayyıldız Matbaası. 10-19.
- Toksöz, C. 1970. *İzmir and Historical Cities of Aegean*. İstanbul: Çınar Matbaacılık. 14-16.
- Tunç, G. 1978. *Taş Köprülerimiz*. Ankara: Karayolları Genel Müdürlüğü Matbaası. 5-8.
- Uğurlu, E. 2005. *Characterization of Horasan Plasters from Some Ottoman Baths in İzmir*. M.Sc. Thesis. Izmir Institute of Technology. İzmir.
- Uğurlu Sağın, E. 2012. *Characteristics of Roman Mortars Produced from Natural and Artificial Puzzolans in Aigai and Nysa*. P.Hd. Thesis. Izmir: Izmir Institute of Technology.
- Ural A, Oruç Ş, Doğangün A. and Tuluk Ö İ. 2008. *Turkish Historical Arch Bridges and Their Deteriorations and Failures*. Engineering Failure Analysis. 15. 43–53.
- Uygun, F. 2011. *Digitizing and Visualization of a 3D Model*, Supervisor: Prof. Dr. Günter Pomaska, Fachhochschule Bielefeld, Minden, Germany.
- Ward-Perkins, J.B., 2003, *History of World Architecture Roman Architecture*, Milano:Electa Architecture Mondadori Electa Spa. 153-181.
- Weber, G. 1889. *İzmir'in Su Yolları*. Translated by: İzmir: İzmir Büyükşehir Belediyesi, 41-50.

Wikipedia. 2013. *Cisterns in Istanbul*.

http://en.wikipedia.org/wiki/Category:Cisterns_in_Istanbul. (accessed May 6, 2013)

Wikipedia. 2010. *Virtual Reality*. http://en.wikipedia.org/wiki/Virtual_reality. (accessed date July 02, 2013)

Yapucu Pullukçuođlu, O. 2011. *Bati Anadolu'nun Yol Ađı Arařtırmaları- III İzmir Ardalarında Kervan Yolları*. Tarih İncelemeleri Dergisi. Volume XXVI, Number 2, 2011, 527-549.

Yapucu Pullukçuođlu O. and Özgün, C. 2011. *Bati Anadolu'nun Yol Ađı Arařtırmaları- III, İzmir'in Ardalanında Kervan Yolları*. Tarih İncelemeleri Dergisi. Volume XXVI. Number 2. 527-549.

Yıldız, N. 2003. *Antikçađ Kütüphaneleri*. İstanbul: Arkeoloji ve Sanat Yayınları. 281-285.

APPENDIX A

MATERIAL CHARACTERISTICS OF THE MORTAR SAMPLE FROM HYPOKREMNOS VIADUCT

The mortar sample taken from Hypokremnos Viaduct was analyzed in order to determine its raw material composition, basic physical, chemical, mineralogical, and hydraulic properties, and pozzolanic activities of aggregates (Figure A.1).



Figure A.1. Sampling

- Basic Physical Properties

Bulk density and porosity values describe the basic physical properties of material. Basic physical properties were determined by standard test methods (Rilem 1980).

M_{sat} = Saturated weight of the sample (g)

M_{dry} = Dry weight of the sample (g)

M_{arch} = Archimedes weight of the sample (g)

$$\text{Porosity (P) (\%)} = [(M_{\text{sat}} - M_{\text{dry}}) / (M_{\text{sat}} - M_{\text{arch}})] \times 100$$

$$\text{Density (D) (g/cm}^3\text{)} = M_{\text{dry}} / (M_{\text{sat}} - M_{\text{arch}})$$

Table A.1. Basic physical properties of lime mortars used in the walls of Hypokremnos Viaduct

Use of Mortar	Density	Porosity
F 1	1.4370	38.1
F 2	1.5943	33.4

Table A.2. Basic physical properties of lime mortars determined by previous studies (Source: Uğurlu Sağın 2012)

Roman Building/ Site (Reference)	Density	Porosity
Aigai- Manisa (Turkey) (Rubble core of the wall) (Uğurlu Sağın 2012)	1.41-1.72	31.05-40.29
Nysa – Aydın (Turkey) (Wall-Mortared rubble throughout) (Uğurlu Sağın 2012)	1.39-1.84	24.79-44.55
The Markets of Trojan- Rome (Italy) (Jackson, et al. 2009 quoted from Uğurlu Sağın 2012)	1.43-1.79	-

Density and porosity values of lime mortars from Hypokremnos Viaduct were almost in the same range with lime mortars used in several Roman period buildings (Table A.1, Table A.2).

- Raw Material Characterization

Raw material compositions of mortars were described by lime/aggregate ratios and particle size distributions of aggregates. Binder-aggregate ratios of the mortars were determined by dissolving the carbonated lime (CaCO₃) from aggregates (Jedrzejewska 1981).

$$\text{Insoluble \%} = [(M_{\text{sam}} - M_{\text{agg}}) / (M_{\text{sam}})] \times 100$$

$$\text{Acid Soluble \%} = 100 - \text{Insoluble \%}$$

Where;

M_{sam} = Dry weight of the sample (g)

M_{agg} = Dry weight of the aggregates (g) (Uğurlu 2005).

Lime transforms into carbonated lime when it reacts with carbon dioxide (CO₂) in the atmosphere. According to the molecular weights as shown in the equation above, 100 gram carbonated lime derives from 74 gram lime. Therefore, lime/aggregate ratio was calculated as following (Uğurlu 2005):

$$\text{Aggregate \%} = (100 \times \text{Insoluble}) / [((\text{Acid Soluble \%} \times \text{M.W.Ca(OH)}_2) / \text{M.W.CaCO}_3) + \text{Insoluble \%}]$$

$$\text{Lime \%} = 100 - \text{Aggregate \%}$$

where;

M.W.CaCO₃ = Molecular weight of CaCO₃ which is 100.

M.W.Ca(OH)₂ = Molecular weight of Ca(OH)₂ which is 74 (Uğurlu 2005).

Table A.3. Lime/ Aggregate ratios of samples from Hypokremnos Viaduct

	Magg	Msam	Insoluable%	Acid soluble %	Aggregate%	lime%	lime/agg
F 1	5,2385	13,5085	61,22	38,78	68	32	0,47
F 2	12,2098	25,4293	51,99	48,01	59	41	0,68
F average	8,7	19,5	56,6	43,4	63,7	36,3	0,6

Lime/aggregate ratios of mortar in Hypokremnos Viaduct were found as 0.6 in average (Table A.3). Lime/aggregate ratios of mortars is 0.22 - 0.64 in Nysa Library, 0.5 - 1 in Saint Callistus and Domitilla catacombs in Roma, Italy. Lime/aggregate ratios of lime mortars From Hypokremnos were similar to the lime/aggregate ratio values of lime mortars from different Roman period buildings.

Determination of particle sizes of aggregates was carried out by sieving them through a series of sieves (Retsch mark). It has the sieve sizes of 53 µm, 125 µm, 250 µm, 500 µm, 1180 µm by using an analytical sieve shaker (Retsch AS200) (Uğurlu 2005). Aggregates which had particals in 500 µm sizes are the 56.7 % of particals (Figure A.2).

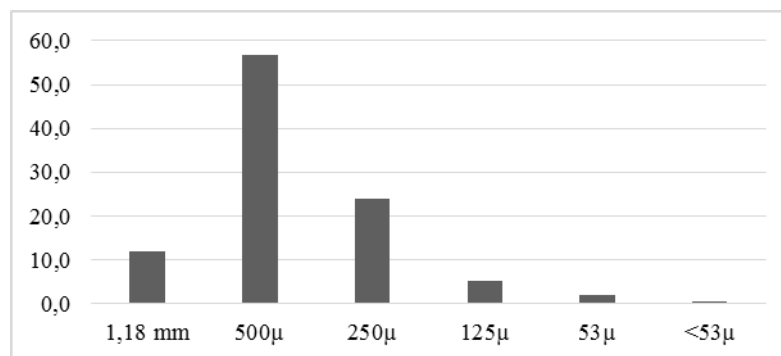


Figure A.2. Partial size of aggregates

Partial sizes of aggregates from Hypokremnos were not similar to the values from different Roman period buildings.

- Chemical Compositions of Mortars

Major chemical compositions of binders of Roman lime mortars were determined by SEM-EDS analysis.

Table A.4. Major chemical compositions of lime mortars from Hypokremnos Viaduct

Sample	CaO	SiO ₂	Al ₂ O ₃	MgO	Na ₂ O	SO ₃	K ₂ O	FeO
Fh1	47.89	30.77	8.00	4.40	3.57	1.28	0.92	0.84
Fh2	46.94	31.26	8.06	4.31	3.57	1.50	0.89	1.09
Fh3	47.08	30.86	8.27	4.48	3.39	1.45	0.89	1.12

Table A.5. Major chemical compositions of binders determined by previous studies
(Source: Uğurlu Sağın 2012)

Roman Building/ Site	CaO	SiO ₂	Al ₂ O ₃	MgO	Na ₂ O	SO ₃	K ₂ O	FeO
Lime mortars with artificial pozzolanic aggregates from Aigai (Uğurlu Sağın 2012)	19.93 - 60.82	23.73 - 52.32	8.57- 17.05	1.66- 2.25	1.19 - 1.58	-	1.10 - 2.25	-
Lime mortars with artificial pozzolanic aggregates from Nysa (Uğurlu Sağın 2012)	13.13 – 50.45	24.78 - 55.59	12.18 - 21.70	2.78- 7.68	0.84- 2.10	-	1.24 - 3.51	-

Binders of lime mortars from Hypokremnos Viaduct consisted of high amount of CaO (46.94 -47.89) and SiO₂ (30.77-31.26), moderate amount of AlO₃ (8.00- 8.27), MgO (4.31-4.40) and Na₂O (3.39-3.57), lower amount of SO₃ (1.28 -1.50), K₂O (0.89 - 0.92) and FeO (0.84-1.12). Major chemical compositions of binders from Hypokremnos Viaduct were similar to the compositions of mortars from Roman Period Buildings (Table A.4, Table A.5).

- Mineralogical Compositions of Mortars

Mineralogical compositions of mortars were determined by XRD analysis. XRD analysis revealed that lime mortars from Hypokremnos Viaduct were found to be composed of calcite, quartz, muscovite, anorthite and albite (Figure A.3).

Binders of Roman period lime mortars were found to be composed of mainly calcite, quartz, muscovite, and anorthite similar to binders of lime mortars from Hypokremnos Viaduct (Uğurlu Sağın 2012).

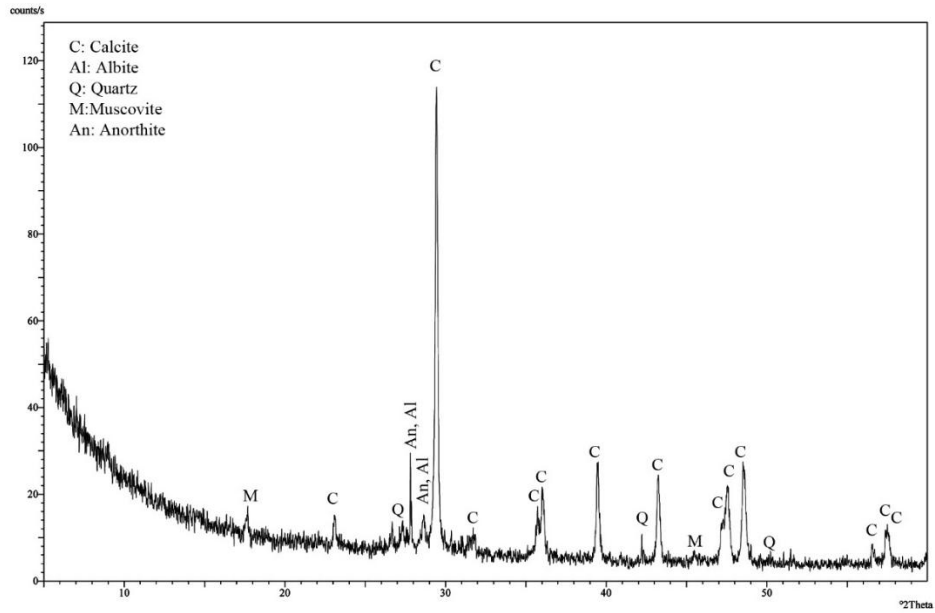


Figure A.3. XRD pattern of lime mortar from Hypokremnos Viaduct

- Pozzolanic Activities of Aggregates

Pozzolanicity of aggregates were investigated by measuring the electrical conductivity differences before and after addition of aggregates (less than 53 micrometer) into saturated calcium hydroxide solution. It was suggested that if the EC is over 1.2 mS/cm the aggregates has good pozzolanicity (Luxan et al. 1989).

Electric conductivity of pozzolans of the case study is 7.496. Therefore it has good pozzolanicity ($1.2 < 7.496$) and was similar to examples from different Roman period buildings (Uğurlu Sağın 2012).

- Hydraulic Properties of Mortars

Hydraulic properties of the mortars were determined by heating the plaster samples in a furnace. The weight loss between 200 °C, 600 °C, 900 °C were measured. Weight losses in the range of 30-200 °C is due to absorbed water, 200-600 °C is due to decomposition of organic matter, 600-900 °C is carbon dioxide. If the ratio between percentage of weight loss in 200-600 °C and 600-900 °C is among 1 and 10, mortar can be accepted hydraulic (Uğurlu 2005).

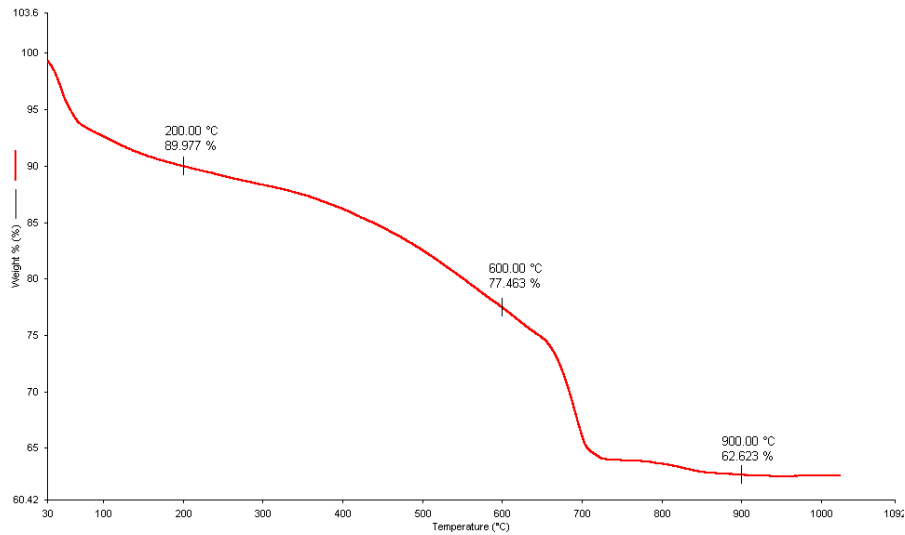


Figure A.4. TGA graph

To determine hydraulicity of mortar taking from Hypokremnos Viaduct, thermogravimetric analysis were carried out. Below, weight losses are observed in the range of 30–200 °C, 200–600 °C and 600–900 °C in the TGA Graph. According to this analysis, the mortar samples of the Viaduct can be accepted as hydraulic (Figure A.4, Table A.6).

Table A.6. Weight losses

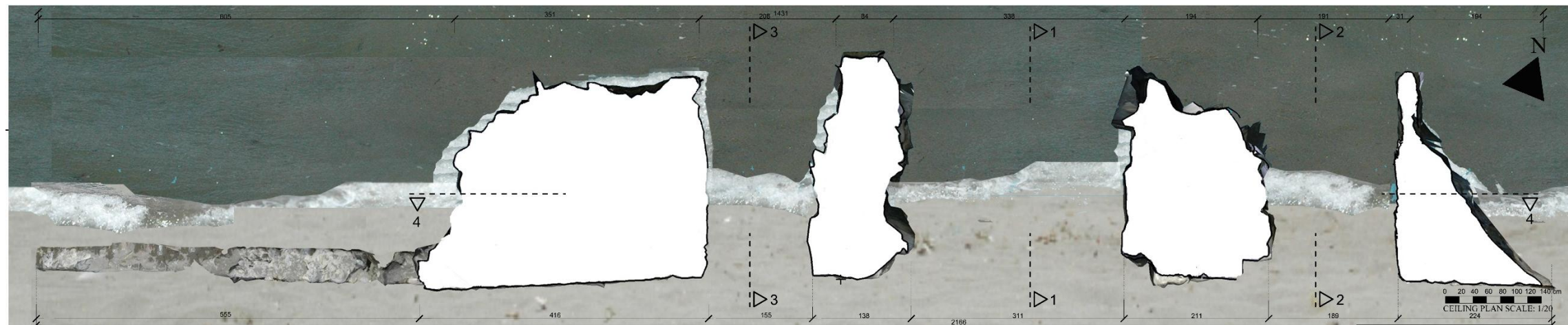
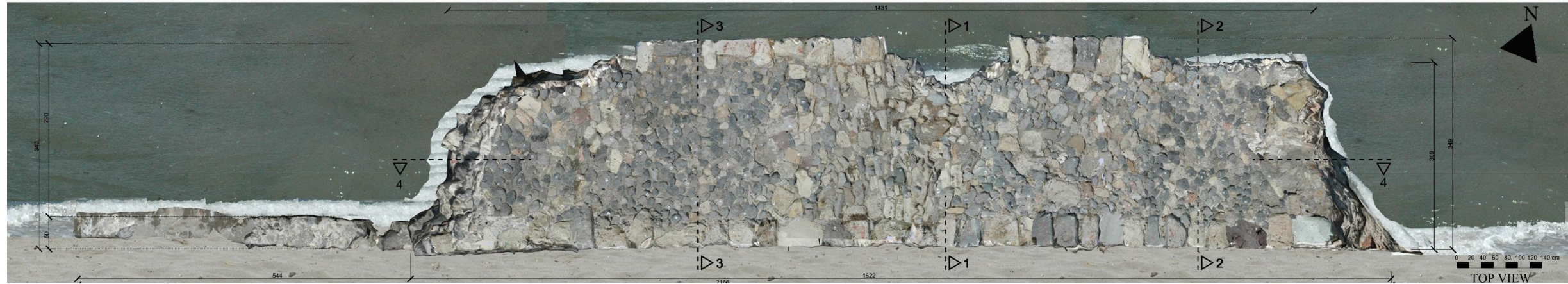
Temperature	30 °C	200 °C	600°C	900°C	200-600 °C	600-900 °C
Weight	2,36gr	2,12 gr	1,83 gr	1,48 gr		
Percentage of Weight loss		89,977 %	77,463 %	62, 623 %	12,514 %	14,84 %

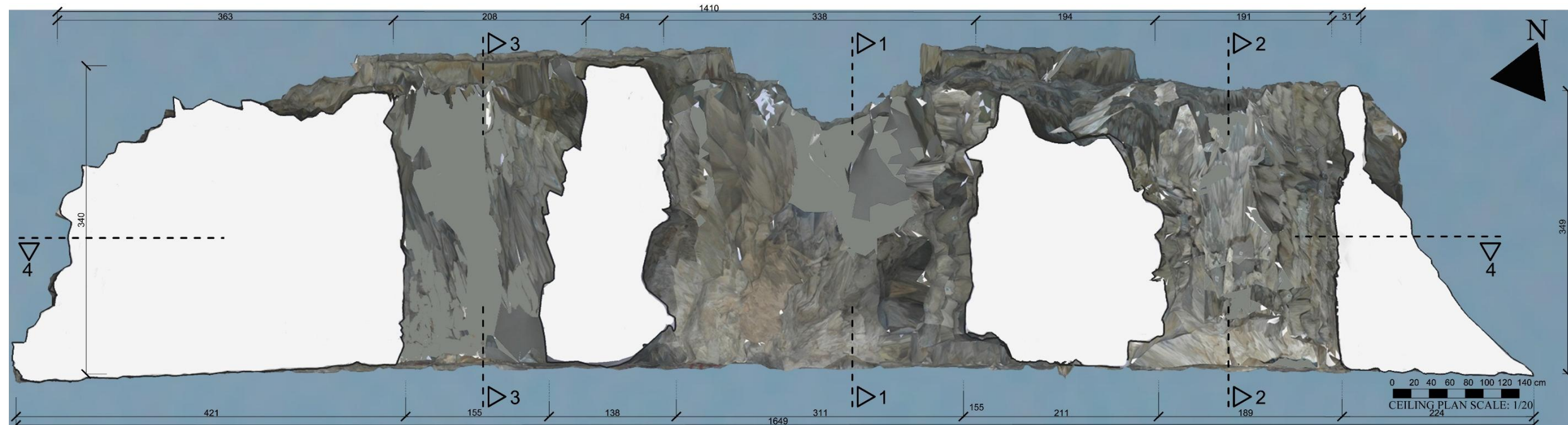
$CO_2/H_2O = 14, 84/12, 514 = 1, 18 > 1$ ➔ Hydraulic Property

Consequently, the mortar sample taken from Hypokremnos Viaduct showed similar features with mortar from Roman monuments in terms of raw material composition, basic physical, chemical, mineralogical, and hydraulic properties, and pozzolanic activities of aggregates.

APPENDIX B

ORTHOGRAPHIC VIEWS OF THE 3D MODEL OF HYPOKREMNOS VIADUCT IN 1/20 SCALE



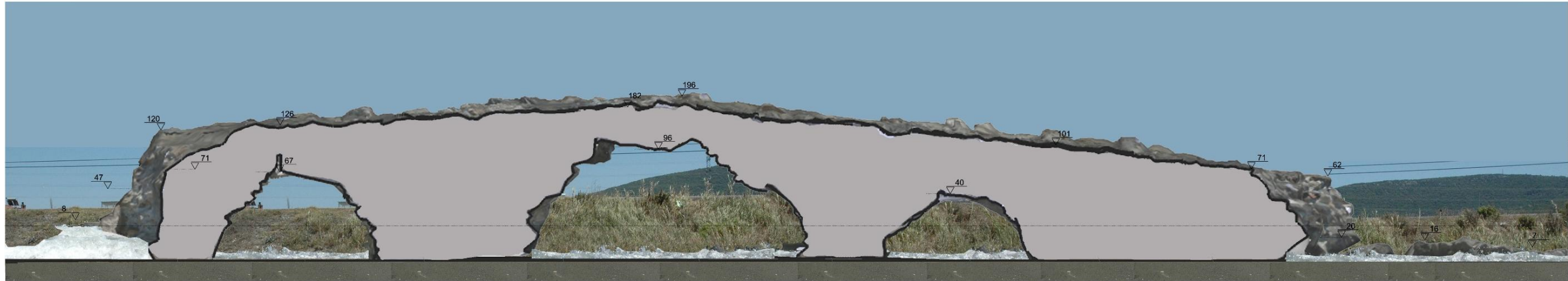


0 20 40 60 80 100 120 140 cm
 SOUTHEASTERN ELEVATION
 SCALE: 1/20



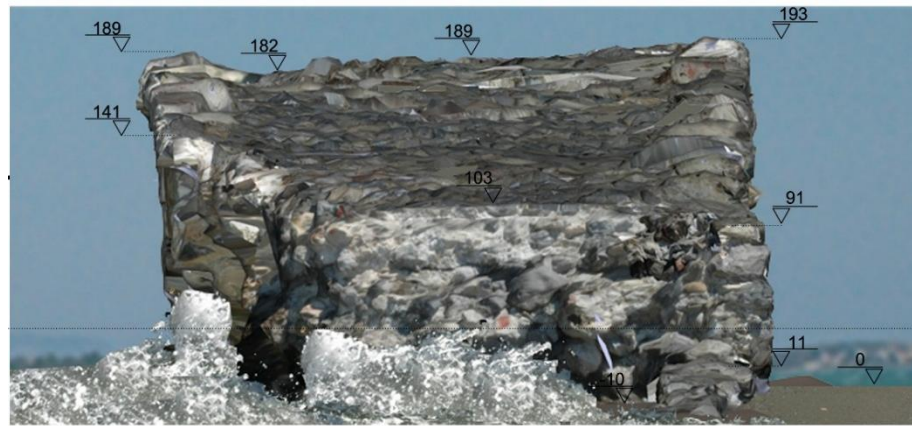
0 20 40 60 80 100 120 140 cm

NORTHWESTERN ELEVATION
SCALE: 1/20

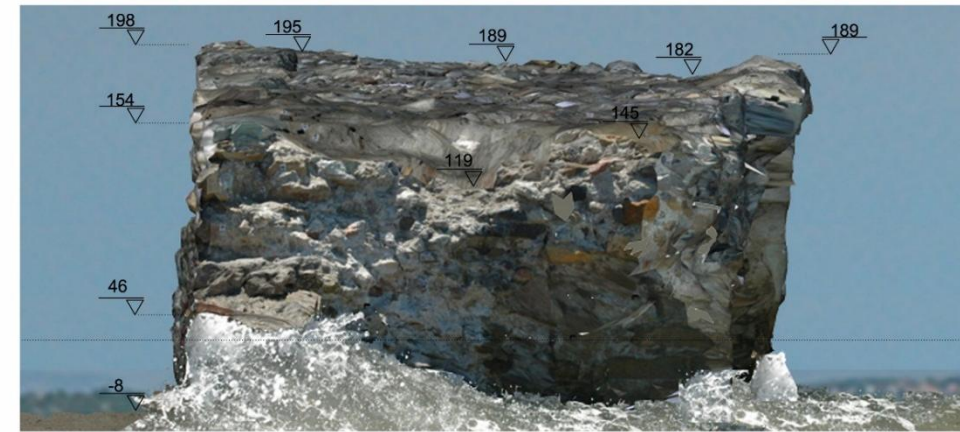


0 20 40 60 80 100 120 140 cm

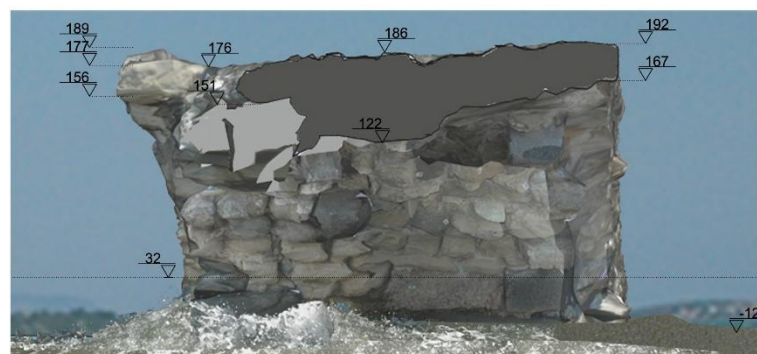
SECTION 4
SCALE: 1/20



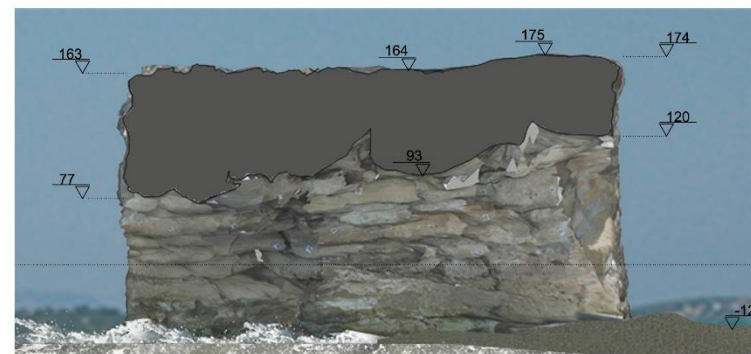
0 20 40 60 80 100 120 140 cm
 SOUTHWESTERN ELEVATION
 SCALE: 1/20



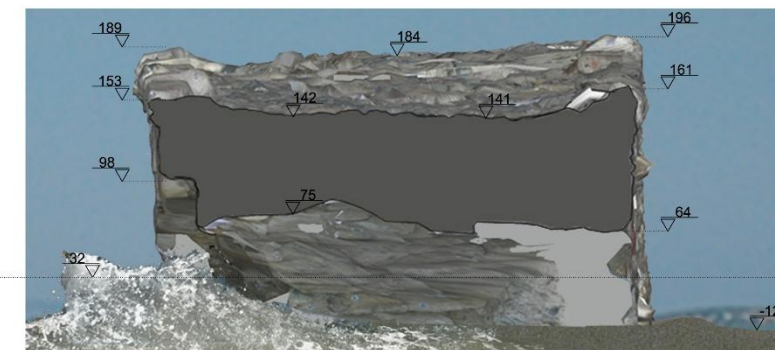
0 20 40 60 80 100 120 140 cm
 NORTHEASTERN ELEVATION
 SCALE: 1/20



0 20 40 60 80 100 120 140 cm
 SECTION 1-1
 SCALE: 1/20



0 20 40 60 80 100 120 140 cm
 SECTION 2-2
 SCALE: 1/20



0 20 40 60 80 100 120 140 cm
 SECTION 3-3
 SCALE: 1/20

APPENDIX C.

AXONOMETRIC VIEWS OF THE 3D MODEL OF HYPOKREMNOS VIADUCT IN 1/20 SCALE



